AN ABSTRACT OF THE DISSERTATION OF

Sarah Burch for the degree of Doctor of Philosophy in Water Resources Engineering presented on August 31, 2018.

Title: Evaluating Biochar for the Sustainable Treatment of Heavy Metals in Stormwater: Characteristics, Mechanisms, and Barriers.

Abstract approved:

_____

Jeffrey A. Nason

Heavy metals, such as copper, zinc, and cadmium, are ubiquitous in stormwater and potentially toxic to aquatic organisms at low concentrations. Removal of heavy metals contamination by conventional treatment is expensive and does not always reduce metals concentrations low enough to ensure safety of all aquatic species. This research seeks to evaluate the effectiveness of biochar as a low-cost, sustainable solution for the remediation of heavy metals in stormwater.

Biochar has proven effective in removing metals; however, specific sorption mechanisms and reactive properties are not well defined. In this work, different biomass feedstocks (Douglas fir chips and hazelnut shells) were pyrolyzed at varying temperatures to determine the effects of biomass feedstock and production conditions on biochar characteristics and metals removal. Adsorption experiments were conducted in batch reactors and constant flow fixed-bed column filtration experiments. Results of copper removal from batch adsorption experiments were used to select an optimal thermally-altered media for further characterization and evaluation in column filtration experiments. Batch and fixed-bed column results indicate that hazelnut shells pyrolyzed at 700ºC exhibit superior performance in copper removal compared to other types of biochar and granular activated carbon (GAC), the current prevailing adsorbent media.

Adsorption results were used in conjunction with biochar characterization and modeling techniques to elucidate the mechanisms for metals removal by biochar. Modeling of batch and continuous flow experiments moved beyond common empirical isotherm models and employed thermodynamically-based surface complexation modeling to predict metals adsorption under varying solution conditions and incorporating electrostatic effects. These electrostatic models are better equipped to evaluate metals removal by biochar in solutions of varying pH, ionic strength, and metals loading, making them more suitable for application in complex stormwater systems. Model parameters, including surface site density and surface complexation constants, were determined by fitting simulation results to experimental results of potentiometric titrations and copper sorption edges over varied pH. Defining the fundamental pathways for metals removal will inform engineering design to optimize biochar production conditions and advance sustainability.

Researchers and practitioners involved in biochar agricultural and environmental applications, bio-energy and biochar production, and forest management were interviewed to determine what questions remained in their fields that were acting as barrier to widespread biochar implementation. Interviews and questions presented in field workshops were video recorded at US Biochar Initiative (USBI) conference hosted at Oregon State University (OSU) in 2016. The "Burning Questions of Biochar" are presented in this document and a complementary edited video. The goal disseminating these questions is to encourage cross-discipline communication between aspects of the biochar business system, to highlight common barriers and to form collaborative solutions. The most common concern presented from all fields examined was that biochar characteristics are not well-documented in the myriad of published studies. Lack of characterization makes it difficult if not impossible to compare biochar results across studies with varying environmental or biochar production conditions. There was a cross-cutting need to understand mechanisms by which biochar provides benefits to environmental and agricultural applications. Defining mechanisms for soil and water improvement must also be linked to biochar characteristics to understand how biochar will affect target

applications based on production and site conditions. Biochar benefits in agricultural and environmental applications need to be confirmed by long-term field-scale trials to understand how environmental conditions affect biochar performance over time.

Evaluating Biochar for the Sustainable Treatment of Heavy Metals in Stormwater:
Characteristics, Mechanisms, and Barriers

by
Sarah Burch

A DISSERTATION

submitted to

Oregon State University

in partial fulfillment of
the requirements for the
degree of

Doctor of Philosophy

Presented August 31, 2018
Commencement June 2019

<u>Doctor of Philosophy</u> dissertation of <u>Sarah Burch</u> presented on <u>August 31, 2018</u>

APPROVED:

_____

Major Professor, representing Water Resources Engineering

_____

Director of the Water Resource Graduate Program

_____

Dean of the Graduate School

I understand that my dissertation will become part of the permanent collection of Oregon State University libraries. My signature below authorizes release of my dissertation to any reader upon request.

_____

Sarah Burch, Author

ACKNOWLEDGEMENTS

CONTRIBUTION OF AUTHORS

Dr. Jeff Nason, was involved with the experimental design, data interpretation and writing. Mark Johnson (US EPA) assisted with production of the pyrolytic biochars and characterization using proximate carbon analysis (PCA), thermogravimetric analysis (TGA), and Fourier Transform Infrared Spectroscopy (FTIR). Joy-Marie Gerould contributed to batch testing and characterization of the adsorbent medias including surface area, pH, PCA, TGA, and FTIR. Jessica Steigerwald collaborated on column testing in competition with metals, electrophoretic mobility (EPM) studies, and FTIR-attenuated total reflectance (ATR).

TABLE OF CONTENTS

LIST OF FIGURES

LIST OF APPENDIX FIGURES

LIST OF TABLES

LIST OF APPENDIX TABLES

1 Introduction

Heavy metals, including copper, zinc, and lead, are common pollutants in stormwater runoff and can be toxic to aquatic organisms at very low dissolved concentrations (2 ppb for Cu^{2+}) (Mcintyre et al. 2008). Current best management practices (BMPs) for stormwater treatment often only target peak flow and total suspended solids reduction and are not designed to remove dissolved metals. Existing BMPs, including bioswales and detention basins, can be amended with adsorbent media to increase removal of dissolved metals from stormwater runoff. Granular activated carbon (GAC) is a common commercially available adsorbent used in drinking water, industrial, and remediation wastewater treatment; however, the cost of GAC makes implementation as an adsorbent media for nonpoint source pollution from stormwater impractical. Alternative low-cost adsorbent medias, such as biochar, could provide a suitable widespread treatment option. Biochar and GAC start with a similar production via pyrolysis, creating particles with medium to high surface areas; however, unlike GAC, biochar is generally not activated or treated (Ahmad et. al. 2014; Cao and Harris 2010) Biochar is a sustainable alternative compared to GAC due to the green energy (syngas, bio-oil, and heat) generated during biochar production and use of biomass waste feedstock in contrast to the high-temperature steam or chemical activation and typically coal feedstock required to produce GAC.

Additionally, the biochar contains a non-carbonized fraction that may interact with contaminants, increasing removal. Specifically, the extent of O-containing carboxyl, hydroxyl, and phenolic surface functional groups in biochar could effectively bind contaminants (Uchimiya et al. 2011). These multi-functional characteristics of biochar show its potential as a very effective environmental sorbent for organic and inorganic contaminants in soil and water without requiring fossil fuel feed stock and energy intensive activation typical in GAC production. Specific biochar properties are mainly affected by pyrolysis temperature, residence time, and feedstock type, which strongly influence biochar sorption properties with respect to various contaminants. Therefore, the selection of biochars produced at different conditions should be targeted for specific contaminant reduction. Biochar has shown potential to remove a variety of organic and inorganic contaminants at a laboratory scale, but which specific biochar properties and corresponding feedstock and production conditions are related to specific contaminant

removal and performance in natural systems are uncertain (Ahmad et. al. 2014; Mohan et al. 2014).

1.1 Objectives This work seeks to reduce uncertainties surrounding biochar effectiveness for copper removal in complex natural systems by accomplishing the following specific objectives:

(1) define mechanisms for copper removal by biochar

(2) link biochar characteristics to performance with respect to metals removal;

(3) evaluate dynamic adsorption and effects of complex aqueous solutions; and

(4) evaluate barriers to biochar application at the field and landscape scale.

1.2 Hypotheses The hypotheses as they apply to the objectives defined were:

(1) Dissolved copper is removed from aqueous solution by a primary mechanism of surface complexation with functional groups located in the internal porous structure of biochar. Due to the formation of large stacked sheets of aromatic carbon rings at high treatment temperature (>700 C), the complex porous internal structure creates a recalcitrant platform for internal organo-metallic complexes.

(2) The biochars obtained at low temperatures are more suitable for removing inorganic/polar organic contaminants by oxygen-containing functional groups and electrostatic attraction (Ahmad et. al 2014). Surface area, pH, and fixed carbon are correlated with increased copper removal and increased production temperature (Mohan et al. 2014). An optimal production temperature balances these opposing trends to maximize copper removal.

(3) Pyrolysis conditions and feedstock type are the main factors influencing biochar characteristics and sorption behavior. One type of biochar is not appropriate for all biochar applications. Even within remediation applications, optimal biochar characteristics vary based on the specific contaminant targeted for removal and environmental conditions. It is important to predict the metal stabilization mechanism of biochar to determine the long-term effectiveness of the remediation technology (Ahmad et. al 2014).

(4) Surface complexation of copper by surface carboxyl, phenolic, and hydroxide groups results in increasing copper removal with increasing pH. Surface complexation modelling can be used to describe and predict experimental proton and copper adsorption results at varying pH.

(5) Natural organic matter (NOM) present in natural waters competes with biochar to complex with copper. Removal of copper by biochar is reduced in the presence of NOM, due to formation of copper-NOM complexes competing with sorption and preventing access to biochar functional groups located within the internal pore structure. Presence of other metals with higher binding affinity in stormwater will complete for biochar binding sites and reduce the removal of copper.

(6) Practitioners and researchers investigating biochar supply, production and market applications have cross-cutting questions that act as universal barriers to widespread biochar implementation. Biochar has demonstrated benefits in several applications, but performance varies based on biochar characteristics, resulting in uncertainty for field scale applications. More thorough and uniform characterization across biochar types is the first step toward understanding biochar characteristics and related feedstock and production conditions and mechanisms that impact performance in targeted end-use applications.

1.3 Approach The approach to evaluate these objectives and hypothesis was pairing laboratory experiments with electrostatic modelling and case studies of field experiences to:

(1) describe proton and copper binding using surface complexation modelling;

Adsorption results were used in conjunction with biochar characterization and modeling techniques to elucidate the mechanisms for metals removal by biochar. Modeling of batch copper removal employed thermodynamically-based surface complexation modeling to predict metals adsorption under varying solution conditions with incorporated electrostatic effects. Electrostatic surface complexation models are better equipped to evaluate metals removal by biochar in solutions of varying pH, ionic strength, and metals loading, making them more suitable for application in complex stormwater systems. Model parameters, including surface site density and binding affinity constants for copper and hydrogen, were determined by fitting simulation results to experimental results of copper sorption edges over varied pH and potentiometric titrations. Identification of reactive site parameters reveal clues to determine how biochar adsorption relates to the types of functional groups (such as carboxyl, hydroxyl, and phenolic) that are key to metals complexation. Modelling of adsorption behavior was

paired with characterization of biochar to identify important properties linked to high copper adsorption.

(2) identify biochar characteristics based on biomass feedstock and production temperature and link characteristics to equilibrium copper removal performance;

Different biomass feedstocks (Douglas fir chips and hazelnut shells) were pyrolyzed at varying temperatures to determine the effects of biomass feedstock and production conditions on biochar characteristics and metals removal. Biochar physiochemical properties were evaluated via measurements of pH, surface area, fractions of volatile matter, fixed-carbon and ash using proximate carbon analysis (PCA), presence of surface functional groups using Fourier Transform Infrared (FTIR) Spectroscopy, and surface potential and isoelectric point using electrophoretic mobility (EPM). Equilibrium adsorption of copper was evaluated in batch experiments by the six types of biochar and GAC. Characterization results were compared with metals removal performance results to identify characteristics linked to high performance. Removal of copper by biochar in batch experiments was also evaluated in the presence and absence of natural organic matter (NOM) to determine the effects of NOM on copper removal.

(3) evaluate dynamic adsorption, predict performance at the field scale and evaluate barriers to performance in complex systems;

While elucidation of the copper removal mechanism by biochar in batch experiments is a critical first step in predicting filtration performance, sorption needed to be experimentally evaluated in fixed-bed column filters to simulate realistic engineering implementation. Results of copper removal from batch adsorption experiments were used to select an optimal thermally-altered media for evaluation of copper removal in column filtration experiments. Rapid small-scale column tests (RSSCTs) were designed to evaluate dynamic adsorption by biochar and predict field scale performance in stormwater treatment of copper. Fixed-bed continuous flow, lab-scale columns were used to evaluate copper removal by biochar in synthetic storm water and solutions containing dissolved organic carbon (DOC) and competing metals (Pb^{2+} and Zn^{2+}). Copper removal in fixed-bed column filtration experiments was evaluated by leveraging surface complexation modelling parameters determined in equilibrium experiments to describe sorption behavior during dynamic flow through a fixed-bed of biochar.

(4) interview biochar researchers and practitioners in fields of production, forest management, remediation, and agriculture to identify questions acting as barriers to widespread biochar implementation.

Researchers and industry leaders were asked to define questions affecting the growth of biochar use in their respective fields of forest waste management, water treatment, soil health, carbon sequestration and policy. These questions are highlighted in concert to alleviate uncertainty surrounding biochar applications and advance the sustainability of the biochar movement. The interviews, presentations, and workshops were filmed at the US Biochar Initiative (USBI) conference hosted at OSU in August 2016 and edited into a complementary video highlighting the questions posed. The manuscript and accompanying video emphasize collaborative efforts of the conference and encourage practitioners and researchers to build on cross-discipline conversations.

The dissertation is organized in the manuscript format, where Chapter 2 describes background information that is not included in the introduction of the three manuscripts. Chapters 3 to 5 are self-contained manuscripts addressing the objectives described. Chapter 3 seeks to define mechanisms for copper removal using characterization, equilibrium batch testing, and electrostatic modelling. Chapter 4 focuses on evaluating dynamic copper removal in RSSCTs with background solutions of synthetic stormwater, river water, and competing metals Pb^{2+} and Zn^{2+}. Chapter 5 identifies the "Burning Questions" defined by biochar researchers and practitioners to link parallel barriers and promote cross-field problem solving. Chapter 6 contains a conclusion that thematically links the findings from the three manuscripts and highlights the contributions and impacts of the work. The bibliography summaries references for the entire dissertation. Appendix A and B contain supplemental information from the first and second manuscript, respectively (Chapter 4 and 5).

2 Background

2.1 Adsorbent Characteristics for Metals Removal Several physical and chemical characteristics of biochar influence its capacity for removal of metals including pH, surface area, fixed carbon, electronegative surface charge, and surface functional groups. Biochar characterization was paired with adsorption results and modelling to evaluate the mechanisms for metals removal by biochar. Characterization of the biochar medias including measurement of pH, surface area, thermogravimetric analysis (TGA), proximate carbon analysis (PCA), electrophoretic mobility (EPM), and surface functional groups by Fourier transform infrared spectroscopy (FTIR) was conducted in concert with batch performance studies to identify specific biochar properties linked to superior metals removal. These specific experiments were chosen to investigate properties attributed to metals removal and to compare with other biochar and adsorptive medias' characteristics frequently reported in literature (Chen et al. 2011; Regmi et al. 2012; Biniak et. al. 1999; Tong et al. 2012; Zhang and Luo 2014; Kim et al. 2012; Manyà 2012).

Adsorption of cationic metals increases with pH; therefore, alkaline biochar pH can influence solution pH and subsequent metals removal. The surface area of biochar is important because high surface area has been shown to increase biochar's ability at adsorption (Chen et al. 2011). Thermogravimetric analysis (TGA) is used to evaluate the release of moisture and the volatilization of organics during biochar production. A more stable form of carbon remains at the higher temperatures (Kim et al. 2012). Proximate carbon analysis (PCA) is performed to determine the amount of fixed carbon, ash, and volatiles present in the biochar. Biochars with higher ash content do not perform as well for copper removal while chars with high fixed carbon perform better (Brewer 2012). FTIR analysis is performed on biochars to determine exactly which functional groups are present on the biochar and to determine correlations between the presence of specific functional groups and increased copper adsorption (Mukherjee et. al. 2011; Regmi et al. 2012).

2.2 Electrostatic Adsorption Modelling Empirical approaches used to model inorganic ion binding such as partitioning coefficients and isotherm equations are limited to particular solution conditions and are not easily extrapolated to other conditions of pH, ionic strength and competition. With known densities of surface functional groups and ion-binding constants, surface charge and ion adsorption can be computed for different conditions in solution using

surface complexation modeling (Dzombak and Morel 1987). An accurate physically-based model needs to be implemented to predict adsorption of protons and metals under varying surface charge conditions. In addition, a wide variety of functional groups in waste biomaterials such as hydroxyl, carboxyl, carbonyl, amine, amide, alcoholic, phenolic, thiol and phosphate have high affinity to form metals complexes (Volesky 2007). Chelation by carboxyl and hydroxyl groups present on bio-sorbent surfaces have been proposed as the mechanism binding (Ravat et. al. 2000; Witek-Krowiak and Reddy 2013). Surface complexation models have been used to accurately predict sorption for varying conditions onto hydrous ferric oxide (Zhu 2002; Dzombak and Morel 1990), calcite (Comans and Middelburg 1987; Zhu 2002) , α-Al_2O_3 (Katz and Hayes 1995), granular activated carbon (Gabaldón et al. 1996), and natural organic matter (Ravat et. al. 2000). These models require quantification of the total number of surface sites available for ion binding and binding affinities to each site. The presence of a variety of surface functional groups and this proposed mechanism of removal give support to the application of a surface complexation model to predict the sorption behavior of hydrogen and metals onto biochar.

Several options exist to model adsorption onto biochar, including multi-site affinity spectrum models that consider a heterogeneous distribution of sites or electrostatic models, with different representations of the solute layer (constant capacitance, diffuse layer, triple layer models). To determine which model is appropriate for describing proton binding to biochar and what type and number of sites to consider, the electrokinetic characteristics of the char were studied. Potential differences across solid/water interfaces can be measured by electrokinetic methods, such as electrophoresis. In this technique, the movement of charged particles in an applied electric field is observed and the average particle velocity is used to estimate the charge per particle. Surface potential is then calculated from the average charge using the Poisson equation (Dzombak and Morel 1987). Zeta potential is often considered to be the potential at the edge of the diffuse layer, Ψ_d. The zeta potential corresponds to the effective shear plane between moving and stationary phases, which does not necessarily coincide with the outer edge of the layer of adsorbed ions. Studies with completely reversible silver iodide have shown that zeta potential and Ψ_d are only equal for low potentials and low ionic strength. With larger potentials and ionic strengths, stronger interfacial electric fields exist, which shifts the shear plane further from the surface, increasing the difference between zeta potential and Ψ_d. Since water near a charged surface has

high viscosity and moves with the solid, the shear plane in aqueous systems occurs beyond the edge of the Stern layer, so that zeta potential is less than Ψ_d. Calculation of zeta potentials from electrophoretic mobility requires that the relationship between mobility and zeta potential be known, which not the case for irregularly shaped particles, such as oxides or bio-sorbents (Dzombak and Morel 1987).

The problem of how to best account for electric field effects on a bio-sorbent surface adsorption reaction is not straightforward. First, it must be determined if the electrokinetic characteristics of the sorbent behave like those of organic macromolecules (bacteria, humic and fulvic acids) or like mineral oxides. The functional groups present on mineral surfaces can be assumed to occupy the outer surface of a rigid plane, while those on organic macromolecule surfaces are present throughout a semi-rigid, three-dimensional fabric of substantial thickness. A single site modeling approach can often be used to describe surface binding with oxide minerals and functional groups are assumed to occur at specific sites of the same character that possess identical binding affinities. Functional groups associated with organic macromolecules occupy a three-dimensional polyelectrolytic mixture of aliphatic and aromatic hydrocarbons. Organic macromolecule surfaces contain a number of chemically distinct functional groups that can only be mechanistically described using multi-site models (Borrok and Fein 2005).

Mineral surfaces typically have a definable point of zero charge (PZC) because the surface functional groups become doubly protonated and positively charged at low pH. Organic macromolecule and bacteria are negatively charged over the pH range for which they are dissolved (above pH 2); therefore, they are absent of a true PZC and the approaches used to describe electric field interactions for mineral surfaces (constant capacitance, double-layer, and triple-layer models) may not be directly applicable for describing electric field interactions with bacterial surfaces. A multi-site non-electrostatic modeling approach has been used to accurately describe proton binding with bacteria (Borrok and Fein 2005; Borrok et. al., 2005) and humic acid surfaces (Westall et al. 1995). These studies conclude that multiple models with differing parameters, including the number of sites and presence of an electrostatic term, can provide equivalently good fits of potentiometric titration; therefore, experimental data from potentiometric titrations alone are insufficient to provide inside into the physical nature of the solid/water interface (Borrok et. al. 2005). Proton binding constants determined from modeling

potentiometric titrations must be tested over a range of ionic strengths and in the presence of other sorbing cations.

The determination of the point of zero charge (PZC) can help distinguish whether the biochar behaves more like a mineral oxide (PZC = 3-4) with distinct reactive surface size or like an amorphous organic macromolecule (PZC < 2) with a range of heterogeneous site distributions. Typically, adsorption of metals onto mineral oxides can be accurately described by electrostatic models while affinity spectrum models are more appropriate for organic macromolecules. It is probable that different bonding mechanisms are dominant at varying pH and surface charge.

Surface complexation models offer advantages over other empirical isotherm models because they can predict adsorption under varying conditions of pH, ionic strength, and sorbate/sorbent ratios. In addition, surface complexation models can accurately predict competition for metals removal in complex waste-streams based on parameters derived from single solute experiments. These models incorporate both surface reactions described by intrinsic binding constants and solution interactions through incorporation of an electrostatic term. The various surface complexation models differ in their physical representation of the solute layer and electrostatic representation. The diffuse layer model is often recommended for modeling removal of heavy metals based on the fact that fewer parameters are required compared to other models with equal accuracy of prediction of adsorption results under varying conditions.

The fundamental concept upon which all surface complexation models are based is that adsorption occurs at a finite number of defined coordination sites and adsorption reactions can be described quantitatively by mass law equations (Dzombak and Morel 1987). Surface adsorption differs thermodynamically from reactions among solutes by the variability of the electrostatic energy of interaction (the coulombic term):

$$\Delta \boldsymbol{G_{adsorption}} = \Delta \boldsymbol{G_{intrinsic}} + \Delta \boldsymbol{G_{coulombic}} \tag{1}$$

The separation of coulombic and intrinsic terms from total Gibbs free energy is necessary because of the long-range nature of electrostatic interactions and the proximity of adsorption sites of varying charge based on reactions with bulk solutes. Intrinsic adsorption coefficients (K_{int}) determined from intrinsic Gibbs free energy ($\Delta G_{intrinsic}$) for the various surface complexation model fits are "intrinsic" in that they are independent of ionic strength and surface charge; however, they are "conditional" in that they are both model and fit dependent. Intrinsic adsorption coefficients are interrelated and dependent on the capacitances and site density, which

must be considered as a complete set (Robertson and Leckie 1997). Electrostatic energy of interaction ($\Delta G_{coulombic}$) depends on both the charges of reacting species and neighboring species.

Various surface complexation models are distinguished by different assumptions concerning appropriate electrostatic interaction terms, or activity coefficients, often described by geometric locations of adsorbed ions at the adsorbent/solution interface. All surface complexation models reduce to a similar set of simultaneous equations to be solved numerically. These equations include (Dzombak and Morel 1987):

1. Mass law equations for all possible surface reactions
2. A mole balance equation for total surface sites (one for each type of surface site)
3. An equation for computation of surface charge
4. A set of equations representing the constraints imposed by the model chose for electrical double layer (EDL) structure

2.3 Surface Charge

Biochars exhibit amphoteric behavior in water, meaning they both bind and release protons based on solution pH. Surface charges are established as result of proton transfer reactions. If H^+ is the only adsorbing ion, the surface charge σ_0 (C/m^2) is computed as (Dzombak and Morel 1987):

$$\sigma_0 = \frac{F}{AS}[(= SOH_2^+) - (= SO^-)] = F[\Gamma_H - \Gamma_{OH}] \qquad (2)$$

Where $(= SOH_2^+)$ and $(= SO^-)$ represent positively and negatively charge surface sites, respectively; ( ) represent molar concentration; F = Faraday constant (96,500 C/mol); A = specific surface area (m^2/g); S = the solid concentration (g/L) and Γ_H, Γ_{OH} = the adsorption densities (mol/m^2) of H^+ and OH^- ions. The pH at which the proton excess at the surface is zero ($\Gamma_H - \Gamma_{OH} = 0$) is known as the point of zero net proton charge. If H^+ is the only adsorbing ion present, the point of zero net proton charge corresponds to the point of zero charge, or PZC. The surface is negatively charged when pH exceeds the PZC and positively charged when pH is less than the PZC. Surface charge can be determined experimentally by comparing a titration curve of an adsorbent suspension versus titration of the background matrix alone. The net consumption of H^+ or OH^- by the solid phase is determined by the difference in titrations. A net adsorption

curve (surface proton excess) can be plotted and surface charge can be calculated as a function of pH.

In the surface complexation approach, surface charge is considered to develop on adsorbent surfaces via chemical reactions at specific surface sites. Adsorption of ions onto absorbent surfaces is considered analogous to the formation of soluble complexes, including H^+ and OH^-. Adsorbates bind to reactive groups at the surface, which can be described by mass law equations. In addition, the surface charge increases with ionic strength as the electrical double layer is compressed and proton exchange reactions are facilitated (Dzombak and Morel 1987). Understanding of processes at the solid/water interface are described by the classical double layer theory (Gouy-Chapman) and its extensions (Stern-Grahame), but some modifications are necessary to describe unique adsorbent surface chemistry compared to mercury and silver iodide electrodes, for which the classical approach was developed (Dzombak and Morel 1987).

2.4 Electric Double Layer (EDL): Surface Potential

When a charged particle is introduced into an aqueous system, a localized disturbance of electroneutrality occurs and is counteracted by the development of an excess density of oppositely charged electrolyte ions near the particle surface. The separation of charges in the electrical double layer (EDL) results in a potential difference across the interface. Although the potential difference across and interface is typically small, the thickness of the interphase region is very small, therefore, the electrical field strength is very large, which dictates the distribution of nearby ions in solution and affects transport of ions at the surface (Dzombak and Morel 1987).

Classical EDL theory (Gouy-Chapman) provides an accurate description of the spatial distribution of counterions in the vicinity of solid surfaces. Stern and Grahame refined to classical model to account for the finite size of ions and proposed that counterions can approach a charged surface only to within a certain distance. Stern and Grahame also introduce specific adsorption, proposing that dissociated ions at the interface bond chemically with the surface. These modifications shift the diffuse layer away from the surface and eliminate predicting physically impossible ion densities close to the surface. Differences among adsorption models occur in the geometric description of specific adsorption related to the treatment of the compact layer at the solid/water interface (Dzombak and Morel 1987).

2.5 Proton Adsorption

The amphoteric ionization reaction of surface groups that cause surface charge development are described below:

$$= SOH_2^+ \rightarrow = SOH^o + H^+; \; K_{a1}^{app} \tag{3}$$

$$= SOH^o \rightarrow = SOH^- + H^+; \; K_{a2}^{app} \tag{4}$$
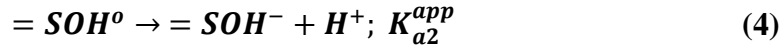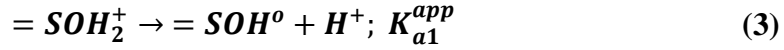
Where K_{a1}^{app} and K_{a2}^{app} are apparent equilibrium acidity constants because they include electrostatic interaction effects (activity coefficients) and are functions of the extent of surface ionization. The corresponding mass law equations are:

$$K_{a1}^{app} = \frac{(= SOH^o)\{H^+\}}{(= SOH_2^+)} \tag{5}$$

$$K_{a2}^{app} = \frac{(= SO^-)\{H^+\}}{(= SOH^o)} \tag{6}$$

Where ( ) represent molar concentration, and { } represent activities. Energy is required to move ions through an interfacial potential gradient (dependent on the degree of ionization); therefore, the electrical interaction energy associated with K_{a1}^{app} and K_{a2}^{app} is variable (Dzombak and Morel 1987). Chemical and electrical contributions to the total interaction energy cannot be separated experimentally, but an ideal expression for the electrical term may be obtained from the Gouy-Chapman EDL theory. For this, reactions are broken into two steps: (1) proton release from the surface; and (2) dissociated proton transported through interfacial potential gradient to the bulk solution. Protons at the surface are distinguished from protons in the bulk solution, because the electrical potential difference between the regions results in a different electrochemical potential of the proton. Under ideal conditions (Gouy-Chapman), the proton concentration at the surface (H_s^+) is related to the bulk solution concentration (H^+) by the expression:

$$(H_s^+) = (H^+) \exp\left(\frac{-F\Psi_0}{RT}\right) \tag{7}$$

Where Ψ_0 represents the surface potential, compared to a reference potential of zero in the bulk solution; $R=$ the gas constant; $T=$ absolute temperature (K); and $F =$ Faraday constant. The exponential term $(\exp\left(\frac{-F\Psi_0}{RT}\right))$ is an activity coefficient for EDL effects on proton exchange, referred to as an electrostatic or coulombic correction factor. This term is useful for accounting for surface charge effects on surface complexation reactions. The coulombic correction factor

can be applied to mass law equations to determine intrinsic acid constants (Dzombak and Morel 1987).

$$K_{a1}^{int} = \frac{\{= SOH^o\}\{H_s^+\}}{\{= SOH_2^+\}} = K_{a1}^{app}\exp(\frac{-F\Psi_0}{RT}) \qquad (8)$$

$$K_{a2}^{int} = \frac{\{= SO^-\}\{H_s^+\}}{\{= SOH^o\}} = K_{a2}^{app}\exp(\frac{-F\Psi_0}{RT}) \qquad (9)$$

Where the intrinsic equilibrium constants, K_{a1}^{int} and K_{a2}^{int}, correspond to chemical interactions only and do not depend on ionic strength or surface charge. Since surface potentials are greater at lower ionic strengths, apparent acidity constants vary more significantly with pH (Dzombak and Morel 1987). Analysis of titration data for determining these mass law constants can be performed using either graphical extrapolation, or objective curve-fitting methods, such as FITEQL (Katz and Hayes 1995), and more recently MINEQL+ combined with minimum residual error calculations (Schecher and McAvoy 1992).

2.7 Cation Adsorption

Adsorption of metal cations is highly pH dependent; the fraction of bound cations increases from zero to one over a narrow pH range, typically only one pH unit in width. These pH adsorption edges shift to increased pH as adsorbate/adsorbent ratio is increased. As cation concentration increases or sorbent concentration decreases, the fractional adsorption at a given pH is reduced. Cation binding can be characterized quantitatively by considering the formation of surface complexes (Dzombak and Morel 1987):

$$= SOH^0 + M^{2+} = = SOM^+ + H^+; K_M^{app} \qquad (10)$$
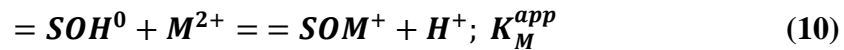
Where M^{2+} represents a divalent cation, and $=SOM^+$ represents a possible cation surface species. The choice of surface species, or multiple surface species, is dictated by the available experimental data. Effects of electrostatic interactions can be accounted for by separation of a coulombic term from the apparent adsorption constant:

$$K_M^{app} = K_M^{int}\exp(\frac{-\Delta ZF\Psi}{RT}) \qquad (11)$$

Where ΔZ = the net change in the charge number of the surface species, Ψ = the potential at the plane of adsorption. Electrostatic interactions have weak influence on cation adsorption (Dzombak and Morel 1987).

2.8 Anion Adsorption

Anion adsorption is referred to as the mirror image of cation adsorption because anion binding decreases as pH increases, and the process involves proton uptake. Specific adsorption of anions is believed to involve ligand exchange reactions in which hydroxyl surface groups are replaced by adsorbate molecules. As with cations, adsorption of anions is highly pH dependent. However, greatest anion adsorption occurs at low pH, and decreases to zero over a range of 3-4 pH units (Dzombak and Morel 1987). Adsorption of natural organic matter (NOM) can be described by anion binding onto positively charge adsorbent surfaces.

2.9 Basic (Two-Layer) Surface Complexation Models

In the basic two-layer model of ion adsorption, adsorbates are considered part of the solid surface (one layer) while resulting electrostatic charge is balanced by an adjacent diffuse layer in the solution (the second layer). The charge on the surface is determined by acid-base reactions and surface coordination reactions with other cations and anions. A classical Gouy-Chapman diffuse layer distribution is typically assumed for the bulk solution. In this diffuse layer model, the relationship between surface charge and potential is fixed by EDL theory:

$$\sigma = 0.1174 I^{1/2} \sinh\left(\frac{ZF\Psi_0}{2RT}\right); \left(\frac{C}{m^2}\right) \tag{12}$$

Where I = the molar electrolyte concentration. The finite number of surface sties limits the value of the surface charge to reasonable values regardless of ionic strength (Dzombak and Morel 1987).

The constant capacitance model is a special form of the diffuse layer model, applicable only to high ionic strength and/or low potential systems. In the constant capacitance mode, surface charge is estimated by:

$$\sigma = C\Psi_0 \tag{13}$$

Where C= a constant with dimensions of a capacitance.

The model parameters that must be determined from experimental data are (Dzombak and Morel 1987):

(1) the concentration of surface sites, N_s;

(2) the intrinsic acidity constants, K_{a1}^{int} and K_{a2}^{int} (determined from acid-base titrations);

(3) the concentration of specific adsorption sites, N_A, N_C;

(4) one or serval intrinsic adsorption constants for each specifically adsorbing cation or anion

2.10 Stern Model

The Stern model for specific adsorption at an electrified interface consists of two discrete planes of charge assumed at the surface with H^+ and OH^- ions binding at the innermost plane, and other specifically adsorbed ions at a second plane, separated by the distance of the Stern layer. The solution side of the interface, beginning at the second plane of adsorption, is described with a Gouy-Chapman diffuse layer. A linear drop in potential between the planes of surface charge is assumed so that the two adsorption planes act as a parallel plate capacitor (Dzombak and Morel 1987).

2.11 Triple Layer Model

In the triple layer model, like the Stern model, specific adsorption of ions is assumed to occur in two separate planes (one for H^+ and OH^- ions and one for other specifically adsorbed ions) and a diffuse layer is assumed for the bulk solution side of the interface. However, the diffuse layer is assumed to begin at the edge of a layer of bound water, at some distance from the second adsorption plane (Dzombak and Morel 1987). The triple layer model has been employed in a widespread number of applications ranging from modeling cation and anions sorption on oxide surfaces to modeling organic acid adsorption on mineral surfaces (Katz and Hayes 1995). In addition, the triple layer model has been used to successfully predict cadmium and zinc removal by activated carbon in competing environments (Gabaldón et al. 1996). An advantage of the triple layer model is its ability to model formation of both inner- and outer-sphere metal ion reactions. Spectroscopic confirmation of the type of surface complexes formed is required for successful selection of the appropriate inner- or outer-sphere surface reactions.

A disadvantage of the triple-layer model is the greater number of model parameters required, which makes it possible to fit titration data equally well with a wide range of surface acidity values (Katz and Hayes 1995). For any given parameter estimation method, there are disadvantages which limit the accuracy or relevancy of the values obtained. For example, surface site density has been estimated by tritium exchange, analysis of crystal structure, dehydration and rehydration with methylation agents, thermogravimetric analysis, gas and water vapor adsorption, solute adsorption, and acid-base titration data (Katz and Hayes 1995). These methods

led to a range of surface hydroxyl site density values for a mineral oxide of 1 to 20 sites/nm^2. The objective curve fitting routine, FITEQL, and titration data was used to attempt to narrow the range for surface site density estimates; however, results indicated site density values ranging from 1 to 100 sites/nm^2 gave equally reasonable fits to the titration data. This experiment highlights a potentially serious shortcoming of objective curve-fitting methods, which should be used in conjunction with other experimental methods to ensure realistic parameter values are utilized (Katz and Hayes 1995).

2.12 Multiple Site Type Model

The multiple site type model of Benjamin and Leckie assumes that adsorbent surfaces consist of serval chemically distinct types of sites with varying affinity for adsorbate cations. Multiple site types are generally not needed to model acid-base data; therefore, different site types can be assumed to have the same proton transfer characteristics. In addition to surface acidity parameters, a minimum of four adjustable parameters are required to model cation adsorption data with a multisite model (for 2 sites). These parameters include total number of binding sites for each type and surface complexation constants for binding to each site type. The multisite approach can be implemented in conjunction with any of the surface complexation models (Dzombak and Morel 1987). A two-site surface complexation model was used to successfully model adsorption of copper onto natural organic matter. In this study, moderate and strong acid sites were chosen as the primary sites necessary to model removal of copper and copper hydroxide (Ravat et. al. 2000).

2.13 Surface Precipitation Model

In the surface precipitation model of Farley et. al. 1985, the mechanism of sorption shifts from surface complex formation to surface precipitation at high adsorbate concentrations. This model describes the continuum between surface complexation and surface precipitation observed for metal oxides which depends on pH, ionic strength, and sorbate/sorbent ratio. Precipitation on the surface is described by the formation of a solid state whose composition varies continuously between the original absorbent solid and the pure precipitate of the adsorbing metal ion. The surface precipitation model contains three adjustable parameters, in addition to the surface acidity parameters (Dzombak and Morel 1987):

1. Concentration of cation binding sites
2. Cation surface complexation constant

3.   The solubility product for the solid hydroxide of the adsorbing cation

The values of these parameters are determined by fitting a constant pH isotherm but can be applied to other solution conditions (pH, ionic strength, adsorbate concentration). The surface precipitation model is not exclusive of the multisite model (Dzombak and Morel 1987). Dzombak and Morel determined a two-site model with surface precipitation on Type 2 sites was most appropriate to describe sorption of Cd on hydrous ferric oxide at high sorbate/sorbent ratios (Dzombak and Morel 1990). The sorption of Cd, Mn, Zn, and Co on calcite has been adequately described by the surface precipitation model (Comans and Middelburg 1987).

Although precipitation is not considered the dominant mechanism for removal at environmentally relevant pH, sorbate/sorbent ratios, and ionic strengths, surface precipitation occurs at lower pH and sorbate concentrations in adsorbent systems with metal hydroxide complex formation than predicted from solubility product of the adsorbing cation hydroxide (Farley et. al. 1985). Surface precipitation could become an important factor during adsorption on a fixed-bed adsorbent media as sorption sites are increasingly complexed with adsorbing metal cations. This scenario depicts a situation where the surface precipitation model may be required to describe surface precipitation occurring at high sorbate/sorbent ratios due to metal complexation of fixed-bed sorption sites, despite influent pH below the solubility limit and low influent metal concentration.

2.14 Model Selection

Westall and Hohl (1980) applied the basic two-layer, stern, and triple-layer models described here to acid-base titration data for two oxides and found all of the models to be equally capable of fitting the data (Westall and Hohl 1980). Based on this observation, the diffuse layer model is recommended for describing adsorption of inorganic ions. The diffuse layer model possesses the attributes of simplicity and applicability to different solution conditions (Dzombak and Morel 1987). Because there is a direct correlation between the complexity of the description of the solid/water interface and the number of model parameters required in the various surface complexation models, it is not always possible to determine a unique set of model parameters in the more complex versions (Katz and Hayes 1995). As a result, surface complexation models with more complex descriptions of the interfacial regions have often been discarded in favor of simpler models with few parameters (Dzombak and Morel 1990).

The primary criticism of the diffuse layer model has been that the surface potentials predicted by the model are higher than the zeta potentials measured by electrophoresis. This can be corrected by expressing the distance from the surface to the shear plane as an empirical function of ionic strength. Additional fitting parameters of electrolyte binding constant and outer layer capacitance are included in the triple layer model to fit zeta potential data. An empirical expression to describe the location of the shear plan can accomplish this objective with fewer fitting parameters and equal or better data fit (Dzombak and Morel 1987).

Ultimately, the validity of a particular model depends on direct elucidation of the surface structure and of surface coordination which should be confirmed independently with spectroscopic evidence. To use surface complexation models in a predictive mode, they should be applied under low adsorbate concentration and low dissolved organic carbon relative to adsorbent solids on a mass basis. These conditions are applicable in many environmentally relevant aquatic systems. Surface complexation models can predict adsorption of inorganic solutes under conditions of changing pH, ionic strength, or solid concentration on the basis of less adsorption data than would be required with a purely empirical approach (Dzombak and Morel 1987).

In this work, experimental metals removal performance results were described using surface complexation modelling. The diffuse layer model (DLM) with two types of binding sites was selected to be the most accurate surface complexation model to describe copper sorption onto biochar based on batch pH sorption edge, net potentiometric titration results, and determination of point of zero salt effect. These experimental results were fit using the DLM to determine model parameters (number of binding sites and site binding affinities) used to describe adsorption. Electrostatic results, DLM parameter values, and DLM representation of experimental sorption of H^+ and Cu^{2+} provide information needed to identify mechanisms of copper removal under varying pH and surface charge conditions. Elucidating the fundamental removal mechanism will support engineering design of stormwater treatment systems using biochar. The scope of this work focuses on removal of copper in stormwater; however, understanding primary cation removal mechanisms will contribute to widespread use of biochar in various treatment applications, including removal of other metal and cationic contaminants and treatment of industrial and municipal wastewater, groundwater, drinking water, and soil.

3 Defining mechanisms for copper removal by biochar using characterization, equilibrium testing and electrostatic modelling

3.1 Introduction

Heavy metals, such as copper, zinc, and cadmium, are ubiquitous in stormwater and are potentially toxic to aquatic organisms at low concentrations. The removal of these contaminants from stormwater has been a persistent problem in environmental water quality. Highway stormwater runoff is a source of contamination to surface waters inhabited by several species listed as threatened and endangered under the U.S. Endangered Species Act (ESA) (Nason et al. 2011). Extremely low concentrations of dissolved copper (2 µg/L or parts per billion (ppb)) can inhibit the olfactory system of salmon, which reduces the ability of juvenile Coho salmon to navigate and avoid predators (Sandahl et al. 2007). The toxicity of copper is dependent on its bioavailability to organisms. The total concentration of dissolved ionic copper and water chemistry parameters including hardness, pH and organic matter influence copper toxicity (Ryan et. al. 2009). Bioavailability and toxicity of copper are generally limited to free ionic copper (Cu^{2+}) and $CuOH^+$; therefore, remediation is focused on reducing this form of dissolved copper. The primary source of copper in highway stormwater runoff is from automobile brake pads, containing up to 20 percent copper by mass (Legret and Pagotto 1999; Davis et. al. 2001; Rosselot 2006). Because brake pads fabricated with copper are ubiquitous, copper deposition occurs on all roadways and must be treated as a non-point source pollutant. High average daily traffic causes increased copper concentrations in aquatic environments adjacent to urban and high-traffic areas (Nason et. al. 2012). Other nonpoint sources of copper to stormwater runoff include engine oil, lubricating oils, roof runoff, corrosion of building siding, fertilizer, pesticides, industrial releases, and wet and dry deposition (Davis et. al. 2001; Joshi and Balasubramanian 2010).

Green infrastructure such as biofilter strips, bioswales and media filters, generally composed of sand or compost, are increasing in use as best management practices (BMPs) for stormwater treatment (Clary et al. 2017) These treatments are typically designed to mitigate peak flow and reduce total suspended sediment concentrations. Typically, BMPs do not reduce metals concentration below approximately 5 ppb, significantly above the 2 ppb concentration threshold for negatively impacting Coho salmon (Clary et al. 2017) There is a need for low-cost, sustainable solutions for remediation of metals from stormwater. Possible methods for improving

current technologies include mixing adsorptive media with existing media to improve adsorption characteristics or augmenting the system with a downstream adsorptive media filter as a finishing step. In industrial wastewater treatment, granular activated carbon (GAC) has been widely used as an adsorptive media to remove metals before discharging to surface waters. However, the cost of GAC makes it undesirable to implement on the scale needed to address nonpoint source pollution of copper in stormwater. Biochar is a material that has potential for landscape-scale implementation as a low-cost, sustainable adsorbent media for stormwater treatment of metals.

Biochar is created as a byproduct during the conversion of biomass to bioenergy by pyrolysis or gasification. Biomass sources, such as manure, organic wastes, and forest and crop residues are readily available as byproducts of other processes. During pyrolysis or gasification, a fraction of biomass is used for bio-oil, heat and energy production and the remaining fraction is converted to solid biochar. The bio-oil, heat and energy are reused in the pyrolytic or gasification system or used to contribute energy to industry, and biochar can be returned to soil to store carbon for CO_2 sequestration and increase nutrient content (Lehmann 2007). Biochar systems have the potential to advance sustainability through clean, carbon-negative energy production, climate change mitigation, increased plant yield and food security, environmental remediation, and water treatment (Ahmad et al. 2014; Lehmann 2007) For wide-scale implementation of biochar, better understanding of how biochar characteristics relate to favorable performance in each application is needed. In addition, mechanisms for removal of specific contaminants need to be elucidated and linked to biochar characteristics.

Previous work has demonstrated the potential for metals removal by biochar in equilibrium batch experiments, but the mechanisms for removal are not well understood (Ahmad et al. 2014). As such, it is difficult to predict copper removal under varying environmental conditions, including small changes in pH. Typical empirical approaches used to model inorganic ion binding such as partitioning coefficients and isotherm equations are limited to specific solution conditions and are not easily extrapolated to other conditions of pH, ionic strength and competition. Surface complexation models improve equilibrium predictions by considering site binding parameters of surface functional groups and pH effects.

Many surface functional groups, including hydroxyl, carboxyl, carbonyl, amine, amide, alcoholic, phenolic, thiol and phosphate have shown high affinity to form proton and metal

complexes on waste biomaterials (Volesky 2007). However, chelation by carboxyl, phenolic, and carboxyl groups has been widely proposed as the mechanism for metals binding (Witek-Krowiak and Reddy 2013; Ravat et. al. 2000). Sorption of metals on several adsorption medias including: hydrous ferric oxide (Dzombak and Morel 1990; Zhu 2002), calcite (Comans and Middelburg 1987; Zhu 2002), α-Al_2O_3 (Katz and Hayes 1995), granular activated carbon (Gabaldón et al. 1996), and natural organic matter (Ravat et. al. 2000) has been accurately described by surface complexation models. Application of surface complexation modelling to describe the sorption of protons and metals onto biochar is supported by the presence of a variety of surface functional groups on biochar surfaces and the proposed mechanism for metals removal of chelation by surface functional groups.

This research evaluated the effectiveness and sustainability of biochar (compared to GAC) for the remediation of copper in stormwater. Removal of metals by plant remains (Douglas fir chips and hazelnut shells) converted to biochar in specific pyrolytic conditions (300, 500, and 700°C) was evaluated to determine favorable biochar characteristics and mechanisms for metals removal. These adsorbents were selected based on availability, favorable characteristics for adsorption, such as high porosity and presence of surface functional groups, and potential to advance sustainability through green heat and energy production with carbon sequestration. Biochar characterization, metals removal in equilibrium batch testing, and electrostatic modelling were conducted in concert to evaluate the mechanisms for metals removal.

Characterization methods were chosen to investigate properties previously attributed to metals removal and to compare with characteristics frequently reported in literature (Tong et al. 2012; Biniak et. al. 1999; Kim et al. 2012; Zhang and Luo 2014; Chen et al. 2011; Manyà 2012; Regmi et al. 2012). Metal removal by biochar and GAC was evaluated through experimental batch testing of different adsorbent medias. The best performing adsorbent was selected for further testing to determine and model copper sorption over a range of pH. In addition, the presence of natural organic (NOM) was evaluated experimentally to provide information about treatment design in natural systems. Experimental metals removal was described by a surface complexation model using the diffuse layer model (DLM) with two types of binding sites. Elucidating the fundamental removal mechanism will support engineering design of stormwater treatment systems using biochar. The scope of this work focuses on removal of copper in

stormwater; however, understanding primary cation removal mechanisms will contribute to widespread use of biochar in various treatment applications, including removal of other metal and cationic contaminants and treatment of industrial and municipal wastewater, groundwater, drinking water, and soil.

3.2 Materials and Methods

3.2.1 Adsorptive media preparation

Six types of biochar were produced from Douglas Fir chips and hazelnut shells. Feedstocks were ground using a course particle mill and dried in a pre-heated oven overnight at 105 °C. Each feedstock type was pyrolyzed at three different temperatures (300°C, 500°C, and 700°C) in a Muffle Furnace (Thermo Scientific Lindberg Blue M™) for one hour in a N_2 atmosphere, resulting in a total of 6 unique biochar media. The biochar media were named by feedstock type (H-hazelnut shells or D-Douglas Fir chips) followed by the pyrolysis temperature. For example, H700 biochar media, was produced by pyrolyzing the hazelnut shell feedstock at 700°C. Calgon F-400 granular activated carbon (GAC) was selected as a comparative industrial adsorbent.

For characterization and batch testing, the produced biochars and GAC were ground further using a mechanical grinder and sieved to 40-50 mesh particle size (0.3 to 0.4 mm). In this work, "fines" were defined as any particles that passed through the 50 mesh sieve (diameter < 0.3 mm). For characterization of surface area and proximate carbon analysis (PCA), potentiometric titrations, and all batch and kinetic performance testing, 40-50 mesh particle size biochar was used for experiments. For characterization of pH, EPM, and FTIR, biochar fines were used.

3.2.2 Characterization

BET Surface Area The surface area of each biochar sample (40-50 mesh size) was measured on a MICROMERITICS ASAP 2020 using the Brunauer, Emmett, and Teller (BET) method. Sample mass of 0.3 and 0.15 g for hazelnut shell and Douglas fir chip biochars, respectively, was based on media density. The samples were de-gassed at 250 °C in a degassing port.

pH Biochar pH was measured using ISO 10390 (Soil Quality--Determination of pH) (ISO, 2005). For each sample (run in duplicate), five mL of biochar fines and 25 mL of 0.01 M $CaCl_2$ solution were combined into 125 mL HDPE bottles and tumbled for 24 hours. The final pH was measured while stirring using a Fisher Scientific accumet pH probe.

Thermogravimetric analysis (TGA) Thermogravimetric analysis (TGA) was performed on both biomass feedstocks. The feedstocks were heated at a rate of 2°C per minute using a Q500 TGA (TA instruments). Samples mass for Douglas fir chips and hazelnut shells was 0.025 and 0.037 g, respectively. The temperature, time from the beginning of the experiment, and the weight percent remaining were recorded.

Proximate carbon analysis (PCA) Proximate carbon analysis (PCA) was conducted on 0.5 g biochar and GAC samples to measure moisture content, ash content, volatile matter, and fixed carbon by ASTM D 1762-84 (ASTM, 2007) using a Muffle Furnace (Thermo Scientific Lindberg Blue M™).

Fourier Transform Infrared Spectroscopy (FTIR) Fourier Transform Infrared Spectroscopy (FTIR) analysis (Thermo Nicolet) was conducted using fines (< #50 mesh) of each biochar media and GAC to identify surface functional groups. Baseline corrected spectra were analyzed using OMNIC^{TM} Spectra software to identify relevant peaks and the associated chemical functional groups. To better identify or confirm lack of chemical peaks for the high temperature biochar results, further experimentation was conducted using a Thermo-Nicolet iS50 FT-IR instrument equipped with an iTX Attenuated Total Reflectance (ATR) accessory with a diamond window. Absorbance measurements were made for 400 - 4000 cm^{-1} and data was corrected with Advanced ATR Correction before exporting.

Electrophoretic mobility (EPM) An electrophoretic mobility (EPM) study was conducted on H700 and D700 biochar fines (< #50 mesh) to determine the isoelectric point (IEP). EPM was measured as a function of pH using a Zeta PALS instrument (Brookhaven Instruments) equipped with an auto titrator. pH was adjusted with 0.01 and 0.1 M HNO_3 titrant solutions from initial solution pH of ~7 for H700 and ~6 for D700 to pH near 1 to capture the IEP. Biochar fines were suspended in 0.01 M $NaNO_3$ and allowed to settle for 24 hours before sonicating for 1 minute to re-suspend particles and break up aggregates. Sonicated solutions were allowed to settle for 5 minutes and then a small volume (10 mL) of supernatant was diluted to a total volume of 30 mL with fresh 0.01 M $NaNO_3$. Dynamic light scattering (DLS) was performed on all samples to ensure the particle size was within an appropriate range for EPM measurements. DLS from the D700 indicated particles size and spread were too large, so these samples were filtered with a 1 µm glass fiber filter (Pall Acrodisc® 4523T). Filters were washed with 1 L of DDI water prior to filtering samples.

3.2.3 Batch Performance Testing

Synthetic Stormwater Suspensions All batch tests were conducted in a synthetic stormwater solution consisting of 1 mM NaCl, 0.185 mM $NaHCO_3$, and spiked copper ranging between 0-1500 µg/L. The initial pH of solutions used for batch isotherm and kinetic tests was adjusted to 6.0 ± 0.1 using HNO_3 and NaOH. Biochar suspensions (#40-#50 mesh) were added at a solids concentration of 0.5 g/L for all batch tests.

Kinetics Initial copper concentrations of 500 and 1000 µg/L were selected for kinetics testing. Samples were placed in a tumbler and collected after 0, 0.25, 0.5, 0.75, 1, 2, 4, 8, 12, 24, and 48 hours. Each sample was removed from the tumbler and filtered (0.45 µm Millipore™ HAWP04700). The final pH was measured immediately after filtration using a Fisher Scientific Accumet pH probe. Filtered samples were acid digested by adding 100 µL of 70.0% ultrapure nitric acid (HNO_3) to 10 mL of sample. Copper concentration was analyzed using Ametek SPECTRO ARCOS™ inductively coupled plasma optical emission spectroscopy (ICP-OES).

Isotherms Bottles prepared for batch isotherm tests were placed in a tumbler for an equilibrium time of 48-hours based on results from the kinetics testing (Appendix A). Triplicate samples of each initial copper concentration (75, 150, 300, 500, 700, 900, 1100, and 1500 µg/L) were used in batch testing of all 6 biochar media and Calgon F-400 GAC.

SRNOM Isotherms Additional batch testing was conducted on the two higher temperature hazelnut shell biochars, H700 and H500, which were determined to be the most promising based on the initial synthetic stormwater testing. These tests were run using the same synthetic stormwater copper concentrations and were prepared according to the same procedure described above with the addition of 2.8 mg C/L of Suwanee River Natural Organic Matter (SRNOM). Preparation of SRNOM stock can be found in Appendix A.

3.2.4 Surface Complexation Modelling

Diffuse Layer Model (DLM) Surface complexation models offer advantages over other empirical isotherm models because they can predict adsorption under varying conditions of pH, ionic strength, and sorbate/sorbent ratios. These models incorporate both surface reactions described by intrinsic binding constants (K_{int}) and solution interactions through incorporation of an electrostatic term (*Coul.*). The various surface complexation models vary in their physical representation of the solute layer and electrostatic representation. The diffuse layer mode (DLM) is often recommended for modeling removal of heavy metals based on results showing that the

DLM can describe metals adsorption results at different initial concentrations, pH, and ionic strengths with equal accuracy compared to other electrostatic models, while requiring fewer fitting parameters (Dzombak and Morel 1990).

The fundamental concept upon which all surface complexation models are based is that adsorption occurs at a finite number of defined coordination sites and adsorption reactions can be described quantitatively by mass law equations (Dzombak and Morel 1987). Surface adsorption differs thermodynamically from reactions among solutes by the variability of the electrostatic energy of interaction (the coulombic term, *Coul.*):

$$\Delta G_{adsorption} = \Delta G_{intrinsic} + \Delta G_{coulombic} \tag{14}$$

The total Gibbs free energy is separated in to the coulombic term to describe the long-range nature of electrostatic interactions and the intrinsic term to describe the proximity of adsorption sites of varying charge due to sorption reactions. Intrinsic adsorption coefficients (K_{int}) describing intrinsic Gibbs free energy ($\Delta G_{intrinsic}$) are intrinsic with respect to ionic strength and surface charge; however, they are conditional with respect to model selection and parameter fit. Intrinsic adsorption coefficients are interrelated and dependent on the capacities and site densities, which must be considered as a complete set (Robertson and Leckie 1997). Coulombic terms (*Coul.*) describing electrostatic energy of interaction ($\Delta G_{coulombic}$) depend on both the charges of reacting species and neighboring species.

Surface complexation models consider surface charge to develop on adsorbent surfaces via chemical reactions at specific sites. Mass law equations are used to described binding of adsorbates to reactive groups at the surface, where ($= SOH^o$) represents a neutral binding site and $K_{a1}{}^{app}$ represents the apparent bulk proton binding constant:

$$= SOH_2^+ \rightarrow \ = SOH^o + H^+; \ K_{a1}^{app} \qquad K_{a1}^{app} = \frac{(= SOH^o)\{H^+\}}{(= SOH_2^+)} \tag{15}$$

A localized disturbance of electroneutrality occurs when a charged particle enters an aqueous system. The charge disturbance is counteracted by development of oppositely charged electrolyte ions in excess density near the surface of the adsorbent. This separation of charges in the electrical double layer (EDL) causes a potential difference across the surface interface, which is typically small but the thickness of the interphase region is very small, causing a very large electrical field strength which dictates the distribution of nearby ions in solution and affects

transport of ions at the surface (Dzombak and Morel 1987). Classical EDL theory (Gouy-Chapman) accurately describes spatial distribution of counterions near the surface interface:

$$\sigma = 0.1174I^{1/2} \sinh\left(\frac{ZF\Psi_0}{2RT}\right); \; \left(\frac{C}{m^2}\right) \tag{16}$$

Where Ψ_0 represents the surface potential, compared to a reference potential of zero in the bulk solution; R= the gas constant; T= absolute temperature (K); and F = Faraday constant (96,500 C/mol). Under ideal conditions (Gouy-Chapman), the proton concentration at the surface (H_s^+) is related to the bulk solution concentration (H^+) by the expression:

$$(H_s^+) = (H^+) \exp\left(\frac{-F\Psi_0}{RT}\right) \tag{17}$$

The exponential term ($\exp\left(\frac{-F\Psi_0}{RT}\right)$) is an activity coefficient for EDL effects on proton exchange, referred to as an electrostatic or coulombic correction factor (*Coul.*), which accounts for surface charge effects on sorption reactions. The Coulombic correction factor can be applied to mass law equations to determine intrinsic binding constants (K_i^{int}), which are converted to the overall apparent bulk binding constants (K_i^{app}) using the coulombic term (*Coul.*) to represent the electric double layer (Dzombak and Morel 1987):

$$K_{a1}^{int} = \frac{\{=SOH^o\}\{H_s^+\}}{\{=SOH_2^+\}} = K_{a1}^{app}\exp(\frac{-F\Psi_0}{RT}) \tag{18}$$

$$Coulombic\ term\ (Coul.) = exp(\frac{-F\Psi_0}{RT}) \tag{19}$$

Biochar potentiometric titration and pH sorption edge batch results were used to determine proton and copper binding parameters of the diffuse layer model (DLM) using equilibrium chemistry software MINEQL+ (Schecher and McAvoy 1992). First, MINFIT (Xie et. al. 2016), an excel macros program, was utilized to calculate the minimum residual using sum of square error (SSE) between experimental and model total bound hydrogen (the net potentiometric titration) to determine proton binding constants and total site concentrations. Then, copper binding parameters were determined from batch pH sorption edge data using the same procedure. Finally, the DLM parameters determined were used to described five separate H700 batch isotherm results over a range of final equilibrium pH.

Potentiometric Titration Proton binding behavior was quantified using potentiometric titrations of the H700 biochar. The titrations were conducted at a solids concentration of 0.3995 g/L H700 in aqueous solutions with ionic strengths of 1 mM and 10 mM NaNO₃. The titrations were

performed in a N$_2$ atmosphere in a jacketed beaker at 25°C. The net titration was determined by subtracting the total hydrogen needed to titrate background NaNO$_3$ at equivalent concentrations from the total hydrogen needed to titrate the biochar suspension to equal pH (Sposito 1981). The point of zero salt effect (PZSE) was identified as the intersection point of the net potentiometric titrations at different ionic strengths (Parker et al. 1979).

pH sorption edge Batch tests were performed identically to the isotherm tests described with the exception that only two initial copper concentrations were utilized (900 and 1500 µg/L) and pH was varied between 2 and 9. Triplicate samples were prepared at each initial pH and copper concentration. MES buffer was added at 1 mM to samples with initial pH between 6 and 7 because of the large pH changes that occurred in this range. The metals binding model parameters were calibrated by minimizing the sum of squared error (SSE) between the measured and modeled percent copper sorbed at an initial copper concentration of 1500 µg/L. The model parameters were validated by pH sorption edge data at an initial copper concentration of 900 µg/L.

3.3 Results
3.3.1 Characterization Results
Surface Area Biochar surface areas range from 0.5 to 600 m^2/g compared to 1730 m^2/g for GAC (Figure 1). Surface area increased with pyrolysis temperature for both hazelnut shells and Douglas fir; however, the biochars made from Douglas fir wood chips had greater surface areas compared to the hazelnut shell biochar produced at the same temperature.
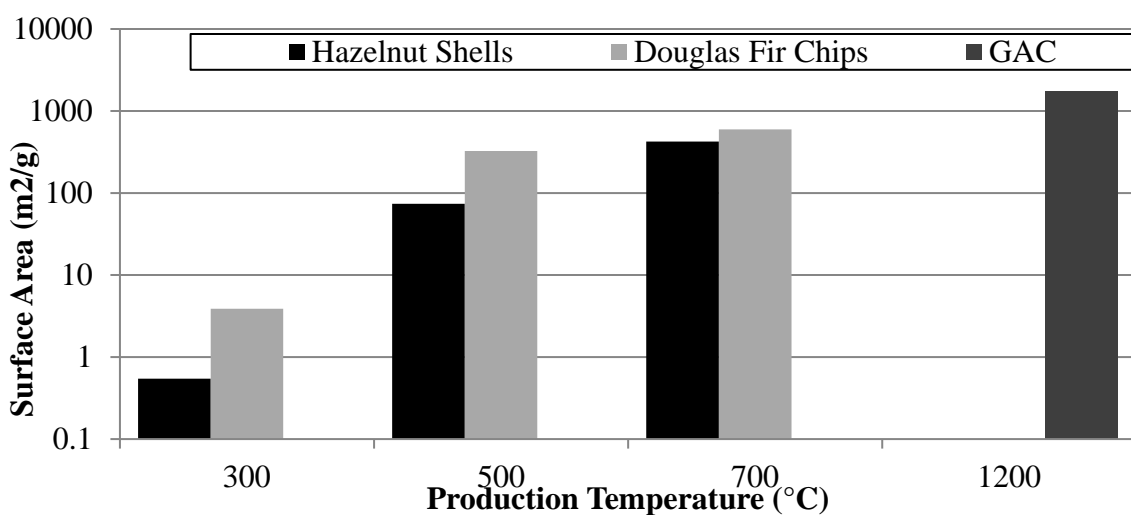
Figure 1 Biochar Surface Area

Biochar pH The average final pH results of duplicate biochar samples are summarized in Figure 2. In general, biochar pH increases with increasing pyrolytic temperature. The only exception to this trend is that the H500 biochar's pH is higher that the H700 biochar's pH. The D300 biochar had a lower pH than the pH of the 0.01 M $CaCl_2$ background solution. Finally, all the hazelnut shell biochars have higher pH than the Douglas fir produced at the same temperature.
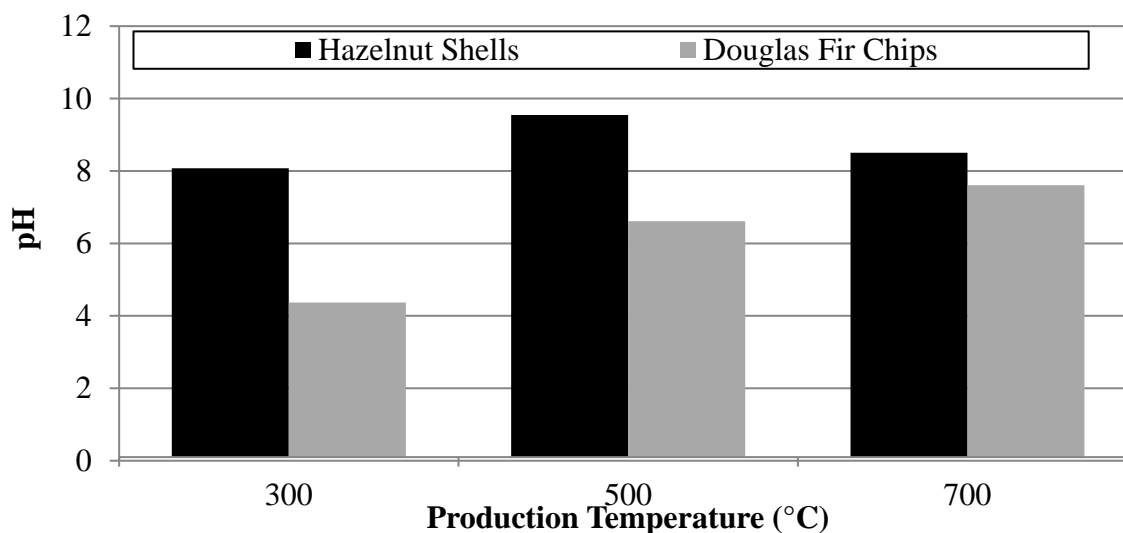
Figure 2 Biochar pH

Thermogravimetric Analysis (TGA) TGA results show both feedstocks lose mass at about the same rate during the same heating period, but the hazelnut shells plateau sooner that the Douglas fir feedstock, resulting in a higher percent remaining for the hazelnut compared to the Douglas fir (Figure 3).
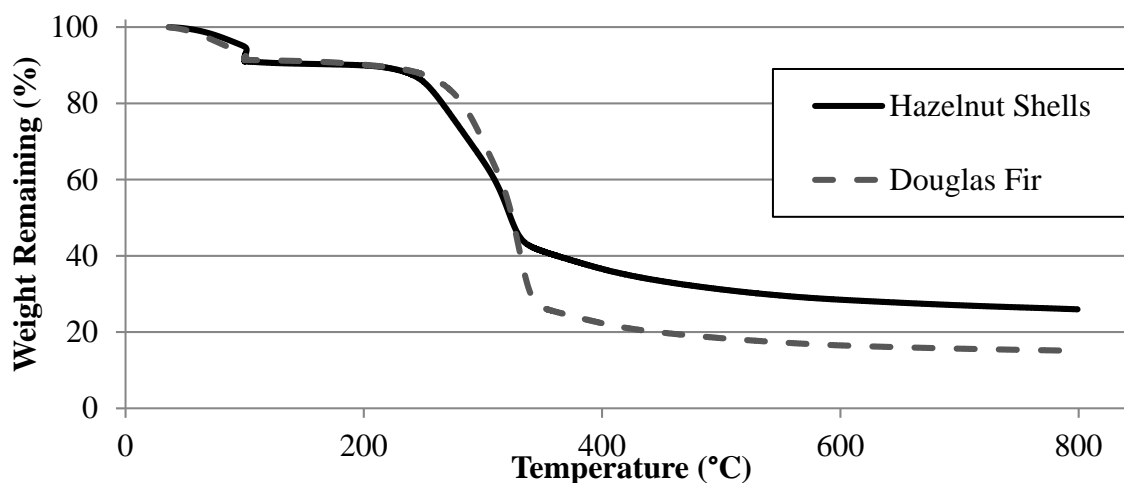
Figure 3 Thermogravimetric Analysis (TGA) - decrease in feedstock mass as temperature increases over time

Proximate Carbon Analysis (PCA) All six biochars and GAC were analyzed by PCA to determine the relative amounts of volatile matter, fixed carbon, and ash (Figure 4). The volatile matter portion of the adsorbent is released first, then the fixed carbon, and the residuals represent the ash content. Both the hazelnut shell and Douglas fir biochars have increasing fixed carbon content and decreasing volatile matter content with increasing pyrolysis temperature. The hazelnut shell biochars had higher fixed carbon content and lower volatile matter content compared with the corresponding Douglas fir chars pyrolyzed at the same temperature.

Additionally, while the hazelnut chars have an ash content of around 2% or higher, the Douglas fir biochars have less than 1% ash content. Ash content does not appear to be largely affected by the pyrolysis temperature of the biochar for either the hazelnut shells or Douglas fir biochars, which is expected for the low-level ash content observed for these wood-based feedstocks. The hazelnut shell biochar ash content ranges from 1.97%-2.9% and the Douglas fir biochar has a range of 0.3%-0.66%, compared to 7.3% for GAC.
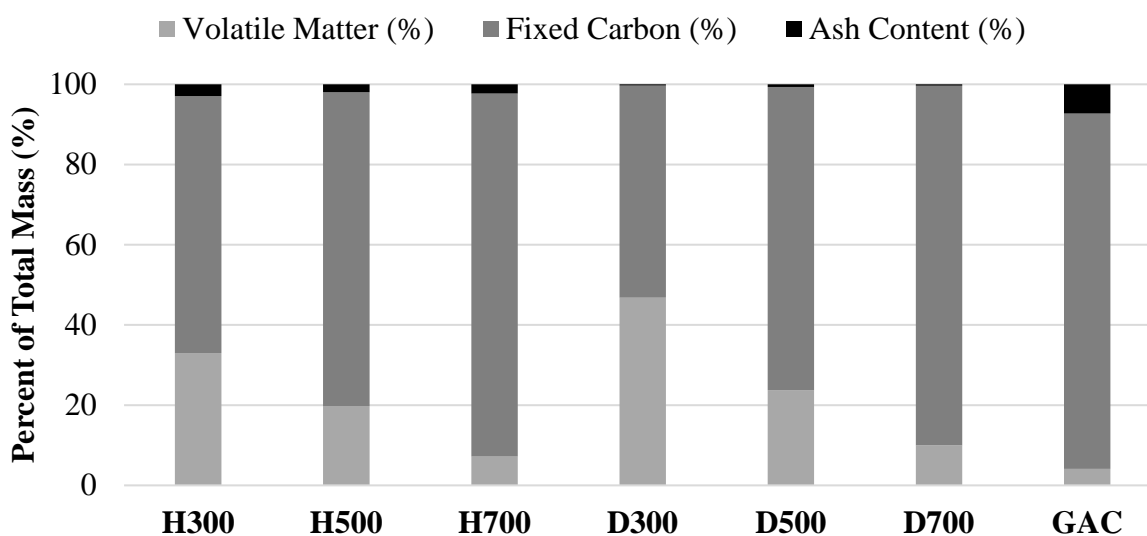
Figure 4 Proximate Carbon Analysis (PCA) results for six biochars and GAC

Functional Group Analysis-Fourier Transform Infrared Spectroscopy (FTIR)

As expected from literature, the number of functional groups measured by FTIR analysis decreases with increasing pyrolysis temperature (Figures 5 and 6). The functional groups found by the IR Spectral Interpretation database from the IR peaks measured for the Douglas fir chip and hazelnut shell biochars are shown in Tables 1 and 2, respectively. The software could not find any matches for the peaks displayed for D700. The phenols and ethers that are present in the

D300 biochar are not present in D500 biochar, likely due to the volatilization between 250-350°C as seen in TGA. The aliphatic amino acids were present in both the D300 and D500 biochars. The sharp peak around 1700 cm^{-1} indicating C=O groups is present for both the D300 and D500 chars, but does not occur in the D700 char. For the D500 char, there were additional IR peaks at the wavenumbers which correspond to inorganic sulfates, which were not present in the D300 char. The broad peak located between 2150-4000 cm^{-1} increases in size as the pyrolysis temperature increases, indicating increasing number of aliphatic carbon groups.

For the hazelnut shell biochar FTIR results, aliphatic hydrocarbons are present for all three different pyrolysis temperatures and are the only functional group in the H700 char. The H500 char has inorganic carbonate groups which are not present in either the lower temperature H300 char or the higher temperature H700 char. This mirrors trends observed for D500 biochar but for inorganic carbonate instead of inorganic sulfates. These groups are potentially formed as an intermediate product during pyrolysis above 300°C (while the majority of volatiles are released around 300-400°C), but below 700°C. Above 500°C, the inorganic carbonate groups (H500) and inorganic sulfates (D500) also volatilize, leaving only aliphatic hydrocarbons (H700) or no detectable functional groups (D700) at 700°C. This temperature dependent formation describes the detection of inorganic carbonates on H500, but not the H700 or H300.
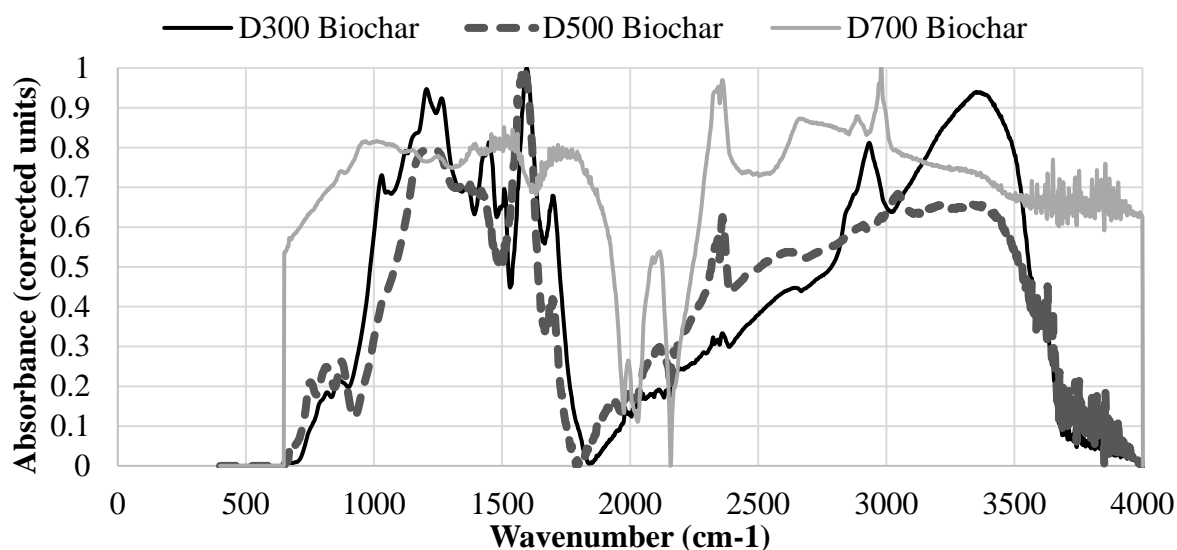
Figure 5 FTIR results for Douglas fir chip biochars

Table 1 FTIR peaks and functional groups for Douglas fir chip biochars (D300 and D500)

Douglas Fir Biochar IR Spectra Peaks				
IR Spectral Analysis Database		Literature Functional Group Analysis		
Experimental Peak Wavenumber Range (cm^{-1})	Database Compound Groups	Literature Wavenumber range (cm^{-1})	Characteristic Vibrations	Functionality
D300 Biochar Peaks				
1180-1265	Phenols	~1200	C-O stretch	Phenol*
3250-3600		3530-3640	O-H stretch	Phenol*
1220-1270	Aromatic Ethers	1230-1270	C-O stretch	C-O-C groups and aryl ethers**
1590-1630	Aliphatic Amino Acids	1580-1615	Aromatic ring stretch	Aromatic amino acid*
2500-3200		~2885, ~2935, ~3050, ~3200	C-H stretch	likely aliphatic CH$_x$**
1340-1380	Aliphatic Hydrocarbons	1330-1350	Methyne C-H bend	Saturated aliphatic group*
1440-1480		1445-1485	Methylene C-H bend	Saturated aliphatic group*
2830-2970		2860-2880, 2845-2865, 2915-2935, 2950-2970	C-H asym/sym stretch (Methyl or Methylene)	Saturated aliphatic group*

IR Spectral Analysis Database		Literature Functional Group Analysis		
Experimental Peak Wavenumber Range (cm⁻¹)	**Database Compound Groups**	**Literature Wavenumber range (cm⁻¹)**	**Characteristic Vibrations**	**Functionality**
D500 Biochar Peaks				
~1400	Aliphatic Amino Acids	~1440	C=C stretch	aromatic C, indicative of lignin, appears when bound to unsaturated group**
~1500		~1510	C=C stretch	aromatic skeletal vibrations, indicative of lignin**
~1600		~1600	C=C stretch	aromatic components**
2840-2970		2860-2880, 2845-2865, 2915-2935, 2950-2970	C-H asym/sym stretch (Methyl or Methylene)	Saturated aliphatic group*
980	Inorganic Sulfates	-	-	-
1050-1200		1080-1130	-	Sulfate ion*
3300-3600		-	-	-

* denotes the source as (Coates and Ed 2000).

** refers to an EPA document assigning characteristic vibrations to individual peaks in wood and grass char ATR FT-IT spectra.

'- ' denotes that a specific functional group determined by the IR Spectral database that was not able to be confirmed using the other two literature sources specified above.
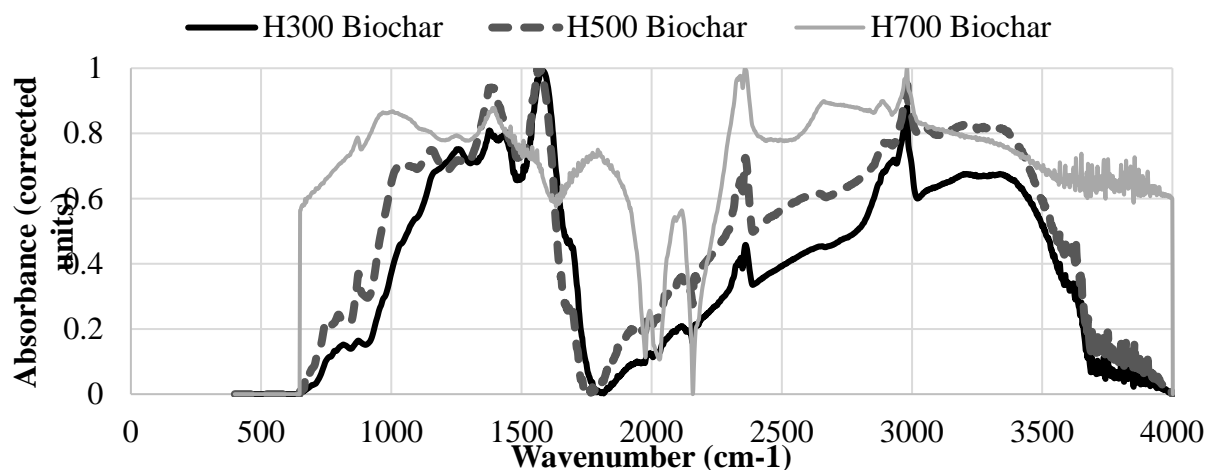
Figure 6 FTIR results for hazelnut shell biochars

Table 2 FTIR peaks and functional groups for hazelnut shell biochars

Hazelnut Shell Biochar IR Spectra Peaks				
IR Spectral Analysis Database		Literature Functional Group Analysis		
Experimental Peak Wavenumber Range (cm⁻¹)	Database Compound Groups	Literature Wavenumber range (cm⁻¹)	Characteristic Vibrations	Functionality
H300 Biochar Peaks				
780-870	Aliphatic Primary Amines	~750, ~815, ~885	C-H bending	aromatic CH out-of-plane deformation**
1070-1095		1020-1090	C-N stretch	primary amine*
1570-1630		1590-1650	N-H bend	primary amine*
3270-3295		-	-	-
3310-3330		3325-3345	N-H stretch	Aliphatic primary amine*

IR Spectral Analysis Database		Literature Functional Group Analysis		
Experimental Peak Wavenumber Range (cm⁻¹)	Database Compound Groups	Literature Wavenumber range (cm⁻¹)	Characteristic Vibrations	Functionality
H300 Biochar Peaks (Continued)				
~750	Aliphatic Hydrocarbon	~750	C-H bending	aromatic CH out-of-plane deformation**
~1380		1380-1385	*gem*-Dimethyl or "iso"-doublet	Saturated aliphatic methyl group*
~1460		1445-1485	Methylene C-H bend	Saturated aliphatic group*
2840-2960		2860-2880, 2845-2865, 2915-2935, 2950-2970	C-H asym/sym stretch (Methyl or Methylene)	Saturated aliphatic group*
H500 Biochar Peaks				
~700	Inorganic carbonate	-	-	-
~900		860-880	-	Carbonate ion*
1300-1500		1410-1490	-	Carbonate ion*
~2500		-	-	-
3200-3560		3200-3500	O-H stretch	H-bonded hydroxyl groups**

IR Spectral Analysis Database		Literature Functional Group Analysis		
Experimental Peak Wavenumber Range (cm⁻¹)	Database Compound Groups	Literature Wavenumber range (cm⁻¹)	Characteristic Vibrations	Functionality
H500 Biochar Peaks (Continued)				
1400-1450	Aliphatic Carboxylic Acid Salts	1300-1420	-	Carboxylate*
1560-1580		1550-1610	-	Carboxylate*
~750	Aliphatic Hydrocarbons	~750	C-H bending	aromatic CH out-of-plane deformation**
~1360		1365-1370	*gem*-Dimethyl or "iso"-doublet	Saturated aliphatic methyl group*
~1450		1445-1485	Methylene C-H bend	Saturated aliphatic group*
2850-2950		2860-2880, 2845-2865, 2915-2935, 2950-2970	C-H asym/sym stretch (Methyl or Methylene)	Saturated aliphatic group*
H700 Biochar Peaks				
~750	Aliphatic Hydrocarbon	~750	C-H bending	aromatic CH out-of-plane deformation**
~1360		1365-1370	*gem*-Dimethyl or "iso"-doublet	Saturated aliphatic methyl group*

IR Spectral Analysis Database		Literature Functional Group Analysis		
Experimental Peak Wavenumber Range (cm⁻¹)	Database Compound Groups	Literature Wavenumber range (cm⁻¹)	Characteristic Vibrations	Functionality
H700 Biochar Peaks (Continued)				
~1450	Aliphatic Hydrocarbon	1445-1485	Methylene C-H bend	Saturated aliphatic group*
2850-2950		2860-2880, 2845-2865, 2915-2935, 2950-2970	C-H asym/sym stretch (Methyl or Methylene)	Saturated aliphatic group*

FTIR-ATR FTIR analysis was repeated for six types of biochar and GAC using an attenuated total reflectance (ATR) attachment (Figure 7-9). The purpose for repeating the experiment was to improve the interpretation of the broad spectrum results for the high temperature biochars.
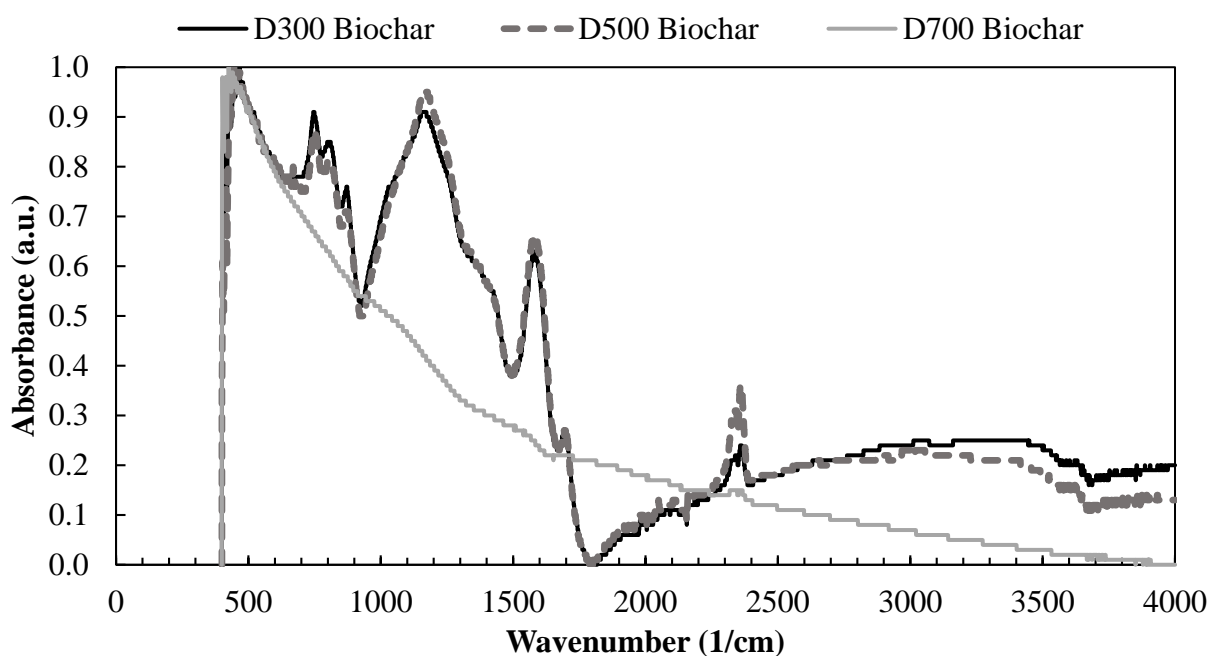
Figure 7 FTIR-ATR results for Douglas fir chip biochars
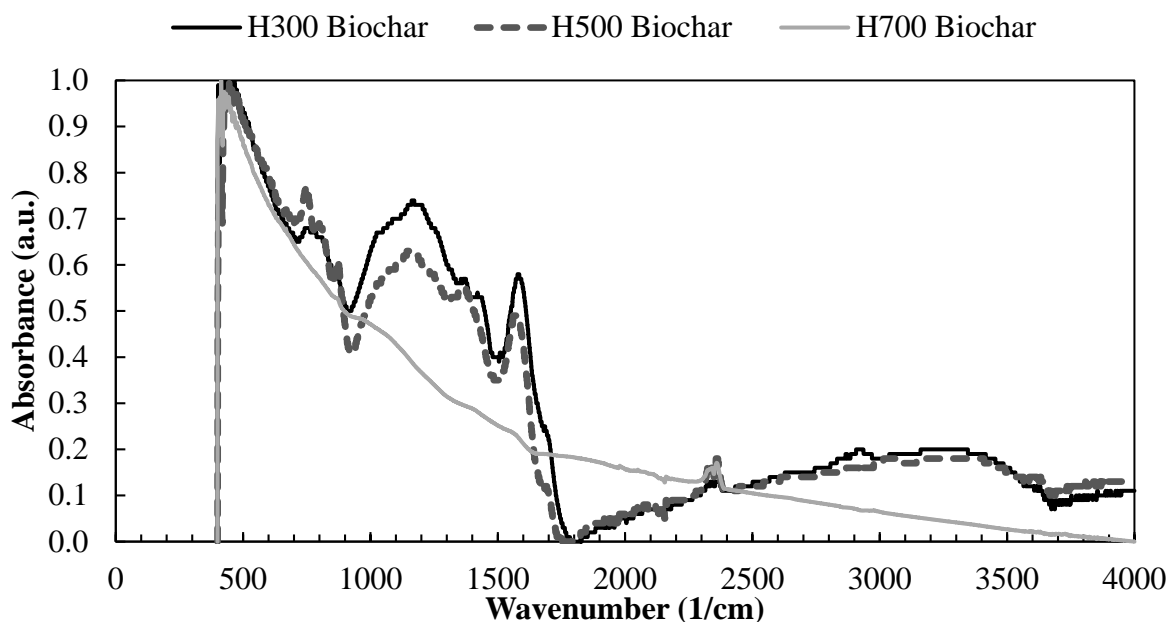
Figure 8 FTIR-ATR results for hazelnut shell biochars
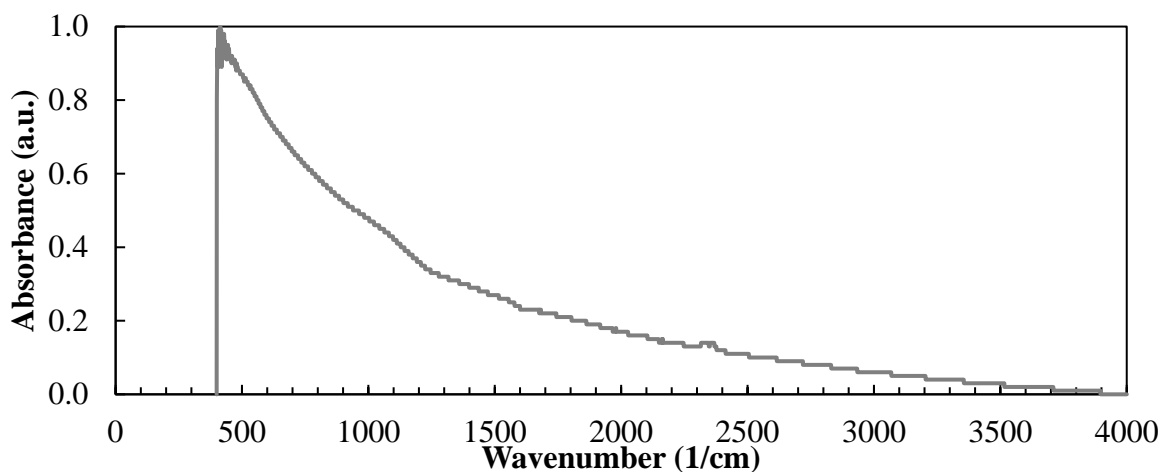
Figure 9 FTIR-ATR results for GAC

For the high temperature chars (H700 and D700), the FTIR-ATR results show no identifiable peaks that would correspond to surface functional groups, confirming the FTIR results without the ATR attachment. The small peak around 2400 cm-1 is from ambient CO_2. The GAC FTIR-ATR results also showed no presence of functional groups. Release of functional groups is expected during high temperature production (~1200°C) of activated carbons.

Electrophoretic Mobility (EPM) EPM testing was conducted with H700 and D700 to evaluate the surface charge of each material. Figures 10 shows triplicate mobility results these chars.
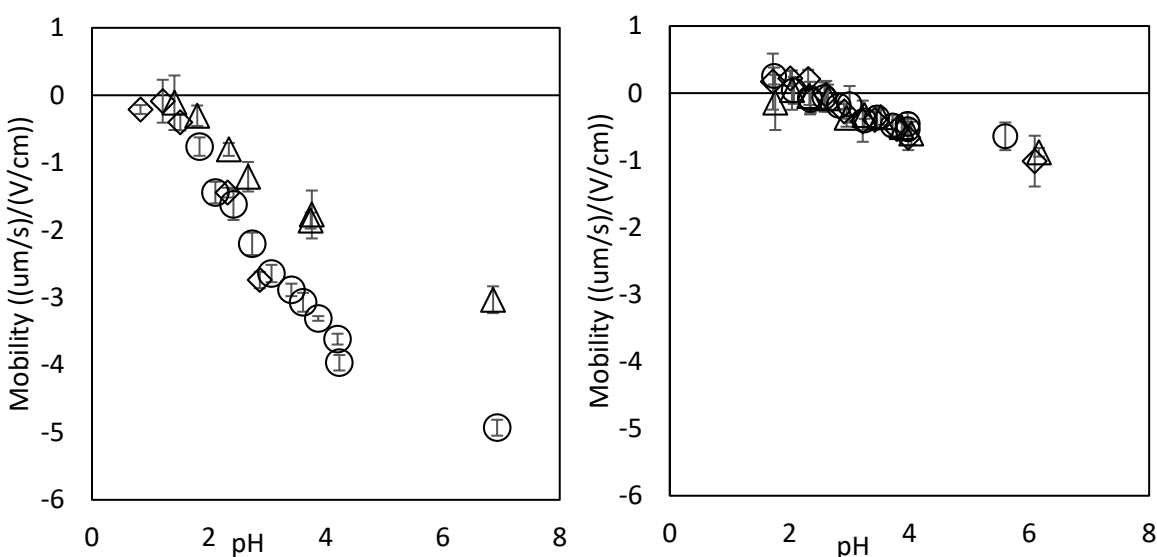
Figure 10 Triplicate EPM results for H700 (left) and D700 (right) fines. Error bars represent standard deviation of 5 measurements at each condition

The three titrations of H700 all show an isoelectric point (IEP) around pH = 1 and a negative surface charge for all higher pH values, indicating a high affinity for positively charged metals ions. The IEP was determined through linear extrapolation. The third experiment had a lower mobility over the entire pH range. This could be a result of a larger average particle size since the sample was extracted last; however, the general trends remained the same. The triplicates for the D700 char agree closely, showing a, IEP around a pH of 2.5 and a negative surface charge at higher pH values, again indicating a high affinity for positively charged metals ions. In addition to IEP at lower pH, H700 surface has more negative electrophoretic mobility at all pH values.

3.3.2 Batch Testing Results

Batch Isotherm Testing An equilibrium time of 48 hours was determined for batch experiments based on kinetics results (Appendix A). Figure 11 shows the experimental batch equilibrium data for the Douglas Fir and hazelnut shell biochars and GAC. Comparing equilibrium results, the H700 char has the highest capacity for adsorption of all the adsorbent medias tested, with the greatest maximum solid copper concentration (q_e). The H500 biochar has the second highest maximum q_e concentration. Both the H500 and H700 are the most promising out of all the biochars due to their high maximum sorption capacity and steep slope, related to copper binding

affinity. These two hazelnut shell biochars have higher maximum copper sorption capacity compared to the GAC, which plateaus near maximum sorption for D500 and D700.
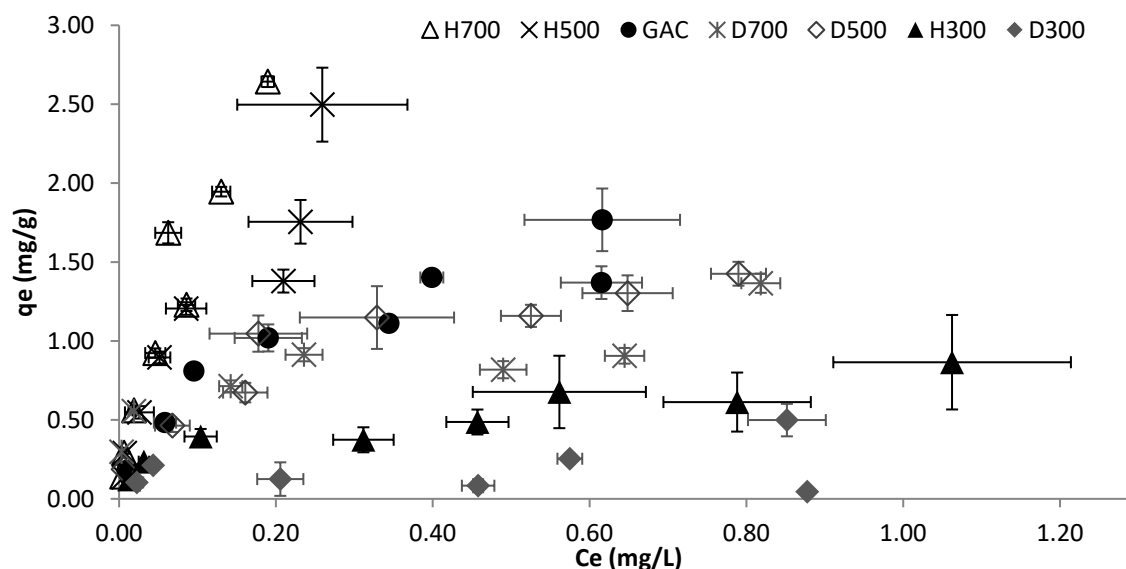
Figure 11 Batch isotherm results for GAC and biochars. Error bars show standard deviation of triplicate samples. Legend is organized from high to lowest maximum solid copper concentration (q_e).

The hazelnut shell biochar removed more copper per gram of material compared to the Douglas fir biochar produced at equal temperature. The batch test results for the higher temperature biochars (H700 and H500) indicates that they have significantly better copper adsorption than the H300. At initial copper concentrations closest to those measured in stormwater (between 9.08 μg/L and 40.9 μg/L) the H700 and H500 biochars performed the best according to percent copper removed from aqueous phase during the 48-hour equilibrium time for the batch isotherm experiments. The high temperature hazelnut shells (H700 and H500) achieved greater removal of copper compared to GAC, D700, and D500, which perform similarly in this copper concentration range.

Final equilibrium pH of the batch isotherm experiments (initial pH of 6.0) are compared for the six biochar medias, GAC, and H500 and H700 medias with SRNOM in Figure 12. All three hazelnut shell biochars had higher final pH (6.4 - 6.7) during batch experiments compared to the Douglas fir chip biochars final pH (6.0 – 6.2). The addition of SRNOM slightly increased the final pH of the batch experiments compared H500 and H700 in synthetic stormwater without dissolved organic carbon. The final average pH (6.6) of the GAC batch experiments was lower than H700, but higher than the other biochars' final pH.
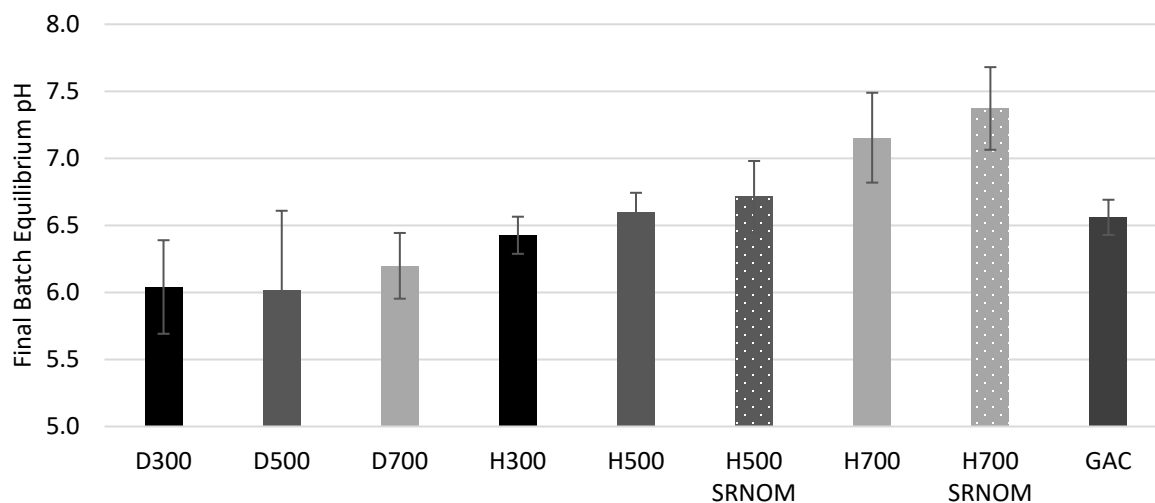
Figure 12 Final Equilibrium pH of batch isotherm experiments. Error bars represent standard deviation of triplicate samples.

H700 was determined to be the most effective media for copper removal under environmentally relevant concentrations and was reevaluated in subsequent batch isotherm experiments. However, a strong correlation was observed between final pH and copper removal, despite all experiments having an initial pH of 6. The H700 batch experiments conducted at the same time as the other biochars and GAC had average final pH of 7.4 (final pH Figure 12, results Figure 11). Successive tests over a period of 24 months had an average final pH for H700 of 8.8 and 6.9 (Figure 13), which could indicate surface aging, but mechanisms controlling variable final batch equilibrium pH are unclear.
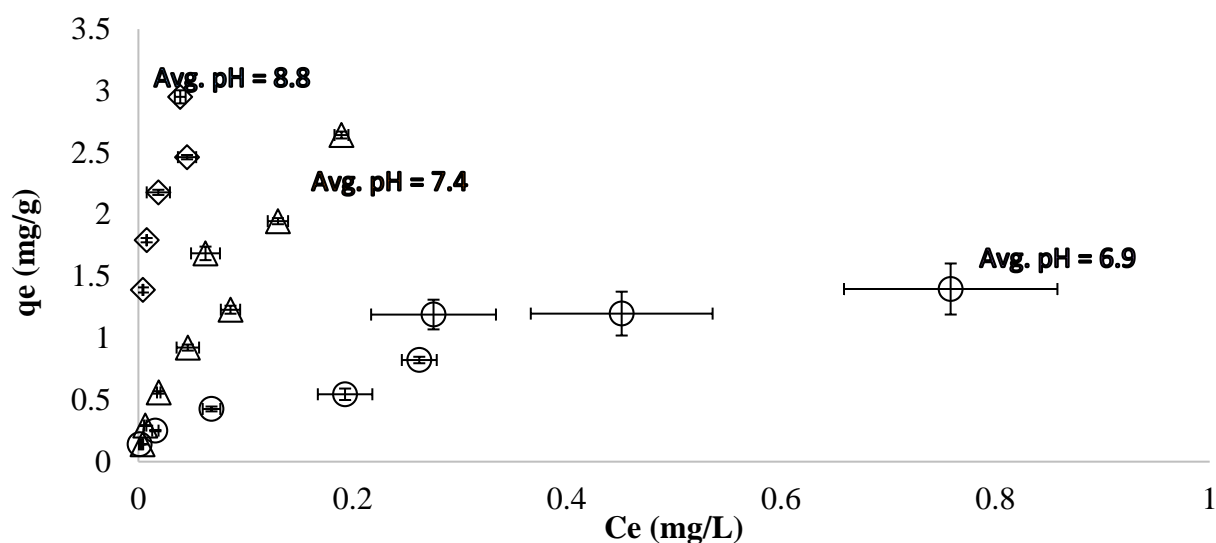
Figure 13 Batch isotherm results of hazelnut shell biochar produced at 700°C (H700) with final average equilibrium pH of 6.9, 7.4, and 8.8

Batch Isotherm Testing including SRNOM The H700 and H500 biochars performed the best for copper removal in synthetic stormwater and were evaluated in additional batch tests with added Suwanee River Natural Organic Matter (SRNOM) to more accurately replicate the NOM that would be present in stormwater. Figure 14 shows the differences between both biochars with and without SRNOM. The slope of the isotherm data and maximum solid copper concentration (q_e) were decreased when NOM was added, resulting in decreased copper sorption in the presence of NOM. The addition of SRNOM produced the same effect on the H700 and H500 biochar isotherm results. Addition of SRNOM masked the performance differences of the H500 and H700 biochars, resulting in equal performance for both biochars when NOM was present.
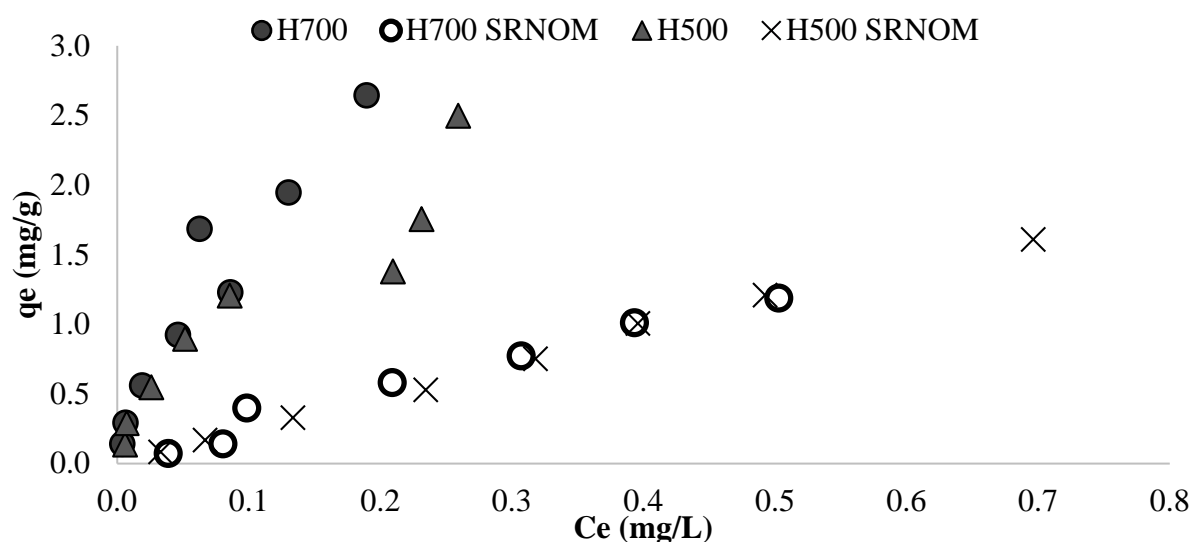
Figure 14 H500 and H700 Batch Isotherm Comparison with and without SRNOM

3.3.3 Surface Complexation Modelling

The diffuse layer model (DLM) with two discrete types of binding sites (strong and weak binding affinities) was employed to represent proton binding by H700 biochar. Strong and weak discrete binding sites correspond to increased binding affinity at low and high pH, respectively. MINEQL+ and MINFIT were used to employ the DLM to fit potentiometric titration and copper pH sorption edge results.

Potentiometric Titration MINFIT and MINEQL+ were implemented to model potentiometric titration results to calibrate proton binding parameters at 1 mM background $NaNO_3$ concentration. Experimental net potentiometric titrations and diffuse layer model fit are shown in Figure 15. The model accurately describes proton binding of the validation potentiometric

titration data at 10 mM background ionic strength. The point of zero charge (PZC) of 8.48 was determined as the intersection of the 2 net titrations at different ionic strength. This represents the pH at which the biochar suspension has neutral charge and above this pH biochar surface is negative, and therefore attracts cations for sorption.

The PZC (8.48) determined from potentiometric titration differs significantly from the isoelectric point (IEP) near 1.0 determined from electrophoretic mobility titration. While the IEP and PZC seem to represent similar surface characteristics, it has been argued that the IEP represents the external surface charges of the materials while the PZC includes both external and internal (pore-related) surface charges (Corapcioglu and Huang 1987; Menendez et al. 1995). How these concepts should be applied to biochar is not clear (Mukherjee et al. 2011). The PZC determined for H700 biochar fits within the PZC range (7.14 to 8.54) determined for three sewage sludge biochars (Lu et al. 2013).The difference (PZC minus IEP) can be interpreted as a measure of surface charge distribution of porous carbons (Menendez et al. 1995). The IEP of various activated carbons has been reported to range from 1.4 to 7.1, indicating that most activated carbons carry a negative charge below neutral pH (Babić et al. 1999; Menendez et al. 1995) . However, there is a lack of IEP and PZC data on biochars to understand of their variability among different biochars (Mukherjee et al. 2011).
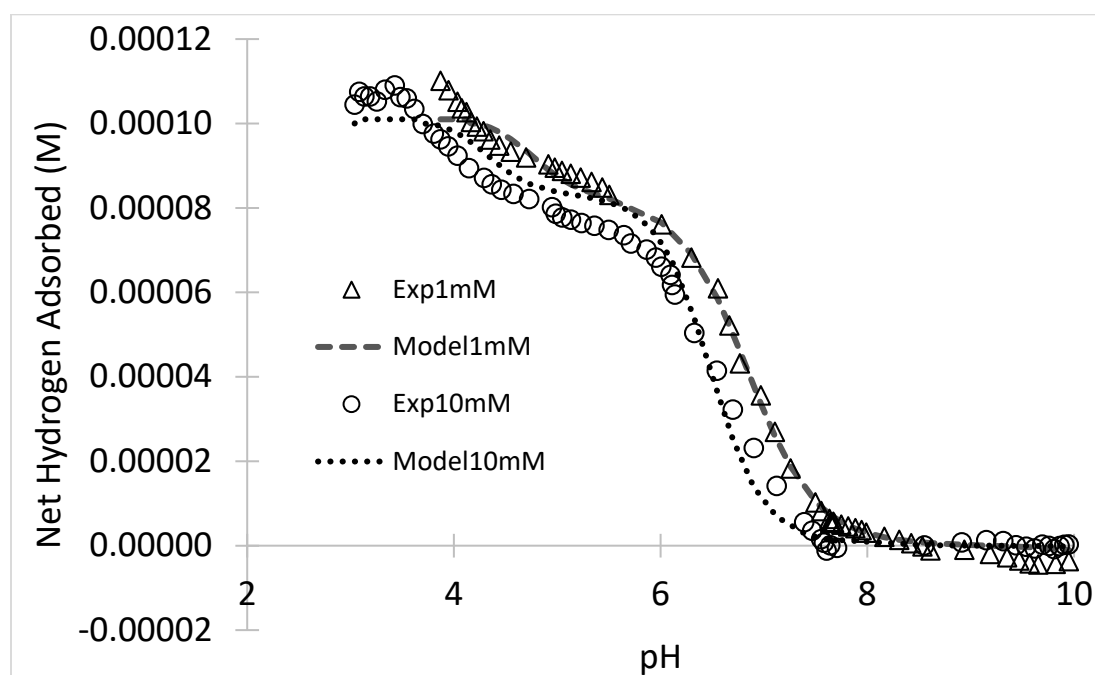
Figure 15 Experimental and model net potentiometric titrations of H700 biochar in 1 mM (calibration) and 10 mM (validation) background $NaNO_3$

The total number of sites were determined to be 0.032 sites/nm^2 (9 x 10^{-6} M) of low pH sites with intrinsic pK_a of 4.0 for monoprotic and 5.9 for diprotic sorption, and 0.15 sites/nm^2 (4.2 x 10^{-5} M) of moderate pH sites with intrinsic pK_a of 6.8 for monoprotic and 7.1 for diprotic sorption (Table 4). These pK_a values correspond to the range for carboxylic (low pH) and laconic and aldehyde-phenolic (moderate pH) functional groups and maximum sorption capacity in the experimental potentiometric titrations.

Acidity equilibrium constant (pK_a) of carboxylic acids range from 2.5 to 5.05 (Namazian and Halvani 2006) which represent the strong binding site type incorporated in the DLM (pK_a 4.0). The pK_a value for phenol is 10.0, and pK_a of phenolic groups of industrial lignins have been reported as 11.0 (soda lignin), 10.9 (sulphate lignin) 10.5 - 11.0 (kraft lignin), and 11.5 (kraft lignin (Indulin-AT)) (Ragnar et al. 2000). However, the pK_a -values for different lignin-related phenolic groups have no typical value, and range between 6.2 and 11.3 depending on the substitution pattern. The acidity of the phenolic group decreases when the oxidation state of the *para*-substituent is changed in the order methyl > hydroxymethyl > acid >> aldehyde (Table 3). In addition, the elongation of a carbon chain from 1 to 2 or 3 carbon atoms generally decreases the pK_a -value (Ragnar et al. 2000). Aging of materials must also be considered, as light-induced excitation of phenols leads to much lower pK_a values (Ragnar et al. 2000). The α-carbonyl function in vanillin strongly lowers the pK_a value, due to the electron-withdrawing effect of the carbonyl function. The pK_a differences due to *para*-substituent group follow the same pattern but with diminished effects as carbon chain is elongated and the functionality is conjugated with the aromatic ring (Ragnar et al. 2000). Aldehyde substituted phenolic groups represent the pK_a (7.4) of the moderate strength DLM binding sites. Conjugation by fixed carbon aromatic structure of H700 biochar is expected to further reduce aldehyde-phenolic pK_a, consistent with DLM fitting parameter (pK_a 6.8).

Carboxyl and low pK_a phenols have been identified on biochars using Bohem titration techniques (Jiang and Xu 2013). Bohem titrations use $NaHCO_3$ neutralization to identify carboxyl groups (the strong acid fraction), Na_2CO_3 neutralization to identify lactones, lactols, and low pK_a phenols (the moderate acid fractions), and NaOH neutralization to identify high pH phenols and any other weak acid components (Boehm 1994; Chun et al. 2004). Bohem titration has been used to quantify carboxyl (strong), low pK_a phenols and lactone hydrolysis products (moderate), and high pK_a phenols (weak) surface functional groups on soybean, crop straw, and

pine needle derived biochar (Ahmad et al. 2013; J. Jiang and Xu 2013; Rajapaksha et al. 2018; Vithanage et al. 2015).

Table 3 The phenolic pK_a-values of *ortho*-methoxyl compounds based on *para*-substituent. Adapted from (Ragnar et al. 2000)
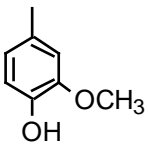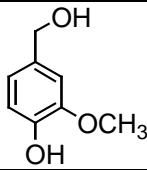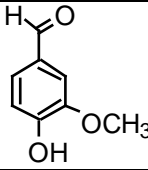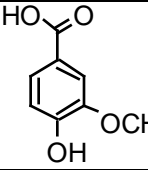
Compound Name	Creosol	Vanillyl alcohol	Vanillin	Vanillic acid
Structure				
Para-substituent	CH_3	CH_2OH	CHO	COOH
Para-substituent	Methyl	Hydroxymethyl	Aldehyde	Acid
Phenolic pK_a	10.27	9.78	7.40	9.39

Table 4 DLM parameters for proton and copper binding

| | | Type I Components in MINEQL+ | | | | |
| | | (st)OH | (wk)OH | | | | |
		strong (low pH) sites	weak (high pH) sites	H^+	Cu^{2+}	Coul.	Log Kint
Proton Binding	$(st)OH_2^+$	1	0	1	0	1	4.0
	$(wk)OH_2^+$	0	1	1	0	1	6.8
	$(st)OH_3^{2+}$	1	0	2	0	2	9.9
	$(wk)OH_3^{2+}$	0	1	2	0	2	13.9
	$(st)O^-$	1	0	-1	0	-1	-11.2
	$(wk)O^-$	0	1	-1	0	-1	-11.2
Copper Binding	$(st)OHCu^{2+}$	1	0	0	1	2	6.4
	$(wk)OHCu^{2+}$	0	1	0	1	2	5.3
	$(st)OCu^+$	1	0	-1	1	1	-1.3
	$(wk)OCu^+$	0	1	-1	1	1	-1.3
	$(st)OCuOH$	1	0	-2	1	0	-8.7
	$(wk)OCuOH$	0	1	-2	1	0	-8.7
	$(st)O\ Cu\ (st)O$	2	0	-2	1	0	3.6
	$(wk)O\ Cu\ (wk)O$	0	2	-2	1	0	-1.6
	Total Conc (M)	0.000009	0.000042	Exp.	Exp.	DLM	
	Surface Area (m²/g)	423	423				
	Total Sites (mol/g)	2.3E-05	1.1E-04				
	Total Sites (sites/g)	1.4E+19	6.3E+19				
	Total Sites (sites/nm²)	0.032	0.150				

pH sorption edge Copper binding parameters were calibrated by fitting pH sorption edge data at an initial copper concentration of 1500 ppb (Figure 16). Intrinsic copper binding constants (log K_{int}) are summarized in Table 4 The K_{int} copper binding parameters were validated with the pH sorption edge data at an initial copper concentration of 900 ppb (Figure 17). The DLM accurately describes copper sorption above pH 5 for the validation data. The low slope and spread of the experimental sorption data between pH 2 and 4 indicate that a spectrum of site types may be available in this range. The two-site DLM accurately describes the capacity for sorption and accurately predicts sorption at different copper concentration over the environmental pH range of interest, above pH 5.
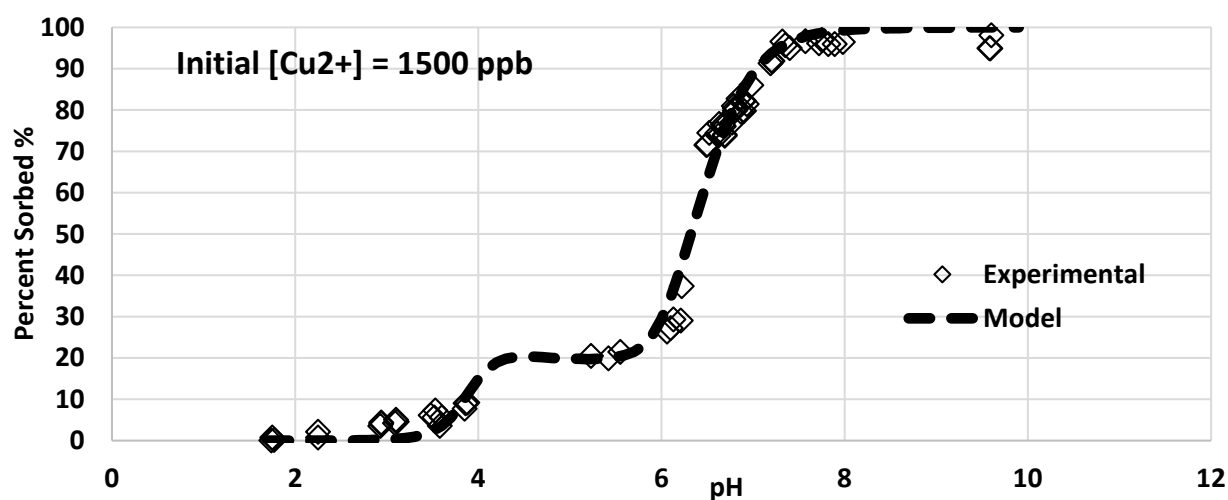
Figure 16 Calibration pH sorption edge of H700 biochar. Batch percent copper sorbed versus final pH. Initial copper concentration of 1500 ppb.
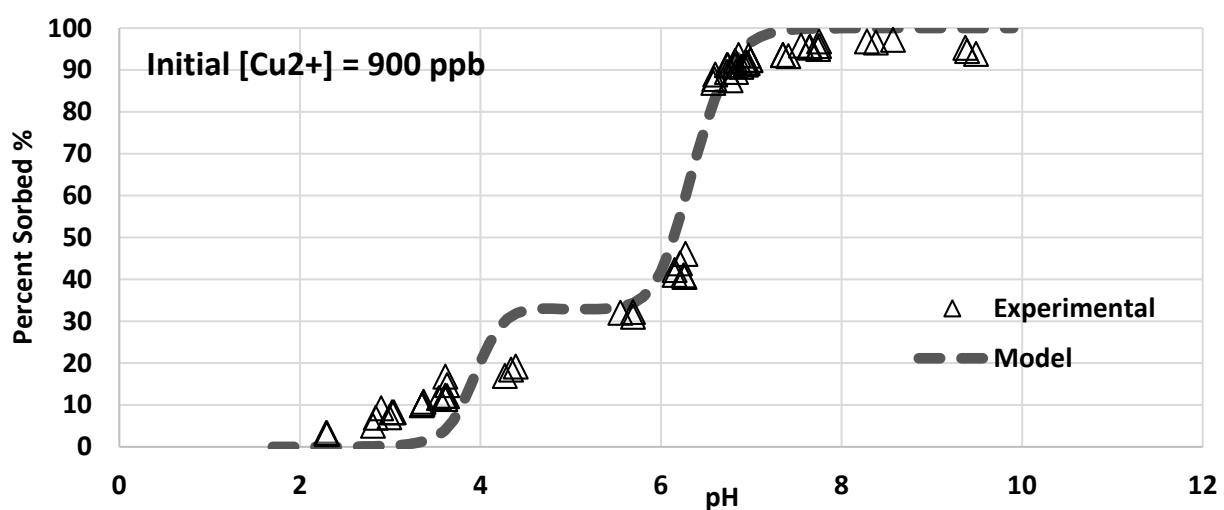
Figure 17 Validation pH sorption edge of H700 biochar. Batch percent copper sorbed versus final pH. Initial copper concentration of 900 ppb.

DLM Model Validation Describing Isotherm Data at Varying pH

The DLM parameters determined were used to describe 5 sets of batch H700 isotherm results with initial pH 6 and a range of final equilibrium pH. This batch isotherm data cannot be described by a single empirical isotherm model (Figure 13). The two-site DLM with parameters determined from pH sorption data and potentiometric titrations accurately describes sorption which can be expressed as percent copper sorbed versus final pH (Figure 18).
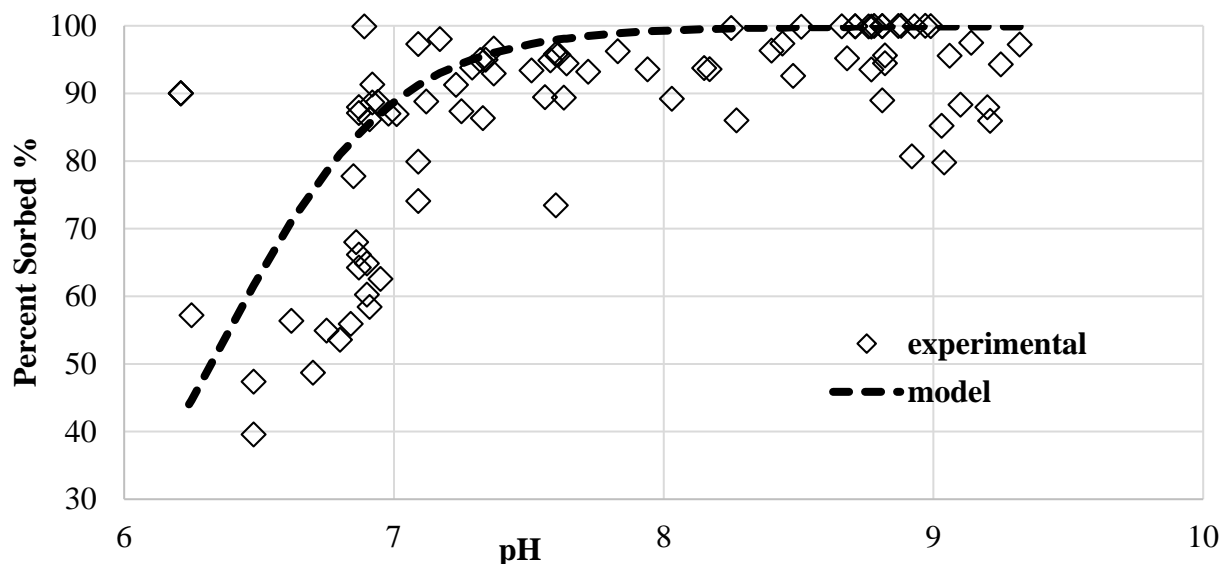
Figure 18 H700 Batch Isotherm shown as percent copper versus final pH

3.4 Discussion

The fact that biochar pH increases with increasing temperature can be attributed to more organic acids being volatilized from the biochars as the pyrolysis temperature increases, which is also observed in TGA where greatest loss of mass occurs between 250 and 250°C. The D300 biochar has a lower measured pH than the pH of the 0.01 M CaCl$_2$ solution, indicating release of acidic functional groups from the surface of this low temperature biochar. Additionally, all the hazelnut shell biochars have higher pH than the Douglas fir produced at the same temperature. In concert with batch performance testing, this data supports the correlation between higher biochar pH and increased copper adsorption due to less competition between copper and protons for available biochar sorption sites.

Surface area increased with pyrolysis temperature for both hazelnut shells and Douglas fir, corresponding to greater metals removal with higher production temperature and surface area. However, the biochars made from Douglas fir wood chips had greater surface areas

compared to the hazelnut shell biochar produced at the same temperature. This is likely due to the wood chips being a more porous feedstock than the hazelnut shells and this property carried over to the biochar when the feedstock was pyrolyzed, observed as differences in media bulk density. Although higher surface area is generally correlated to better copper adsorption in biochars, the higher surface areas for the Douglas fir did not result in increased copper removal compared to the hazelnut shell. Interestingly, the GAC has much higher surface area than any of the biochars tested but does not perform as well as the H700, D700, and H500. These results indicate that while surface area corresponds to increased metals removal for the same type of feedstock and production method, surface area alone is not an adequate indicator of metals removal performance. Pore structure, size, and accessibility must also be considered when relating surface area to sorption performances, as nanoscale pores within the biochar structure may not be available to containments for sorption. The combined surface area and performance results shown that larger surface area does not necessary indicate greater metals removal, instead metals removal is controlled by surface functional groups and bulk solution conditions.

By pairing the results from proximate carbon analysis (PCA) with the batch isotherm results, it can be concluded that increased fixed carbon content in the pyrolytic biochars is correlated to increased copper adsorption. However, despite a much higher fixed carbon composition for GAC, it did not adsorb as much copper as the high temperature pyrolytic biochars. This could be due to the much higher ash content of GAC compared to the biochar medias tested. Results indicate that when ash content is low (<3%), fixed carbon can be used as an indicator of comparative metals removal performance. Increased ash content above this level can be caused from residual minerals and metals from the feedstock material and production conditions that will limit adsorption of metals from solution. Thermogravimetric analysis (TGA) results confirm greater fixed carbon and less volatile matter for hazelnut shells compared with Douglas fir chips. Lower volatile matter was confirmed by faster stabilization of weight change between 250 and 400°C. TGA results indicate that the feedstocks release similar percent of volatiles up to 330°C; above this temperature, hazelnut shells retain more mass. At pyrolytic temperatures of 500 and 700°C, the hazelnut shell biochar retained a larger portion of fixed carbon, which corresponded to increased metals removal performance; therefore, fixed carbon can be used as a quick indicator to determine if biochar medias should be further evaluated for surface functional groups with high metals affinity.

Aliphatic carbon groups increase with increasing pyrolysis temperature. This group may be linked to the increased copper adsorption compared to the Douglas fir chars at each temperature but providing a substrate for reactive groups. The lack of functional groups identified in FTIR was unexpected for the 700ºC since a key mechanism proposed for heavy metal adsorption onto biochar materials is through interaction with oxygen containing surface functional groups which can deprotonate to accept a metal cation (Regmi et al. 2012). Higher temperature chars have shown increased removal of metals. However, high production temperatures have also correlated to loss of surface functional groups, which are released completely above 650°C (Fuchs et al. 2014). FTIR analysis with and without ATR attachment showed decreasing surface functional groups with increasing production temperature, despite increased copper removal. However, increased buffering capacity in two discrete ranges and corresponding pH dependent copper removal provide evidence that strong and moderate acidic surface functional groups control proton and copper binding. RAMAN spectroscopy analysis should be conducted to confirm the presence or absence of surface functional groups on the high temperature biochars.

Electrophoretic Mobility (EPM) results show H700 biochar has an isoelectric point (IEP) around 1 and a negative surface charge for all higher pH values, indicating a high affinity for positively charged metals ions. The D700 biochar follows the same trend but has less mobility over the pH range and a higher IEP of 2.5. The lower IEP and more negative electrophoretic mobility of H700 compared to D700 indicate greater electrostatic affinity for copper and other cations, which agrees with performance results.

The top two adsorbent medias evaluated in batch equilibrium tests (H700 and H500) followed the expected tread of increasing copper removal with increasing pH; however, the pH effect alone does not explain the performance of the other biochar and GAC medias. Final average pH of H500 batch experiments was equal to GAC, but H500 showed much greater capacity to remove copper. H300 had higher final pH than the Douglas fir chip biochars, but much lower copper removal compared to D500 and D700. GAC performed similarly to D500 and D700 despite a higher final pH. The presence of SRNOM slightly increased final pH compared to SRNOM absence, but also decreased copper removal.

Adding SRNOM to the stormwater in batch adsorption tests simulates the effect that organic material present in stormwater runoff has on Cu^{2+} adsorption by biochar medias. The

lower adsorption observed when SRNOM is added to the aquatic matrix was expected due to complexation of copper with the NOM which prevents it from being adsorbed by the biochar medias. In many cases, Cu-NOM complex formation reduces partitioning into the solid phase of adsorbent medias (Lu and Allen 2001) including: calcite (Lee et. al. 2005); goethite (Buerge-Weirich et al. 2002); montmorillonite (Martinez-Villegas and Martinez 2008), compost, and Apatite II™ (Silvertooth 2014). Copper removal can also be inhibited by sorption of organics onto the solid phase, thereby blocking surface adsorption sites. This effect was observed with NOM reducing adsorption of organic contaminants onto activated carbon (Morley et. al. 2005; Speth 1991) and copper sorption onto ferrihydrite (Martinez-Villegas and Martinez 2008).

Results from the potentiometric titrations and pH sorption edge batch experiments indicate two discrete areas of increased buffering capacity; therefore, a surface complexation with specific sites such as the diffuse layer model (DLM) is a more representative of proton binding to biochar surfaces compared to other types of affinity spectrum models or empirical Langmuir and Freundlich models.

Potentiometric titration data shows two distinct regions of increased buffering capacity near pH 4-5 and pH 6-7 which correspond to binding affinities (pKa) of two discrete binding site types. These experimental observations provide evidence to support surface complexation by two discrete surface functional groups (e.g. strong and moderate acids) as the mechanism for copper removal by biochar.

3.5 Conclusions

Biochar properties and performance in copper removal were evaluated for six types of biochar and GAC. Plentifully available waste biomass consisting of Douglas fir chips and hazelnut shells were selected to investigate the effects of wood feedstock type and pyrolytic temperatures (300, 500, and 700°C). The highest temperature (500 and 700°C) hazelnut shell biochars had the greatest capacity for copper adsorption, exceeding performance of GAC. For each feedstock, performance increased with temperature. High temperature Douglas fir chip biochar performed similarly to GAC. The low temperature (300°C) biochars exhibited the lowest removal of copper. Addition of NOM reduced copper removal and should be investigated further to aid design of treatment in natural environments.

For each pyrolytic temperature, the hazelnut shell biochars removed more copper compared to the Douglas fir chip biochars despite a lower surface area. Although performance

and surface area both increase with increasing pyrolytic temperature, surface area does not explain the improved performance of the hazelnut shells. Similarly, pH effects do not explain all the performance trends observed.

Thermogravimetric analysis (TGA) showed stabilization of weight change at a lower temperature for hazelnut shells, indicating less volatile matter in the biomass feedstock. The hazelnut shells had a greater residual mass at high temperature. Proximate carbon analysis (PCA) showed that both biochar feedstocks have increasing fixed carbon content and decreasing volatile matter content with increasing pyrolysis temperature. The hazelnut shell biochars had higher fixed carbon content and lower volatile matter content compared with the corresponding Douglas fir chars pyrolyzed at the same temperature.

Pairing PCA with the batch isotherm results, increased fixed carbon content in the pyrolytic biochars is correlated to increased copper adsorption. However, despite a much higher fixed carbon composition for GAC, it did not adsorb as much copper as high temperature hazelnut shell biochars. This could be due to the much higher ash content of GAC caused from residual feedstock minerals that limit adoption of metals (Fuchs et al. 2014). Results indicate that when ash content is low (<3%), fixed carbon can be used as an indicator of comparative metals removal performance.

FTIR analysis shows a decrease in surface functional groups with increasing production temperature despite increasing metals removal results. However, increased buffering capacity in two discrete ranges and corresponding pH dependent copper removal provide evidence that strong and moderate acidic surface functional groups control proton and copper binding. Literature shows that with increasing heat treatment temperature or time biochar increases in aromaticity, including the degree to which C rings exhibit electron delocalization, the extent to which aromatic rings are fused into larger polycondensed units, and the proportion of C in condensed ring structures with reference to total C, providing a substrate of organo-metallic complexes.

Out of all the characterization results, electrophoretic mobility (EPM) was the clearest first screening indicator of adsorbent copper binding affinity, as linked to more negative mobility and lower isoelectric point (IEP), which should be confirmed by identification of surface functional groups. EPM investigations required less experimental time compared to batch performance and other characterization methods. High temperature hazelnut shell biochar had

greater negative mobility and lower IEP compared to high temperature Douglas fir chip biochar, which were correlated with increased copper removal as expected electrostatically.

Copper removal results were highly dependent on final solution pH, as expected for metals sorption. Performance prediction under varying pH is unfeasible using typical empirical isotherm models. The diffuse layer model (DLM) was used to described proton and copper binding over the environmentally relevant pH range. DLM predictions can be used to predict equilibrium performance at varying solution conditions without the extensive experimental time and resources required for batch performance studies.

Characteristics of potentiometric titration and pH sorption edge results indicate two-discrete site types can be used to describe proton and copper binding onto high temperature hazelnut shell biochar. DLM binding parameters correlated to strong binding and low pH (carboxylic) and weak binding and moderate pH (lactonic and aldehyde-phenolic) surface functional groups. After calibration, the DLM successfully described copper removal at varying initial copper concentration and final pH conditions. Successful description of multiple batch copper removal isotherms using the two-site DLM indicates that two main biochar surface functional groups dominate copper removal by surface complexation. This allows biochar production for metals sorption to be optimized to focus on feedstock characteristics and production methods that will maximize high affinity functional groups, while maintaining high fixed carbon component. In addition, the DLM predicts equilibrium sorption at varying pH conditions, which yields to better prediction of field scale performance of adsorbent media in natural systems.

3.6 Future Work

Further studies need to be conducted to evaluate surface structure and define the extent of the aromatic domain of different types of biochar compared to standard activated carbon. In concert with results presented here, biochar and GAC should be examined spectroscopically to determine aromatic domain and confirm the presence of surface functional groups with techniques including Boehm titrations, RAMAN spectroscopy, near-edge x-ray adsorption fine structure (NEXAFS), and CHNO elemental analysis.

4 Evaluating dynamic copper removal by hazelnut shell biochar in fixed-bed column experiments: synthetic stormwater, river water, and metals competition

4.1 Abstract

Copper, zinc and lead are heavy metals commonly present in highway stormwater runoff where discharges to surface waters inhabited by sensitive aquatic species including threatened and endangered salmonids has necessitated the need for improved treatment techniques. Hazelnut shell biochar (H700) was compared to granular activated carbon (GAC) in parallel fixed-bed continuous flow column tests to evaluate copper removal from synthetic stormwater runoff and river water. Rapid small scale column tests (RSSCT) were used to simulate dynamic operation in continuous systems and predict performance of field scale systems. H700 results demonstrated superior performance in synthetic stormwater (SSW) compared to GAC. Varying solution conditions, including presence of natural organic matter (NOM) from river water (RW) and competition with zinc and lead, decreased copper removal by H700 biochar.

Equilibrium isotherm predictions of adsorption capacity greatly overestimated experimental RSSCT breakthrough times. Surface complexation modelling improved breakthrough predictions of dynamic copper adsorption by incorporating pH effects on copper removal. The diffuse layer model (DLM) improved predictions of breakthrough time by accurately describing copper adsorption as a function of influent pH. The DLM combined with RSSCT scaling ratios can be used to predict field-scale breakthrough of natural systems based on varying influent solution pH. This provides a significant advantage to the extensive experimental work required to evaluate copper removal at the lab and field scale under varying solution and environmental conditions.

4.2 Introduction

Stormwater runoff has been shown to be a significant source of heavy metals to surface waters (Chen et. al. 1996; Cole et. al. 1984; Kayhanian et al. 2007) with significant concerns of ecological impacts. Copper is deposited onto roadways primarily from brake pad wear and building siding (Davis et. al. 2001) and enters aquatic systems through highway and urban stormwater runoff. Zinc is commonly found in vehicle tires, motor oil, and as a biocide in paints (Nunes et al. 2015; Shaheen 1975). Lead is less commonly used in production due to its toxicity to humans, but is still found in runoff from sites with old paint or old piping, or from mining (Gerould 2016; Shaheen 1975; Steigerwald 2018). Although copper and lead pose greater

toxicological concern, zinc is often present at several times higher concentrations and may compete with copper during adsorptive treatment processes.

Dissolved copper has been shown to have negative impacts on many aquatic organisms, including Coho salmon (Sandahl et al. 2007), chinook salmon (Hansen et al. 1999), rainbow trout (Julliard et. al. 1996), brown trout (Moran et al. 1992), fathead minnow (Carreau and Pyle 2005), Colorado pikeminnow (Beyers and Farmer 2001), and tilapia (Bettini et. al. 2006). Recent research has shown that temporary exposure to dissolved copper concentrations as low as 2 µg/L causes impairment of the olfactory sense of juvenile Coho salmon (Mcintyre et al. 2008; Sandahl et al. 2007). This is a significant concern because four major populations of Coho salmon are listed as either threatened or endangered under the Endangered Species Act, and 2 µg/L is a concentration that is widely exceeded in stormwater runoff (Cole et. al. 1984; Kayhanian et al. 2007; Nason et al. 2011).

Copper (Cu^{2+}), lead (Pb^{2+}), and zinc (Zn^{2+}) are all contaminants of concern in stormwater runoff and are monitored by the EPA due to the potential for negative environmental and human health effects when they are present in the environment. Increasingly stringent regulations on allowable levels of these three metals in stormwater runoff has made it necessary for some industrial and municipal sites to treat their runoff (US EPA 2016). The US Environmental Protection Agency (US EPA) Aquatic Life Criteria has set toxicity levels for Pb^{2+} (acute: 65 µg/L; chronic: 2.5 µg/L) and Zn^{2+} (acute and chronic: 120 µg/L) (US EPA 2016). The toxicity level for Cu^{2+} is determined using the Biotic Ligand Model which takes into account aquatic chemistry parameters such as hardness, alkalinity, pH, and dissolved organic carbon (US EPA 2016). Recent studies on stormwater quality in Oregon found Cu^{2+}, Pb^{2+}, and Zn^{2+} at concentrations higher than the toxicity levels (Lopez 2015; Nason et. al. 2012). These high levels of metals in stormwater can present an issue around points of entry to local water bodies, when sufficient mixing has not yet occurred to dilute metals concentrations. This is particularly true during a first flush storm event where metals levels are elevated due to accumulation on land surfaces during an extended dry period (Sansalone and Buchberger 1997).

Current best management practices (BMPs) for stormwater treatment only reduce dissolved copper concentrations to 5 µg/L (Wright Water Engineers and Geosyntec Consultants 2011), so amendments to current methods or novel treatment approaches need to be developed to avoid harmful impacts on aquatic systems. Due to the nature of existing roadway infrastructure,

it is often impossible to treat stormwater runoff at a central location. This makes active treatment methods such as chemical precipitation or membrane filtration unreasonable in most instances, based on the requirement of skilled operators and consistent maintenance. Economically feasible, passive treatment technologies need to be developed that can be installed and left to operate with minimal maintenance for long life cycles. Numerous studies have been carried out on the remediation of heavy metals by a variety of methods, such as chemical precipitation (Singh and Rawat 1985; Wu et al. 2003), membrane filtration (Fu and Wang 2011), bio-remediation (Imani et al. 2011; Joshi et al. 2011), ion exchange (Genç-Fuhrman et. al. 2007; Wu and Zhou 2009), and adsorption processes (Lee & Davis, 2001; Swami & Buddhi, 2006). Most of the removal processes were indicated to be effective at high concentrations (mg/L levels); however, few studies have focused on metals remediation at trace levels. Among the processes mentioned above, adsorption, ion exchange, and bio-remediation are suitable for metals remediation from stormwater runoff, where metal concentrations are typically at trace levels (Davis et al. 2003; Genç-Fuhrman et. al. 2007; Pitcher et. al. 2004; Sun and Davis 2007; Wu and Zhou 2009).

A variety of best management practices (BMPs) are commonly employed to mitigate negative effects on aquatic environments due to contaminants in stormwater runoff. Considering the construction costs and treatment effectiveness are both important when selecting BMPs. Generally, BMPs can be categorized by several removal processes or mechanisms, such as sedimentation, filtration, biological uptake, and infiltration through soils. Some BMPs rely on a single removal mechanism, while others may involve a combination of several processes. A report summarizing the performance of BMPs for metal abatement from international stormwater BMP databases showed that BMPs were less effective at reducing dissolved copper compared to total copper and total and dissolved zinc (Wright Water Engineers and Geosyntec Consultants 2011). For total zinc removal, all the tested BMPs showed significant reductions, where effluent concentrations were typically reduced to 15-30 µg/L with influent concentration of 50-99 µg/L. Similar results were reported for total copper remediation; most types of BMPs resulted in statistically significant reductions of copper except wetland channels. Bioretention ponds, bioswales, filter strips, media filters, porous pavement, retention ponds, and wetland basins all successfully reduced dissolved zinc to 8-25 µg/L. Fewer BMPs are effective for the removal of dissolved copper. Only detention basins, filter strips, and retention ponds showed significant decreases of dissolved copper, where the corresponding effluent (influent) concentrations were

4.8 (5.3), 5.3 (11.1), and 5.0 (7.5) µg/L, respectively. However, no BMPs reduced dissolved copper to below 5 µg/L, a level which is not safe for all aquatic life, including endangered Coho salmon.

Adsorption is a common removal method for metals like Cu^{2+}, from stormwater and involves accumulation of an adsorbate (e.g. Cu^{2+}) onto the surface of an adsorbent through physical and chemical interactions. Alternative sorbents or ion exchange media can be applied to BMPs, such as detention basins, filter strips and retention ponds, to improve removal efficiencies. Activated carbon, a commercially available adsorbent produced from coal or other organic materials, is commonly used for stormwater filtration. Contaminants adsorb to the surface of the activated carbon via physical and chemical processes. A second treatment option that is gaining popularity is adsorption with biochar, a carbon-based sorbent often generated as a byproduct of energy production processes. Locally sourced biochar has the potential to become a cheaper and more sustainable option than granular activated carbon. However, biochars produced via different methods or from different feed stocks (e.g. hazelnut shells or Douglas fir chips) have varying removal capabilities for metals owing to variation in chemical composition and physical structure (Chen et al. 2011; Fuchs et al. 2014; Gerould 2016). Finding low cost and highly effective adsorbent media which can be applied in the existing BMPs represents a promising solution for remediating metals from stormwater runoff.

Biochar has potential for metals removal due to the presence of surface functional groups that bind with contaminants. The binding affinity and competition for removal of different metals needs to be evaluated to design treatment to target specific metals from complex solutions containing multiple metals. In addition, solution conditions such as pH, ionic strength, and natural organic matter (NOM) affect metals sorption. Removal efficiencies increase with increasing pH due to precipitation as metal hydroxides above pH 6 and deprotonation of surface oxide groups resulting in increased negative surface charge and increased available sites for binding with metal ions. Similarly, at low pH, protons outcompete metals for adsorption sites on the surface (Moreno-Piraján and Giraldo 2011; Nadaroglu et. al. 2010).

Metal speciation and complexation affects the bioavailability and toxicity of metals to aquatic organisms. Bioavailability and environmental fate and transport are strongly dependent on metal speciation (Bhavsar et al. 2004; Luoma 1983). For copper, speciation in the environment is typically governed by the presence of organic ligands (Buck and Bruland 2005).

Stormwater runoff samples from four locations in Oregon shows results >99.9% of total dissolved copper was complexed with organics (Nason et al. 2012). Complexation of dissolved copper with NOM also affects adsorbent medias' ability to remove copper and should be investigated when evaluating treatment performance.

It is important to better understand the extent and mechanism of copper removal by biochar before application for stormwater treatment, including assessing dynamic copper removal in synthetic stormwater and natural water conditions. The objective of this work was to evaluate the dynamics of copper removal by biochar produced via pyrolysis of locally sourced hazelnut shells (H700) compared to commercially available granular activated carbon (GAC). The approach to evaluate this objective was designing rapid small scale column tests (RSSCTs) in a fixed-bed filtration system to simulate and predict full-scale implementation. RSSCTs were used to better understand the dynamic adsorption behavior and to predict adsorption behavior in full scale applications (Crittenden et al. 1987; Crittenden et. al. 1986). The continuous flow set up of a column test provides results that more closely mimic what is expected from adsorbent media implementation in full-scale stormwater filtration (Crittenden et al. 1991; Zhang et al. 2015). Hazelnut shell biochar has the capability to remove metals from stormwater runoff and to be incorporated into existing BMPs. The dynamic adsorption behavior of H700 and GAC were evaluated through RSSCTs drawing on the results from batch testing and parameters estimated for a full-scale installation. Column studies for biochar and GAC were evaluated in a synthetic stormwater (SSW) media containing copper, river water (RW) containing copper, and SSW media with Cu^{2+}, $Zn^{2+,}$ and Pb^{2+}.

4.3 Materials and Methods

Adsorbent Media Calgon F-400 granular activated carbon (GAC) was selected as a comparative commercially available adsorbent. Hazelnut shells were ground using a course particle mill, dried in a pre-heated oven overnight at 105 °C, and pyrolyzed at 700°C in a Muffle Furnace (Thermo Scientific Lindberg Blue M™) for one hour in a N_2 atmosphere. The high temperature hazelnut shell biochar media is referred to as H700. This biochar media was selected based on superior performance for copper removal compared to 5 other biochar types and GAC (Burch et al. in preparation). For lab-scale column testing, the H700 and GAC were ground using a mechanical grinder and sieved to 40-50 mesh particle size (0.3 to 0.4 mm).

Column Sizing Rapid Small Scale Column Tests (RSSCT) (Crittenden et. al. 1986) were used to simulate the operation of adsorbent media in a continuous system and to predict performance at field-scale. Building on previous work that employed RSSCTs to evaluate dynamic copper removal using Apatite II™ (Huang 2012; Provolt 2013; Silvertooth 2014), parallel column experiments were performed to evaluate dynamic copper removal by H700 and GAC in synthetic stormwater, in river water, and in competition with zinc and lead. A field-scale (large) adsorbent media layer consisting of 4 inches (0.102 m) bed depth containing 12×40 mesh particle size (R=0.42 mm) and a superficial velocity of 58.69 m/d (1 gpm/ft^2) was implemented for scaling of the RSSCT tests (Huang 2012). A field scale filter depth of 4 inches was chosen to represent a reasonable depth in engineered stormwater systems of a layer of adsorbent media in an infiltration bioswale or detention pond (Huang 2012). A loading rate of 1 gpm/ft^2 was chosen as a practical stormwater flow rate, which fit within the range of loading rates (0.005-24.54 gpm/ft^2) reported for filtration and infiltration velocities of other adsorbent medias (Champagne and Li, 2009; Hsieh et. al. 2007; Johir et al. 2009).

Lab-scale column parameters were designed to maintain sizing ratios developed for RSSCT so that lab-scale results can be used to design and predict field-scale performance (Crittenden et al., 1986). The ratio of column diameter and media diameter was 27.9 to minimize any wall effects (Rose 1951). The adsorbent media particle size used in the RSCCT (R = 0.179 mm) was selected within the range used for other adsorbent media (Genç-Fuhrman et al. 2007; Jiang et al. 2010; Vijayaraghavan et. al. 2010). The superficial velocity and empty bed contact time (EBCT) of the RSSCT design were determined based on the appropriate scaling relationship relating the RSSCT (small) and representative field-scale (large) bed (Crittenden et. al. 1986):

$$\frac{EBCT_{small}}{EBCT_{large}} = \left(\frac{R_{small}}{R_{large}}\right)^2 \qquad (20)$$

$$\frac{v_{large}}{v_{mall}} = \frac{R_{small}}{R_{large}} = \frac{l_{small}}{l_{large}} \qquad (21)$$

Where *EBCT* is the empty bed contact time; *R* is the radius of the adsorbent particle; *l* is the length of the bed depth; and *v* is the superficial velocity. The characteristics of the RSSCT and hypothetical full-scale system are displayed in Table 5.

Table 5 Parameters of RSSCT (small) and field scale (large) filtration systems

Symbol	Column Test Parameter	RSSCT (small)	Field-scale (large)	units
R	particle radius	0.179	0.42	mm
D	column diameter	0.01	NA	m
A	cross-sectional column area	7.85E-05	0.465	m^2
Q	flow rate/infiltration rate	0.0108	27.26	m^3/day
l	bed depth length	0.043	0.103	m
EBCT	empty bed contact time	0.46	2.53	minutes
V	superficial linear velocity	137.5	58.7	(m/d)
Vol	Bed Volume	0.003	48	L

Column Setup A glass column (Omnifit^{TM}) with 10 cm length and 1 cm internal diameter fitted with adjustable PTFE media bed supports and flow diffusers was used for RSSCTs. Two identical columns were setup with parallel peristaltic pumps to compare adsorption from two separate media beds receiving the same influent solution. Prior to media packing, the columns were purged with 10% HNO_3 for 30 minutes, followed by deionized water for 3 hours at a flow rate of 20 mL/min. The column was then wet packed with 1.73 to 2.22 g (Table 6) sieved media to 4.3 cm bed length. The mass of media was determined by media bulk density to assure constant bed length and a stable packed bed that will not fluidize at the design flow rate of 7.5 mL/min. Influent and effluent samples were taken on regular intervals to monitor dynamic adsorption performance and copper breakthrough times.

Spiked synthetic stormwater (SSW) Synthetic stormwater (SSW) solution containing 1.0 mM NaCl, 0.185 mM $NaHCO_3$, and 100 µg/L spiked copper was mixed in an influent reactor for parallel RSSCTs. Solution pH was adjusted to 6.0 ± 0.1 using HNO_3. Stock solutions of Cu^{2+}, NaCl, $NaHCO_3$, and HNO_3 were pumped into a mixing reactor via syringe pumps, diluted with deionized water via a peristaltic pump, and stirred thoroughly . The resulting SSW solution was pumped from the mixing chamber through the parallel columns using parallel peristaltic pumps. Pressure leading into the column was monitored to ensure tubing stability.

Spiked River Water (RW) To provide for an adequate source of NOM and closer approximation of natural conditions, parallel river water RSSCTs were performed for H700 and GAC. Due to similarities in organic matter, pH, and conductivity, water from the Willamette

River near Corvallis, OR was chosen as a reasonable stormwater surrogate for experimentation. River water samples were filtered with a 0.45 µm filter and stored at 4°C prior to being added to the influent tank. The experimental setup was equivalent to RSSCTs described for SSW, but the deionized water was replaced with collected river water and syringe for background salt additions of NaCl and NaHCO$_3$ was removed.

Competition with Zinc and Lead Conditions for RSSCTs for copper removal with competition from zinc and lead were the same as for the SSW RSSCTs with the addition of 400 µg/L zinc, 100 µg/L lead (ratio typical for stormwater runoff in Oregon (Lopez, 2015)) and 1 mM MES buffer to control pH.

Desorption Potential for the adsorbents to release captured metals in clean water was evaluated after each adsorption experiment. The metals stock solution was removed from the syringe pump and a background mixing solution (SSW or RW) was pumped through the RSSCTs. Effluent samples were collected to measure metals released.

4.4 Results

        Column Performance Results Dynamic adsorption behavior of H700 biochar and GAC was evaluated via parallel continuous-flow rapid small scale column tests RSSCTs in synthetic stormwater (SSW), river water (RW), and competing metals (Comp.) solutions. Breakthrough curves (effluent copper normalized by influent copper concentration of 100 ppb (C/C$_{in}$) over volume treated) are compared in Figure 19. Only H700 in SSW was able to produce an effluent containing less than 2 µg/L of copper. Other treatment options would need to rely on adequate mixing with the receiving water to achieve a treatment threshold safe for endangered aquatic species.

        In the H700 column experiments in SSW, total removal of copper occurred for the first 6.1 treated L, before initial copper breakthrough began. Alternatively, copper breakthrough occurred much faster in the GAC column, with initial copper breakthrough after 0.5 and 0.6 L in SSW and RW, respectively. Although H700 exhibited superior performance in SSW, breakthrough curves (performance over time) in other solutions were similar to performance of GAC. Competition with other metals and natural organic matter (NOM) greatly reduced H700's initial breakthrough time.
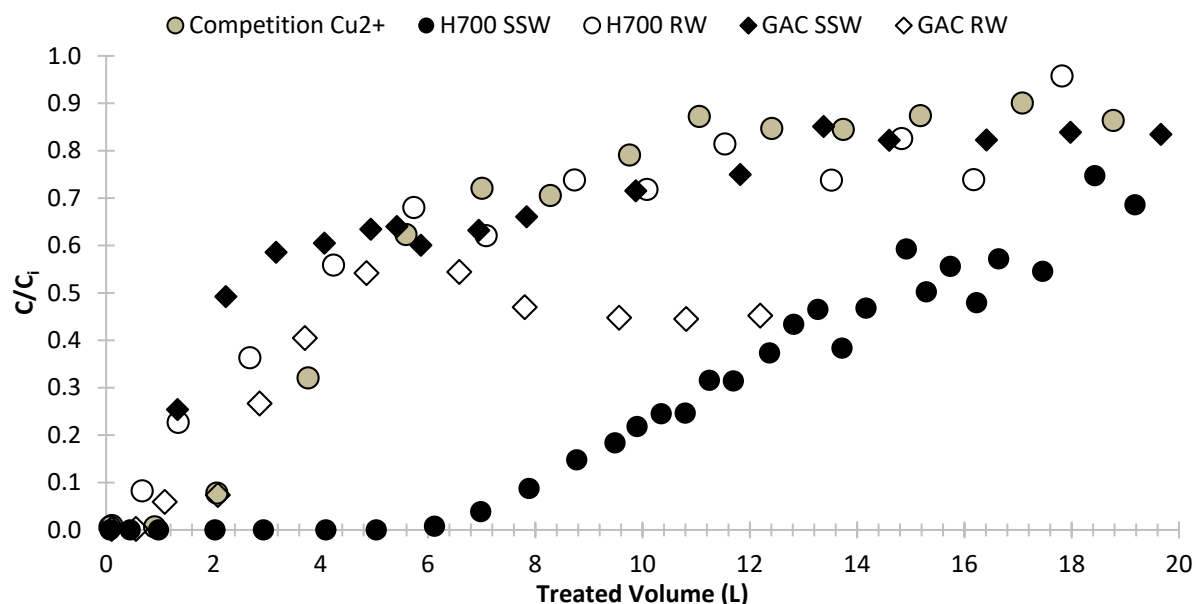
Figure 19 Column Adsorption Breakthrough Curves

Column test adsorption results were compared by two methods: (1) experimental breakthrough times (t_{B20} and t_{B50}) and (2) mass balance calculating total sorption capacity (q_e). Breakthrough times t_{B20} and $t_{B50\ were}$ defined as the time when copper concentration in the column effluent is equal to 20% and 50% of the influent concentration. Sorption capacities were calculated based on the mass of metal accumulated in the column per unit mass of media over the total volume treated.

Fifty percent breakthrough (t_{B50}) time (volume) was selected as an evaluation criterion defined as the time (volume treated) when,

$$\frac{C_{out}}{C_{in}} = 0.5 \tag{22}$$

to estimate total filter treatment capacity in an ideal plug-flow reactor with rapid mass transfer, although filters are often changed before breakthrough is reached to meet discharge requirements. Twenty percent of the influent copper concentration 100 ppb, was also evaluated to estimate treatment capacity based on industrial stormwater discharge regulations of copper in Oregon (20 ppb). RSSCT breakthrough times and volumes (Figure 20 and Appendix B, respectively) were converted to equivalent field-scale parameters based on equivalent number of filter beds treated (Appendix B). This scaling relationship maintains similitude ratios designed for RSSCTs to accurately predicted dynamic field-scale adsorption performance (Crittenden et.

al. 1986). Field-scale breakthrough treatment time capacity predictions assume a continuous influent flow with 100 ppb [Cu^{2+}]. Intermittent flows and contaminant concentrations of storm events will affect performance during in-situ stormwater treatment.
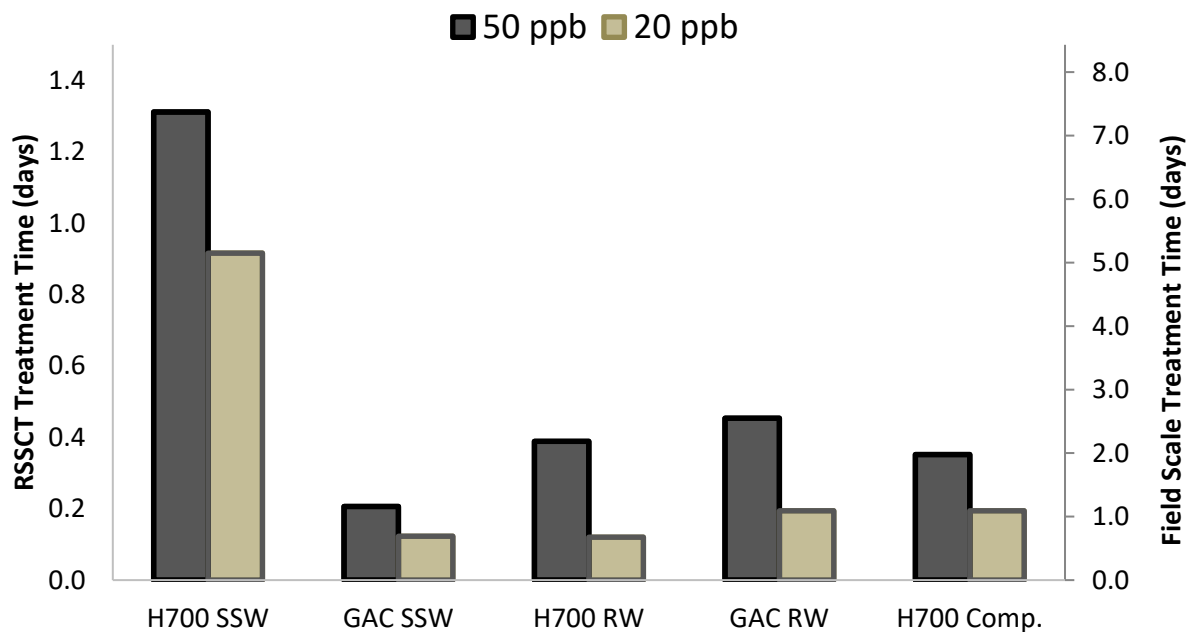
Figure 20 RSSCT and Field Scale Breakthrough Times for effluent treatment levels of 20 ppb (t_{B20}) and 50 ppb Cu^{2+} (t_{B50}).

Sorption Competition between Metals Column breakthrough treatment volumes indicated binding affinity of $Pb^{2+} > Cu^{2+} > Zn^{2+}$ on H700 (Figure 21). Sorption capacity results confirmed this trend when compared on a mass basis (Table6). Minimal sorption of Zn^{2+} was due to high influent (400 ppb Zn^{2+}) concentration and competition for binding sites with Pb^{2+} and Cu^{2+} which had stronger adsorption affinities for the H700 adsorbent.

Metals competition performance results indicate that Pb^{2+} has higher sorption affinity for H700. Competition with Pb^{2+} for surface binding sites was the main mechanism for reduction of Cu^{2+} sorption by H700 from 1.35 to 0.38 mg/g. Methods were the same between column experiments with Cu^{2+} in SSW alone and in competition with Zn^{2+} and Pb^{2+}, except for MES pH buffering, which occurred during the competition run only. Average effluent pH values were 6.04 with competition, and 6.20 without competition or MES buffering. This likely accounts for some of the observed decrease in adsorption during the competition run since adsorption is improved at a higher pH (Chen et al. 2011; Gerould 2016; Regmi et al. 2012).
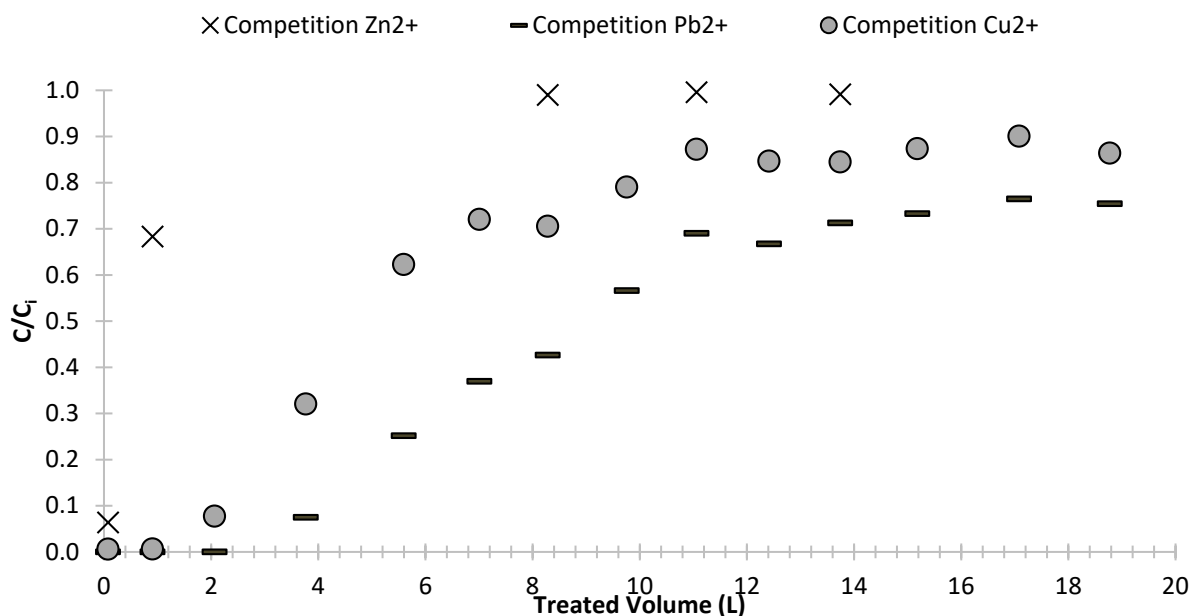
Figure 21 Competition of Cu^{2+}, Zn^{2+}, and Pb^{2+} adsorption of H700 in SSW

Column adsorption media, solution conditions and results of metals sorption capacity are summarized in Table 6. Sorption capacity of H700 in SSW was greatest (1.35 mg/g) of all column experimental conditions. However, sorption of copper by H700 was significantly decreased in RW background (0.28 mg/g) and when in competition with Pb^{2+} and Zn^{2+} sorption (0.38 mg/g). Sorption of copper by GAC was similar (0.38 mg/g) to H700 in RW and less than H700 (0.55 mg/g) in SSW. However, copper removal by GAC increased in RW compared to SSW and plateaued near 50 percent removal. GAC is often used in treatment to adsorb NOM (Weber 2004); therefore, increased copper removal by GAC in RW could be due to adsorption of Cu-NOM complexes by the GAC column that are not adsorbed by H700. Pressure in the RW columns increased much higher and faster compared to the SSW column experiments. Eventually, built-up pressure caused the experiment to terminate due to a rupture of the system tubing. Effluent copper concentration leveled of a treatment level of 0.5 C/C_{in} after the first 5 L of treated volume, supporting evidence that Cu-NOM complexes are removed by GAC in the RW system. While performance of GAC appears to improve in natural waters, NOM induced fouling and pressure issues in the filter, limited the effective filter lifetime.

Unlike batch testing (Burch et. al. in preparation), very little change occurred between influent and effluent pH (Table 6) values due to the shorter contact time and constant influent flow at pH 6. In the case of the metal competition solution, added MES pH buffer controlled effluent pH to 6.04. The total treated volume through the H700 column was slightly larger than the GAC column due to blockage in the GAC column resulting in increased pressure and slightly decreased flow rate. This is thought to be the result of migration of small particles which consequently blocked pore spaces, and not due to copper buildup. Because the removal mechanism is adsorption and not chemical precipitation, precipitation was not the cause of observed pressure buildup. The volume difference occurred after 50% breakthrough time and did not impact adsorption results.

Table 6 Column Adsorption Capacity and Desorption Results

Solution	Adsorbent Media	Metal Treated	bed mass (g)	bulk bed density (g/cm^3)	metal sorbed (mg)	sorption capacity (q_e) (mg/g)	Vol Treated (L)	Avg. pH influent	Avg. pH effluent	Desorption (%)
Synthetic Stormwater (SSW)	H700	Cu^{2+}	1.73	0.51	2.34	1.35	65.0	5.99	6.29	13.2
	GAC	Cu^{2+}	1.88	0.56	1.03	0.55	59.7		6.25	NM
River Water (RW)	H700	Cu^{2+}	2.06	0.61	0.58	0.28	17.8	5.92	6.21	24.6
	GAC	Cu^{2+}	1.73	0.51	0.66	0.38	12.2		6.41	NM
Metals Competition (Comp.)	H700	Cu^{2+}	2.22	0.66	0.82	0.37	31.2	6.01	6.04	16.0
	H700	Pb^{2+}	2.22	0.66	1.33	0.6	31.2		6.04	13.0
	H700	Zn^{2+}	2.22	0.66	0.11	0.05	31.2		6.04	73.0

NM – Denotes Not Measured. Increased pressure due to blockage in GAC column during adsorption did not permit pumping for desorption experiments

Desorption Results Desorption experiments evaluated copper released from the filtration media when copper-free background solution (SSW or RW) was pumped through the exhausted column following adsorption experiments. Desorption results indicate potential for the adsorbent media to discharge metal into clean influent solutions. All desorption experiments produced a similar effluent copper concentration over desorption volume. SSW resulted in the smallest percent of sorbed Cu^{2+} released (13.2 %) despite the largest mass released per gram media (0.18 mg/g) due to the large sorption capacity of copper in SSW. Desorption curves of H700 in RW and competition with other metals released 0.06 and 0.07 mg/g Cu^{2+}, respectively. Similar desorption results (Figure 22) were observed for Pb^{2+} in SSW (0.08 mg/g). Effluent Zn^{2+} concentration reduced to zero much faster than the other two metals evaluated due to weaker binding affinity and minimal amount (0.05 mg/g) sorbed. Desorption results indicated 2 L of clean water was required for effluent concentration of completely sorbed media to fall below 20 ppb. Effluent copper concentration leveled to 5 ppb after 10 L of desorption.
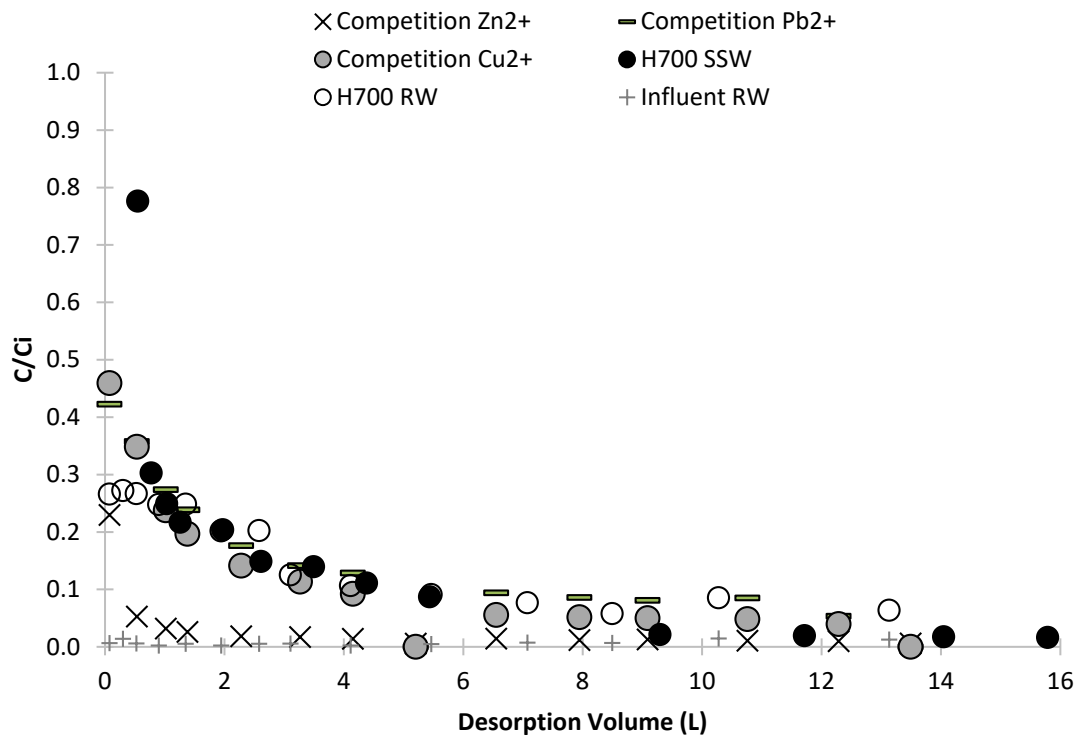
Figure 22 Column Desorption Results

Comparison to isotherm predictions Theoretical breakthrough times calculated from Langmuir isotherm constants were compared with experimentally determined breakthrough times. Experimental breakthrough times were smaller than calculated values for all cases. This is caused by dispersion of the pollutant in the pore spaces and diffusive transport limitations of pollutant molecules to and into the pores of the adsorbent media. Differences in solution pH likely had a significant effect as well: effluent pH during the column test was maintained at 6.1 - 6.2, while pH during batch testing was more variable, reaching as high as 7.4 for the H700. The higher pH during batch testing would have increased adsorption, resulting in an over prediction of breakthrough time in a lower pH environment.

Isotherm parameters derived from batch test results are used to calculate the expected time to equilibrium breakthrough:

$$t_B = \frac{M_{ads} * q_{in}^*}{Q * C_{in}} \tag{23}$$

Where t_B is the time to equilibrium breakthrough, M_{ads} is the mass of adsorbent, q_{in}^* is the adsorption capacity at the influent adsorbate concentration, Q is the flow rate through the column, and C_{in} is the influent adsorbate concentration. Adsorption capacity (q_{in}^*) is determined from batch isotherm data and can be calculated using empirical Langmuir isotherm or surface complexation modeling. Equation 10 assumes plug-flow through the column and adsorption characterized by rapid equilibrium, resulting in a square wave breakthrough curve.

RSSCT results for H700 and GAC indicated a shorter breakthrough time and lower removal capacities for copper when compared to batch equilibrium tests. Experimental breakthrough times are typically smaller than theoretical times due to inefficiencies in the column bed such as pore access, dispersive, and diffusive mass transport limitations. Experimental breakthrough curves are typically asymmetrical, exhibiting a steeper slope before breakthrough, and then tailing off as adsorbents reach capacity.

The experimental copper breakthrough time for H700 (1.3 days) was significantly shorter than the predicted breakthrough time of 2.8 days based on the batch isotherm data Langmuir q_e of 1.76 mg/g (Appendix B). Experimental

breakthrough time was consistent with duplicate H700 column results (Appendix B). Faster experimental breakthrough compared with batch predictions could be due to the lower effluent pH of the column experiments compared to the final pH of the batch isotherm experiments. Influent column pH was kept constant at 6.0 ± 0.1, resulting in an average effluent pH of 6.28. In the batch isotherm experiments, initial pH was adjusted to 6.0 ± 0.1, but the pH increased during the 48-hour experiment, resulting in a final average pH of 7.4 (Burch et al., in preparation). The column experiments have reinforced a significant relationship between pH and copper removal. A spike in effluent copper concentration was observed at slightly lower influent pH, and a decrease in effluent concentrations was observed at slightly higher pH values (Appendix B). This confirms greater removal of copper at higher pH, which can be accurately described and predicted using surface complexation modelling.

Surface complexation modelling provides a better prediction of the removal of copper by biochar at varying pH by representing both proton and metals adsorption. Equilibrium chemical software, MINEQL+, was used to fit experimental proton and metal binding data to calibrate and validate diffuse layer model (DLM) parameters (Burch et al. in preparation). The validated DLM can be used to predict equilibrium sorption at a specified pH to match effluent column pH. At C_{in} of 0.1 mg/L Cu^{2+} and pH of 6.28, the DLM predicted an equilibrium solid concentration (q_{in}*) of 0.7 mg/g, resulting in a breakthrough prediction of 1.1 days, much closer to experimental breakthrough time for H700 of 1.3 days.

In contrast to the H700 column experiments, the breakthrough of copper begins immediately in the effluent of the GAC column and 50 percent breakthrough occurs at 0.6 days. A duplicate GAC column exhibited a similar experimental breakthrough time and curve behavior (Appendix B). As in H700 column experiments, the experimental GAC breakthrough time is significantly shorter than the Langmuir isotherm predicted breakthrough time of 1.18 days. The shape of the breakthrough curve is significantly spread resulting in earlier partial breakthough which indications that dynamic adsorption is affected by transport limiting processes including diffusion, dispersion, reaction transport kinetics, and inaccessibility of

nanoscale pores. In addition, changes in pH between batch and column experiments account for earlier experimental breakthrough time.

Field-Scale Prediction The diffuse layer model (DLM) with calibrated and validated parameters for copper and proton sorption, was used to predict equilibrium sorption (q_{in}^*) as a function of influent copper concentration and pH. Influent copper concentration (31 ppb) was set to a maximum concentration from the stormwater concentration range reported (8-31 ppb Cu^{2+}) (Walaszek et al. 2018). Equilibrium copper sorption capacity by H700 biochar (q_{in}^*) was estimated as 0.65, 1.0, and 1.6 mg/g using DLM calculations at influent pH of 6.2, 6.5, and 6.8, respectively. Lab and field scale column equilibrium breakthrough times and volumes were estimated based on q_{in}^* and RSSCT scaling ratios (Figure 23 [time], Appendix B [volume]). Initial breakthrough time was determined based on the length of the experimental mass transfer zone of RSSCTs, determined from breakthrough curve results. In experimental RSSCTs, initial copper breakthrough occurred 0.75 days (8.1 L) before lab scale equilibrium (t_{B50}) breakthrough time. Based on similitude ratios maintained in RSSCT sizing, breakthrough curve shape is expected to be maintained at the field scale (Crittenden, Berrigan, and Hand 1986), resulting in initial breakthrough occurring 4.2 days (115 m^3) before field-scale equilibrium breakthrough time (Figure 23, Appendix B). Field scale equilibrium breakthrough varied from 47 days (1290 m^3) at influent pH of 6.8 to 19 days (518 m^3) at influent pH of 6.2 for a constant infiltration rate, demonstrating the need to consider pH effects in treatment design. The DLM can support field scale design and performance predictions, limiting required experimental resources.
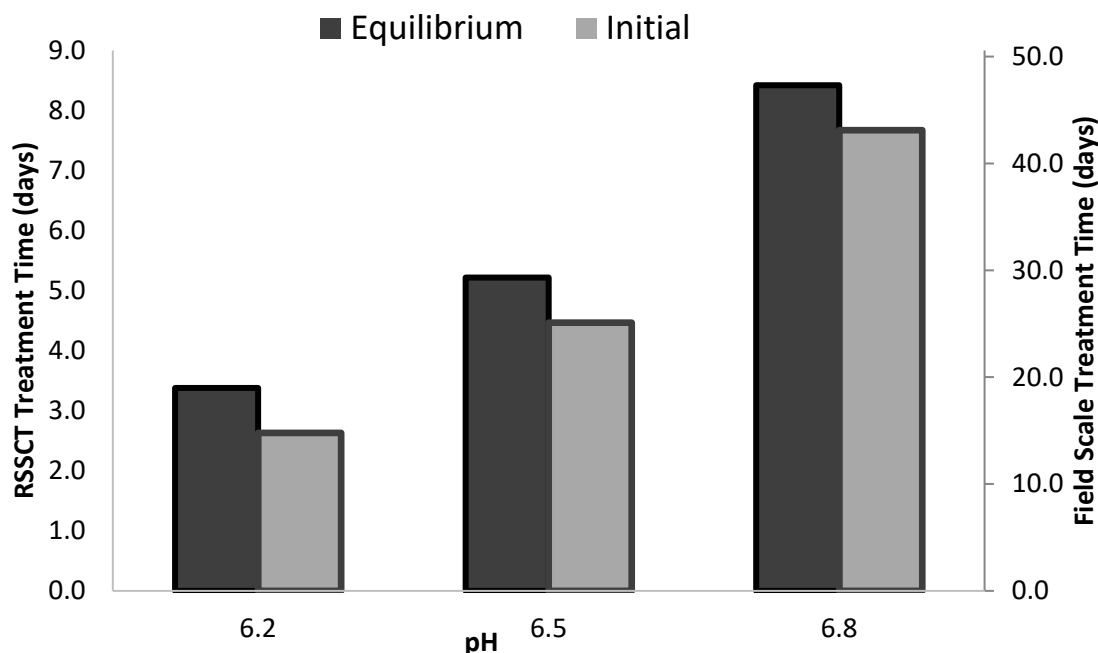
Figure 233 RSSCT and field scale DLM initial and equilibrium and breakthrough time predictions at influent copper concentration of 31 ppb

4.5 Discussion

Effluent pH was in the same range for all column experiments, demonstrating that pH was not the primary cause for the dissimilar curves. The difference in ionic strength of synthetic stormwater and river water is small, and ionic strength has been shown to have little effect on copper partitioning (Lu and Allen 2001). Many studies have demonstrated that NOM has a significant impact on copper speciation and removal with variable effects depending on specific combinations of solid phase, metal species, and type of organic matter. Interactions can be grouped based on the mechanism by which NOM affects removal. In many cases, Cu-NOM complexes form and subsequently reduce partitioning into the solid phase (Lu and Allen 2001) of many adsorbent medias including: calcite (Lee et. al. 2005); goethite (Buerge-Weirich et al. 2002); montmorillonite (Martinez-Villegas and Martinez 2008), compost, and Apatite II™ (Silvertooth 2014). Removal can also be inhibited by sorption of NOM onto the solid phase, thereby blocking surface adsorption sites, which reduced adsorption of organic contaminants onto GAC (Morley et. al. 2005; Speth 1991) and reduced copper sorption onto ferrihydrite (Martinez-Villegas and Martinez 2008).

NOM can also reduce precipitation and solubilize copper precipitates (Gao and Korshin 2013).

Conversely, in some instances NOM has been shown to improve metal adsorption rates, which occurs when NOM serves as a bridge between the adsorbent and metal, observed with humic acid increasing the uptake of copper by goethite (Tipping, et. al. 1983). Furthermore, the effect of NOM can be a function of solution pH. This was demonstrated in experiments with copper and colloidal hematite particles in solution with fulvic acid, where sorption of copper onto hematite increased in the presence of fulvic acid at pH values below 6 and decreased at pH values above 6 (Christl and Kretzschmar 2001). It is important to note that NOM partitioning onto the solid phase is not uniform among different types of organic sorbents. Molecular weight, aromatic fraction, and abundance of phenolic and carboxylic functional groups dictate adsorption and complexation reactions (Gao and Korshin 2013).

In general, there are far more examples of NOM inhibiting metal removal as opposed to promoting removal. Effects of NOM are not uniform among different treatment processes; therefore, experiments must incorporate NOM to evaluate specific treatment options. When NOM does inhibit metal removal, it may be unclear if NOM inhibition is occurring due to metal-NOM complexes or NOM adsorption onto the solid surface, which impacts treatment process design. Results showed that presence of NOM inhibited sorption of copper by H700 biochar, but slightly increased copper sorption by GAC.

The purpose of small column tests was to simulate the performance of metals remediation in field-scale systems. The results of the RSSCTs suggested approximately 7.3 days to breakthrough for copper in field scale columns if treated with continuous flow containing 100 ppb Cu^{2+}. However, stormwater flows are highly intermittent and concentrations are variable. In addition, average stormwater concentrations are much lower (near 30 ppb Cu^{2+}) than the influent column solutions. Both of these factors are likely to impact full scale breakthrough times. The theoretical field scale system was designed to treat 1585-2172 m^3 of stormwater per m^2 of bed when packing conditions and the superficial velocity are the same as

described in Table 5. The location of sites and amount of rain will affect the calculated amount of stormwater that can be treated in a given field-scale system. These results provide an initial estimate of the capacity of H700 and GAC for Cu^{2+} removal and provide the basis for field testing.

For the target field site (1.5 acres capture area) annual rainfall is 40 inches (US Climate Data 2018), resulting in an annual treatment volume of 6167 m^3. Assuming constant infiltration rate and influent maximum copper concentration (31 ppb), bed depth of the specified field scale system (Table 4) needs to be increased to 1.5, 0.8, and 0.5 m to treat 1 year of stormwater at influent pH of 6.2, 6.5, and 6.8, respectively. Actual field storm conditions would vary in influent flow rate and concentration, but DLM predictions provide an estimate of sizing requirements as a function of pH.

The percent desorbed, calculated as the ratio of adsorbate mass desorbed to mass adsorbed, was low for Cu^{2+} and Pb^{2+}. Cu^{2+} desorption was more favorable than Pb^{2+} desorption due to the higher affinity H700 had for Pb^{2+}, as seen in the metal competition column adsorption results. Desorption of Zn^{2+} from the H700 was high relative to the other metals (73%), reflecting the low binding affinity seen during batch testing when competition with other metals exists. The desorption results indicate there is potential for release of sorbed metals, which increases in solutions with metals of strong binding affinity.

4.6 Conclusions

The longer removal time for initial and equilibrium copper breakthrough coupled with the increased sorption capacity indicated that H700 has superior copper removal performance compared to GAC in SSW. Copper sorption capacity by H700 was greatly reduced in river water (RW) background and by competition with Pb^{2+} and Zn^{2+}. H700 copper breakthrough in RW and metal competition were similar to GAC copper breakthrough in both RW and SSW. When metals compete for sorption, later breakthrough time occurred for Pb^{2+} compared to Cu^{2+} and Zn^{2+} indicated higher affinity for $Pb^{2+} > Cu^{2+} > Zn^{2+}$. Adsorption of Zn^{2+} was minimal under the conditions tested. Competition from Pb^{2+} and Zn^{2+} significantly decreased both the mass of Cu^{2+} adsorbed and the time to breakthrough on H700 when compared to adsorption

without competition. Metal competition sorption results on H700 followed the general trend of metal adsorption affinity to a metal oxide:

$Ca^{2+} < Cd^{2+}, Ni^{2+} < Zn^{2+}, Co^{2+}, Cu^{+} < Cu^{2+} < Pb^{2+} < Cr^{3+}, Fe^{3+}, Hg^{2+}$ (Benjamin 2014).

Experimental copper breakthrough time was shorter compared to batch isotherm predictions. Surface complexation modelling improved breakthrough time prediction by accurately accounting for the effect of effluent column pH on adsorption. Desorption of copper was low, with releases of 0.06 to 0.18 mg/g Cu^{2+} in background RW and SSW solutions. Completely sorbed media required 2 L desorption volume for effluent concentration to reach below 20 ppb. Effluent copper concentration leveled to 5 ppb after 10 L of desorption. The favorable comparison of H700 to GAC in batch tests demonstrated initial promise for copper removal from stormwater. This was further exemplified by the high removal efficiencies observed in the synthetic stormwater column tests. However, the introduction of NOM significantly altered removal characteristics, rendering H700 less effective. This is problematic due to the ubiquitous nature of NOM in stormwater runoff.

When considering biochar application for stormwater treatment in natural systems, the presence of organic matter and other metals in stormwater runoff resulted in lower removal capacities and shorter breakthrough time compared to RSSCTs conducted in SSW. NOM inhibits copper removal through the formation of Cu-NOM complexes, which do not adsorb as readily as Cu^{2+}. Other metal species compete with copper for available biochar binding sites so that the removal capacities for copper will decrease in complex stormwater systems. In addition, field performance also depends on the amount of rain and sites' metals loading rates. High rainfall and sites with heavy traffic (more metals in runoff) may lead to earlier breakthrough resulting in shorter filter operation time. Also, considering that zinc broke through the column faster than copper, improvement of media (e.g., mixture of biochar with other materials with high zinc binding or multiple filter sets) is preferred so that multiple metals can be removed, achieving maximum efficiency of biochar for stormwater treatment.

Results indicate lab-produced H700 pyrolytic biochar could be a viable alternative to the commercially available GAC for applications as stormwater filtration media. Performance of H700 was reduced in realistic waters including competition from other metals and NOM, demonstrating the need to evaluate complex solutions for field application. Further work should be done to compare adsorption behaviors of these two adsorbent medias in pilot scale and full-scale systems. Improved methods for pH control during batch testing would eliminate pH as a confounding variable and allow for improved comparison of adsorption behaviors between medias. Field scale stormwater filtration testing of the H700 and would validate scalability of RSSCT results.

5 Burning Questions of Biochar

5.1 Introduction

Biochar has the potential to make significant economic and ecological impacts in agriculture, remediation, forest waste management, and sustainable energy production. Biochar production companies are actively engaged in developing commercial-scale market opportunities. Some examples in the Pacific Northwest include BioLogical Carbon, Sunmark Environmental, Freer Organics, Biochar Supreme, and Walking Point Farms, but biochar production companies are emerging nationally and internationally, targeting locations with surplus biomass supply. The near-term national market potential is estimated at more than $5 billion within the agriculture, horticulture, environmental remediation, and stormwater filtration sectors (Delaney 2015). The current market value of biochar is about $400,000 on an annual basis in the Pacific Northwest region. Prices for raw biochar are highly variable, reported costs ranged from $90 to as high as $600 per yard (Delaney 2015).

Biochar has many commercial uses including expanding use in horticulture and agriculture, as well as remediation. Some commercial uses include biochar as part of a soil amendment blend and in a prill or prill-like form as a fertilizer supplement. Biochar is also used commercially as filtration media to remove pollutants from stormwater and wastewater. Like any new industry, the biochar industry faces several barriers. These include: lack of policy incentives for biochar use; lack of product standardization; an incomplete understanding of end-user customer needs; as well as a lack of demonstration projects. These barriers currently hamper market demand for biochar (Delaney 2015).

While biochar has proven benefits across applications in agriculture, soil health, remediation, forest management, and green energy production, it is not clear if these benefits can be met simultaneously. Biochar physical, chemical and mechanical properties can vary with production conditions, making it challenging to engineer biochars that are simultaneously optimized for carbon sequestration, nutrient storage, water-holding capacity and adsorption (Sun et al. 2012). Questions of burning importance remain in these applications, preventing growth of the biochar markets.

This paper aims to highlight questions presented by researchers and practitioners at the US Biochar Initiative (USBI) bi-annual conference hosed at Oregon State University in August 2016. Examples described center around case studies in the Pacific Northwest, but questions and problems examined preventing biochar applications are universal. The end-goal is to encourage cross-application communication in biochar supply, production, and market application to identify key biochar characteristics and optimize the biochar life cycle system.

5.2 High Value Biochar Markets: Remediation and Agriculture

Soil Remediation Harsh conditions of mine waste soils such as low pH and high metals content challenge plant and microbial growth, which leads to increased erosion and acid mine drainage (AMD). Historical mining in the United States left 161,000 abandoned mines in the western states and Alaska, of which 33,000 have polluted surface or groundwater (Phillips et al. 2016). The Formosa mine in southern Oregon was abandoned in 1993 and designated as a USEPA superfund site; the $12 million remediation project is funded through federal revenues. Every year, millions of gallons of acid mine drainage contaminate surface water, groundwater, soil and sediment with heavy metals (US EPA 2018). The 76-acre mine was added to the USEPA's National Priorities List due to AMD that has severely degraded 18 miles of river and destroyed a steelhead fishery (Phillips et al. 2016). The remediation consists of excavating or capping mine soils due to their high metal concentrations and low pH which results in leaching during precipitation events.

EPA received multiple public comments indicating a desire to utilize biochar for site remediation. Commenters suggested the use of biochar might help in various ways, including: immobilizing metals and toxics, raising the pH of contaminated soil, stabilizing soil, assisting in soil fertility, assisting in tree growth, and providing local economic opportunities. EPA included the evaluation of utilizing biochar as a soil amendment during design of the remedy to enhance plant growth, sequester metals, and raise the pH of soils.

Two gasification biochars, produced from mixed conifer wood and Kentucky bluegrass seed screenings were investigated as amendments for mine soils at rates

ranging from 0 to 9% (w/w). Both biochars promoted plant establishment by increasing soil pH, increasing concentrations of macro-and micro-nutrients, and decreasing the solubility and plant uptake of heavy metals. The Formosa mine soil required at least 4% biochar amendment to promote healthy wheat growth. This addition rate neutralized the elution pH and reduced concentrations of metals (Zn, Cu, Ni, Al) to levels near or below concern (Phillips et al. 2016). In a similar study, Miscanthus biochar and lime additions were evaluated to remediate Formosa mine soil by reducing metal availability, improving soil microbial enzymatic activity, and promoting the initial growth of native vegetation. Lime additions significantly reduced extractable metals concentrations. Increasing biochar addition rates significantly reduced leachate DOC and metals concentrations. By itself, Miscanthus biochar had limited effects, but when combined with lime, the extractable metals concentrations were further reduced and microbial enzyme activity improved at a biochar application rate of 5% (w/w) (Novak et al. 2018).

These greenhouse studies showed favorable results with biochar additions above 5% (w/w) combined with lime can remediate Formosa mine soil by increasing microbial activity and nutrient availability, promoting plant growth, increasing pH, and decreasing leachable DOC and metals. A biochar addition solution requires less invasive mechanical work compared to the standard excavation and capping remediation, and therefore less risk for large unplanned discharge events caused by disturbing the abandoned mines. In addition, natural vegetation growth promoted by biochar functions as an erosional cap and pathway for metals uptake.

Biochar has been shown to adsorb metals, increase pH, and promote microbial and plant growth in greenhouse studies, but long-term, field-scale feasibility studies in natural conditions are lacking. This creates a barrier to biochar implementation in large remediation projects. Biochar was not considered in the original feasibility study of solutions for the Formosa mine site and was only evaluated after intense community involvement through several letters and comments at public meetings. Successful large-scale case studies like the Formosa mine should be well-documented to promote adaptation of biochar solutions to other mine remediation projects, including reporting of how biochar types affect soil characteristics and microbial

biodiversity. The Formosa mine site could be a leading example to answer the following critical question preventing widespread application of biochar solutions for less invasive mine capping and soil improvement:

How do biochar types and characteristics affect microbial biodiversity, soil and plant health in harsh mine soils at a field scale over long life cycles?

Farm Soil Improvement

Because of its high organic carbon (C) content, biochar has the potential to serve as a soil conditioner to improve the physicochemical and biological properties of soils (Ahmad et al. 2014) . Increase in organic C also increases soil water retention capacity, and an 18% increase in the water holding capacity of soil containing biochar has been reported (Glaser et. al. 2002). Biochar accelerates the decomposition of native soil C by improving microbial populations (Kuzyakov et al. 2009) and increasing the chemical hydrolysis due to increasing soil pH (Yu et al. 2013). Other studies show contradicting results where biochar increases the adsorption of native organic C (Kwon and Pignatello 2005; Zimmerman et. al. 2011), thereby decreasing its decomposition rate, resulting in a decrease in microbial activity (Zimmerman et. al. 2011). Physicochemical properties of biochar such as mobile and resident organic matter and sorption capacity influence the priming effect of biochar on soil C. Differing effects of diverse biochar characteristics on soil native C contribute to uncertainties regarding biochar effects on plant growth, earthworm populations, and microbial diversity that serve as barriers to field-scale application of biochar for soil improvement.

Despite the benefits of biochar applications to soil, the mechanisms explaining the interaction between biochar and soil properties are not fully understood. The long-term effects of biochar applications to different soils should also be monitored (Singh et. al. 2012). Soil water holding capacity is related to the hydrophobicity and surface area of biochar, as well as the improved soil structure following biochar application (Verheijen, Jeffery, Bastos, der Velde, et al. 2010). A decrease of nutrient leaching due to biochar application was also reported (Sohi et al. 2009). Biochar generally has a neutral to alkaline pH; however, acidic biochar pH has also been measured (Chan et

al. 2007). The pH of biochar depends on various factors including feedstock type and the thermochemical process of production. The alkaline pH of biochar induces a liming effect on acidic soils, thereby possibly increasing plant productivity. The extent of this effect depends on the acid neutralizing capacity of a given biochar and varies depending on the feedstock and pyrolysis temperature. Increased microbial population and microbial activity in soils amended with biochar have been reported (Lehmann et al. 2011; Verheijen et. al. 2010), which influence biogeochemical processes in soils (Awad et. al. 2012; Lehmann et. al. 2011). Significant increases in seed germination, plant growth, and crop yields have been reported in the soils amended with biochars (Glaser et. al. 2002). Applying biochar together with organic or inorganic fertilizers can even enhance crop yields (Lehmann et al. 2002).

Biochar is highly porous; thus, its application to soil is considered to improve a range of soil physical properties including total porosity, pore size distribution, soil density, soil moisture content, water holding capacity or plant available water content (PAWC), and infiltration or hydraulic conductivity (Atkinson et. al. 2010; Major et al. 2012; Sohi et al. 2009; Sohi et al. 2010; Zwieten et. al. 2012). However, there are few field-scale demonstrations showing that biochar application significantly improves the physical properties of in-situ agricultural soils (Atkinson et. al. 2010; Hardie et al. 2014; Shackley et al. 2010; Sohi et al. 2009). In addition, the mechanisms by which biochar influences water retention, macro-aggregation, soil stability (Sohi et al. 2009) and soil pore size distribution (Verheijen et al. 2010) are poorly understood.

Several studies indicate that various types of biochars applied at sufficiently high rates improved soil physical properties of some soils (Chan et al. 2007; H. X. Chen et al. 2011; Kameyama et al. 2012; Mukherjee and Lal 2013; Novak et al. 2012; Streubel et al. 2011) . However, many studies are of questionable relevance to agriculture (Hardie et al. 2014) due to use of:

(1) ancient anthropogenic soils (Ayodele et al. 2009; Glaser et al. 2002; Glaser and Woods 2004) ,

(2) non-agricultural soils (Belyaeva and Haynes 2012; Jones et al. 2010; Uzoma et al. 2011),

(3) impractically high application rates of biochar for agriculture >40 Mg/ha (Gaskin et al. 2007; Hardie et al. 2014; Jones et al. 2010) , or

(4) re-packed rather than in-situ soils (Belyaeva and Haynes 2012; K. Chan, Zwieten, and Meszaros 2008; Dugan et al. 2010; Kameyama et al. 2012; Laird et al. 2010; Novak et al. 2012; Streubel et al. 2011; Uzoma et al. 2011; van Zwieten et al. 2010).

Pot trials and experiments using sieved re-packed soils for the study of soil physical characteristics are of significant concern because soil structure, pore architecture, and pore size distribution affect field capacity, PAWC, infiltration, hydraulic conductivity, and drainable porosity are an artefact of the sieving and the re-packing process that do not directly resemble in-situ soil properties (Hardie et al. 2014). To be relevant to agriculture, these studies need to be conducted in situ in agricultural production systems employing biochars containing a large proportion of pores within the PAWC pore size range (0.2–30 μm).

Hardie et. al. (2014) conducted a long-term in-situ agricultural study to investigate the mechanisms of biochar influences on orchard soil physical properties including hydraulic conductivity, PAWC, and aggregate stability 31 months after biochar application. Biochar application was expected to increase plant available water through direct pore contribution of 0.2 to 30 μm diameter pores; however, biochar application had no significant effect on drainable porosity, field capacity, PAWC, soil water retention parameters, or soil moisture content of the loamy sand orchard soil. Lack of a significant difference in all soil physical properties between the control and biochar treatments resulted in part from the high spatial variation in pore size and architecture at the site. Despite no significant change in soil plant available porosity, biochar-amended soil had significantly higher near saturated hydraulic conductivity, total porosity, and soil water retention due to large macropores (> 1,200 μm). The formation of large macropores was attributed to observed but unrecorded increased earthworm burrowing, requiring further investigation (Hardie et. al., 2014). The effects of biochar on soil fauna have been scarcely studied, except earthworm activity in soil, which has demonstrated conflicting results based on biochar types and application conditions (Ahmad et al.

2014; Li et al. 2011; Weyers and Spokas 2011). Diverse effects of biochar types and application procedures on earthworm populations demonstrate the critical nature of biochar selection to match site characteristics and target application. Evaluation of biochar application in long-term natural systems is necessary for agricultural adoption, but complex environmental effects of soil and site heterogeneity and uncontrolled microbial and large soil fauna conditions complicate interpretation of results.

For agricultural uses, due to the high cost of the product, current primary users are those producing high value crops. A source in USBI and Dovetail Partners Inc.'s commercial market survey stated, "If a grower is going to spend $30,000 per acre on biochar, they need to be able to recover those costs quickly" (Groot et al. 2017). Another factor reported for implementing biochar from a lender perspective was the fraction of added cost for biochar amendments compared to the overall investment. For example, a vineyard may cost $100,000 per acre to install, so if biochar is 30% of the cost and the returns are going to be $20,000 to $50,000/acre (for a 5 to 10-year payback), then biochar use becomes a more acceptable risk for the lender. For lower value crops, where use of biochar would account for a high cost relative to potential returns, additional cost would more likely be viewed as unacceptable from an investment perspective. It is critical for adoption that farmers and investors understand that biochar is a one-time investment rather than an annual application and will return value to treated soils for multiple decades. For instance, some high value crop growers have reported doubled yields or halved inputs over multiple crop rotations (Groot et al. 2017). This added profit that continues after return on investment can markedly change the value proposition for farmers with long-term soil improvement goals. The long-term effects of biochar amendments to soils need to be investigated and well-documented with respect to both soil and biochar physical characteristics to provide critical forecasting for farmers to make informed investments.

A market analysis needs to be conducted to determine the maximum price farmers could afford for biochar given the expected increase in yield and reduction in the costs of other inputs (such as irrigation) for a variety of crops: potatoes, alfalfa,

wheat, barley, oats and hay. This would also include an estimate of the quantity of biochar that would be needed to supply these farms. The volumes of biochar required to alter soil properties are quite high in comparison to other soil amendments (Novak et al. 2016), thus prices and costs of applications of other sources of soil amendments must also be investigated to determine the potential demand for biochar from forests and other biomass supplies. Determining the price that a farmer could afford to pay for biochar along with the quantity that will be demanded will help determine what type of biochar processing plant will be feasible to build (Houston , 2018). With respect to biochar applications in agriculture, the following questions remain unanswered:

- **How do biochar and soil characteristics influence biochar impacts on soil native organic C through microbial and pH effects?**

- **What mechanisms dominate biochar impact on in-situ soil physical properties and soil fauna?**

- **How do long-term effects of biochar amendments on in-situ agricultural soil pore size and plant water availability relate to biochar and soil characteristics?**

- **What price can farmers afford to purchase biochar for amendment to poor soils based on long-term increased yields and reduction in water and fertilizer inputs to grow high valued crops?**

Water Remediation Discharge of environmental contaminants from industrial, residential, and commercial sources threaten surrounding ecosystems. Technologies are advancing to remediate contaminated water by reducing the bioavailability of contaminants, and consequently decrease their accumulation and toxicity in plants and animals (Ahmad et al. 2014). Biochar is emerging as an ameliorant to reduce the bioavailability of contaminants in the environment (Ahmad et al. 2014; Cao et al. 2011; Sohi et al. 2010). Pyrolysis conditions, including residence time, feedstock types, temperature and heat transfer rate, determine biochar properties, and consequently its efficacy for contaminant remediation (Ahmad et al., 2014).

In stormwater treatment, regulations drive the market. Regulations are determined by technologically feasible limits and environmental health. If contaminants are harmful at low concentrations, improving technology sets the standard for achievable regulations. The National Pollution Discharge Elimination System (NPDES) permit program requires updated permit applications for stormwater discharge permits every 5 years, which provides opportunity for regulatory agencies to review achievable technological treatment levels. The updated regulations provide the catalyst for facilities to reevaluate their stormwater treatment technologies, creating a market entry point for biochar filtration solutions.

A survey of the stormwater treatment market in Oregon and Washington was conducted in January 2017 in collaboration with BioLogical Solutions (a commercial biochar producer) as part of the Oregon State University (OSU) Advantage Accelerator Program, a National Science Foundation (NSF) Innovation Corps (iCorp) site, to evaluate the potential market for biochar amendments in stormwater treatment. Interviewees consisted of 40 industrial facility managers, 6 environmental engineering consultants, 3 municipal stormwater managers, and 2 state regulators. Questions focused on current stormwater treatment technologies, costs, management requirements, and potential problems meeting reduced allowable discharge regulations.

In Washington and Oregon, ODEQ and Washington Department of Ecology (DOE) issued 1,812 industrial stormwater discharge permits. Of 40 industrial permit holders surveyed, 25 percent of interviewees did not use any kind of treatment because they "have no stormwater leaving their site". To prevent off-site discharges, some facilities install retention ponds to capture water and promote infiltration into the soil profile. Biochar amendments have demonstrated increased soil saturated hydraulic conductivity and infiltration rates (Hardie et al. 2014; Novak et al. 2016; Verheijen et. al. 2010) so there is a potential market for biochar application to industrial sites seeking to promote infiltration and reduce or eliminate off-site discharge. Further work is needed to investigate the potential market for biochar to improve infiltration basins by increasing hydraulic conductivity to prevent off-site stormwater discharges requiring regulation.

The market survey findings revealed that industrial permit holders deploy a variety of strategies to meet state water pollution benchmarks, including elimination of any run-off via the use of detention ponds or alternative materials (like permeable pavement) to reduce the need for stand-alone filter systems. The three municipal representatives interviewed followed a combined approached to manage and reduce stormwater runoff, including bioswales and porous pavement. The market for stand-alone stormwater filters and filter media is complicated and driven by a variety of factors including state & local laws and regulations, variations in approaches between industrial and municipal customers and other issues. For sites requiring treatment, facilities reported spending an average of $15,000 annually on stormwater compliance. Based on this information, the size of the filtration market in Oregon and Washington is estimated as $16.7 million dollars annually with annual expenditures on media expected to be about $2.5 million.

State regulators were asked if any changes to Federal regulations based on uncertainties from changes in U.S. Environmental Protection Agency (USEPA) administration would impact state stormwater programs and enforcement of regulations. The state agency personnel indicated that state regulations are more conservative than Federal regulations and would not be impacted by policy changes at the Federal level. In fact, Oregon, Washington, and California state agencies have been expanding their stormwater programs to apply to more organizations and introducing more stringent treatment requirements. For example, new state regulations were developed by the Washington Department of Ecology that require vineyard owners to meet total maximum daily load (TMDL) water quality benchmarks in the near future (Stang 2017).

Based on survey results, market opportunities for biochar media in stormwater treatment are particularly focused on industrial segments. Biochar can be incorporated into existing stormwater applications such as waddles that line catch basins to capture sediment. Adding biochar provides an additional treatment component for dissolved contaminants. These applications can be deployed quickly for use in temporary stormwater mitigation such a wildfire events or during construction or remediation excavation. Currently, specifications for bioswale media

and other Low Impact Development (LID) strategies in places like the City of Portland or the City of Seattle do not include biochar. Before biochar can enter these public-sector marketplaces, more data will need to be collected to prove to regulators that the material offers filtration performance improvements at a reasonable cost compared to existing common materials (like sand and compost).

Biochar and biochar-based filters may also be suited for new markets within the stormwater filtration sector where there are no other practical solutions (filtering pharmaceuticals, for example). However, these potentially new markets for biochar media will require additional research to see if they can perform at a reasonable cost. Uncertainties of future regulations for emerging contaminants create a huge unknown future cost for treatment. Wastewater treatment plants were not designed to remove emerging and trace contaminants, including pharmaceuticals, and future regulations of emerging contaminants could require significant treatment upgrades, costing $100 to $365 million forecasted future regulations for Corvallis, Oregon (Kennedy/Jenks Consultants 2013).   In the near-term, biochar market opportunities with municipalities will require more data and research to show that biochar has a sufficient value proposition for municipal and state specifications.

The variety of types of biochars and their differing characteristic and effects on contaminant removal makes it difficult to predict treatment performance in variable field solution conditions. Biochar has been shown to remove a variety of pollutants including mercury and pharmaceuticals during laboratory studies (Jung et al. 2015; Tan et al. 2016) but long-term site-specific studies at a field-scale are lacking. A long-term field trial is underway for the next 3 years at the OSU-Benton County Green Stormwater Infrastructure Research (*OGSIR*) Facility to investigate optimizing removal of PAHs, PCBs, PFASs, and Metals from stormwater at Department of Defense (DoD) Sites. If this study at a certified technology testing site shows favorable biochar performance results in a natural environment, biochar solutions in water treatment could escalate rapidly. Biochar has shown potential to remove a variety of organic and inorganic contaminants at a laboratory scale, but which specific biochar properties and corresponding feedstock and production conditions are related to specific contaminant removal and performance in natural

systems are uncertain (Ahmad et al. 2014; Mohan et al. 2014). To reduce uncertainties surrounding biochar effectiveness for copper removal in complex natural systems, a combined approach pairing laboratory experiments with electrostatic modelling to define mechanisms for copper removal by biochar, link biochar characteristics to metals removal performance, and evaluate dynamic adsorption and effects of complex aqueous solutions has been performed (Burch et. al., in preparation).

If the uncertainty surrounding future regulations and long-term biochar performance in complex natural systems was reduced by researchers and early commercial adopters, more industrial and municipal sites could be economically motivated to consider biochar medias as a passive alternative for stormwater treatment. In addition, biochar amendments have demonstrated increases in soil hydraulic conductivity and infiltration; therefore, bioswales and detention ponds constructed using biochar to promote subsurface infiltration could be a favorable solution for industrial and municipal stormwater discharge reduction or elimination. Meeting contaminant TMDL regulations is a universal problem that is compounded by uncertainties related to regulatory changes. Better understanding of biochar performance and characteristics linked to specific site conditions and potential changes over time is needed for widespread adoption of biochar solutions. Questions that need to be answered to advance application of biochar in water treatment include:

- **Does biochar media offer filtration performance improvement at a reasonable cost compared to existing common materials (like sand and compost) to meet current and future regulations for stormwater, industrial, and wastewater discharge?**
- **What mechanisms and biochar characteristics are related to contaminant removal and how do they vary among specific contaminants and biochar feedstock and production conditions?**
- **How do natural environmental conditions affect biochar performance over long-term field application?**

5.3 Biochar Supply - Production Technology and Biomass Availability

Forest to Farm: Market, Supply, and Production Economics Biochar amendments have proven benefits in agriculture including increase plant productivity, crop yield, and total soil carbon (Biederman and Harpole 2013) but it is not clear if the benefits outweigh the costs. The cost of biochar has been too high to permit breakeven investments in all but the most favorable circumstances (Ronsse et al. 2013). For widespread adoption of biochar in agriculture to occur, the market must be economically profitable for forest managers, biochar processors, and farmers. This requires large quantities of biomass, proximity to a processing facility, and co-location near farmland (Houston 2017). Researchers at Oregon State University (OSU), US Department of Agriculture (USDA), and Oregon Department of Forestry (DOF) collaborated to investigate the biochar business model, combining supply, production, and market to identify a scenario that will make economic sense for all parties involved. They have found that forest to farm biochar has the greatest potential in areas that raise dryland food crops, have limited water availability, and are designated high-fire hazard forests (Houston 2017).

Three important components that must be favorable for forest to farm biochar to be profitable are farm market, forest supply, and production technology. Questions related to biochar influences on soil improvements and barriers to biochar implementation in agriculture are presented in the market section above. Forest supply depends on large quantities of low-value biomass, including high fire risk forestland requiring management. Estimating the supply chain costs is necessary to determine if forests located near a farm market can produce enough feedstock (recovered biomass) at a reasonable cost to supply the quantity of biomass required to feed a large-scale biochar production plant. This includes estimating the quantity of biomass that can be harvested on a yearly basis as well as the transportation costs.

Klamath County, Oregon was chosen as a case study to investigate forest to farm biochar economics due to plentiful forest supply, including high fire risk forestland, and a large proportion of dryland agriculture, but there is no biochar production facility. Large quantities of low-value Ponderosa pine biomass do not currently have a market in this region and are burned in slash piles for wildfire

mitigation. The lack of a pulp market for the small diameter pulpwood sized logs, non-commercial species, and other low-value biomass makes biochar production more economically feasible in Klamath County. Thus, creating a biochar market for these materials can reduce restoration costs and reduce the release of carbon and other particulates into the atmosphere that result from burning these materials (Houston 2017).

A similar situation is occurring in California, where Ponderosa pine timber is plentiful, but does not have a very lucrative market; forest sales are mostly for a limited firewood market. The situation creates a problem for government foresters charged with thinning overstocked forests to minimize risk of wildfire and beetle infestation. Ponderosa pine in the San Juan National Forests are in large stands with dire need of thinning. David Casey, forest supervisor, sees biochar as a good value-added product for the forests to benefit the agricultural community and that bringing the biochar market to San Juan National Forest would help forest restoration efforts. Casey stated, "We have 90,000 acres of harvestable ponderosa pine within the Dolores District, but we are lacking a market. Biochar could prove an output for the material, lessen the burden on the U.S. government and create jobs" (Mimiaga 2016). Supply chain estimates and answers to farm market questions will determine if capital investments of a biochar production facility are economically feasible. The technical feasibility of biochar production at the landscape scale to support the development of forest to farm biochar markets, benefiting rural economies that are typically based on forest and agricultural commodities is investigated further in the following section. To understand if biochar and production application is a feasible and sustainable industry at the landscape scale, supply and demand costs and benefits must be understood by answering the following question:

Can forest-to-farm markets be economically competitive based on farm market, forest supply, and large-scale biochar production?

Large-Scale Biochar and Green Energy Production

Optimal plant scale depends on feedstock availability and transport costs. For the forest-to-farm project currently investigated by OSU, USDA, and ODOF in the

Klamath basin, the plant construction cost, capitalization, and operation costs are being evaluated for two potential sites. Researchers are also exploring two different biochar conversion technologies along with several different configuration scenarios to determine the best fit considering the feedstock supply and the price point needed for farmers to choose forest biochar over other soil enhancements (Houston 2017).

Preliminary research on plant designs and placements suggests economically viable biochar operations located near forest biomass supplies are close, especially as the cost of harvests decline with new harvest technologies. It is expected that forest biochar has the greatest potential when applied to high valued crops such as potatoes, alfalfa, onions, and strawberries on farms that have limited water supplies (Houston 2017). In Archuleta County, California, construction of a biochar production facility is planned with a target forest supply of low-value pine under a long-term contract with the Rio Grande National Forest. The developer's vision is to create a local biochar industry to improve forest health, create jobs and provide an alternative energy source (Mimiaga 2016). Production technology and conditions must be optimized for sustainable and economically beneficially combined production of bioenergy and biochar.

Converting biomass into biochar and its application to soils have been proposed as one of the best ways to mitigate climate change by sequestering C in soil (Lehmann et al. 2008). The long-term stability based on mean resident time of C of biochar in soils varies from 90 to 1600 years, depending on the labile and intermediately stable C components which are key factors affecting decrease of CO_2 emissions into the atmosphere (Cheng et al. 2008; Kuzyakov et al. 2009; Singh et. al. 2012). Biochar has demonstrated reduction of nitrous oxide (N_2O) and methane (CH_4) through stabilization during pyrolysis of waste biomass (Woolf et al. 2010) and reduction of soil emissions by both biotic and abiotic mechanisms (Zwieten et al. 2009). Bio-oil produced by pyrolysis retains half of the fixed C from the biomass feedstock (Woolf et al. 2010) and can be used as an alternative to fossil energy with low fossil CO_2 emissions (Bolan et al. 2013). Biochar has been estimated to be capable of offsetting a maximum sustainable technical potential (12%) of current anthropogenic CO_2–C equivalent emissions (Woolf et al. 2010). A biochar production

facility in Philomath Oregon demonstrated that 2.18 tons of CO_2 can be sequestered per ton of C harvested as biochar (Miedema 2011). For every 3 tons of biomass feedstock, the combined gasifier and pyrolytic retort production equipment produced approximately 1 ton of carbon, 1 MW bioenergy, and the inherent thermal energy to drive the pyrolytic process (Miedema 2011). However, bioenergy production and carbon sequestration are dependent on the pyrolysis conditions, in which the slow pyrolysis results in a lower yield of liquid fuel and more biochar, whereas the fast pyrolysis generates more liquid fuel (bio-oil) with relatively less biochar (Mohan et al. 2006). It is assumed that with an intermediate yield of 35% biochar, a maximum bioenergy output of 8.7 MJ/kg of biomass could be obtained (Woolf 2008). However, the production of biochar and/or bioenergy from biomass is still controversial (Ahmad et al. 2014) because biomass fuel has less energy output compared to fossil fuel sources, but replenishes via biomass growth on a much faster timescale.

Production facilities have found that with current energy pricing and competition, heat is the most valued component of biochar production, compared to bio-oil and syngas components. To make biochar production economically profitably, production companies must resolve the following question:

How can the heat released during biochar production be utilized for beneficial reuse?

5.4 Conclusions

Although biochar benefits in agricultural and environmental applications have been widely reported at the laboratory scale, field scale studies and applications have been limited. The conflicting results of multiple laboratory studies due to differing biochar physical and chemical characteristics that have not been sufficiently reported creates uncertainty regarding the translation of biochar benefits to complex environments. Matching favorable biochar characteristics with target biochar benefits in applications for specific soils and environmental conditions has proven a successful start to optimize biochar benefits, but the mechanisms underlying biochar impacts remain largely undefined.

Researchers should collaborate to define biochar characteristics related to biomass feedstock and production conditions and determine which characteristics influence biochar benefits in target applications. Understanding mechanisms for biochar improvement of environmental and agricultural systems including contaminant removal, soil health, and water retention is the most critical barrier to field-scale application. How variable environmental characteristics, including soil heterogeneity, soil fauna, and complex aqueous solutions impact biochar's fundamental mechanisms for soil and water improvement must also be understood for biochar application to complex natural sites. Forest supply and biochar and bioenergy production should be evaluated in concert with target biochar market to determine if landscape scale biochar production is economically feasible.

Researchers and practitioners must make a concerted effort to characterize physical and chemical properties of biochar and document characteristics based on biomass feedstock and production. Only then can valuable characterization clues can be linked to performance in target biochar applications. Finally, mechanisms of biochar benefits in agricultural and environmental applications must be defined to optimize biochar market performance potential, based on biomass supply, production conditions and economics.

6 Conclusions

The primary mechanism of copper removal as surface complexation with biochar surface functional groups was confirmed through a combined approach that evaluated biochar characteristics, metals removal performance, and electrostatic modelling. Performance results showed that copper removal increased with increasing pyrolysis temperature and hazelnut shell biochar outperformed Douglas fir chip biochar at each temperature. The high temperature hazelnut shell biochar (named H700) performed best in batch equilibrium copper adsorption experiments, with superior removal capacity compared to GAC. Because of environmental benefits of the biochar industry through biomass waste management, green energy production, and carbon sequestration, biochar is a more sustainable alternative to GAC. Based on demonstrating equal or superior metal removal capacity compared to GAC in equilibrium and dynamic sorption, biochar could be a feasible adsorbent alternative; however, for widespread application of biochar in complex environmental conditions, metals removal mechanisms by biochar must be well understood and linked to biochar characteristics.

Characterization results showed that greater fixed carbon and more negative electrophoretic mobility were successful first screening indicators adsorbent medias that could contain surface functional groups with high copper binding affinity. Due to the formation of large stacked sheets of aromatic carbon rings at high treatment temperature (700°C), the complex porous internal structure creates a recalcitrant platform for surface functional groups to form internal organo-metallic complexes. Conversely, increasing surface area and pH with increasing biochar production temperature correlated with increasing copper removal with increasing temperature but did not describe performance variations between feedstock types. FTIR analysis showed decreasing surface functional groups with increasing production temperature, despite increased copper removal. However, increased buffering capacity in two discrete ranges and corresponding pH dependent copper removal provide evidence that strong and moderate acidic surface functional groups control proton and copper binding.

Surface complexation modelling was used to described proton and copper binding to H700 in potentiometric titration and pH sorption edge experiments. The diffuse layer model with two discrete site types accurately described sorption results. The pK_a value of the binding sites and areas of increased proton and copper binding corresponded to strong acid (carboxylic) and moderate acid (lactonic and aldehyde-phenolic) surface functional groups. Based on increased binding capacity in these pH regions and validation of the DLM parameter at varying solution conditions, surface complexation by two discrete surface functional groups in the pK_a range represented above is proposed as the mechanism for copper removal by H700 biochar.

Natural organic matter (NOM) present in natural waters competes with biochar to complex with copper. Removal of copper by biochar is reduced in the presence of NOM, due to formation of copper-NOM complexes competing with sorption and preventing access to biochar functional groups located within the internal pore structure. Presence of other metals with higher binding affinity in stormwater competed for biochar binding sites and reduce the removal of copper. Rapid small scale column tests (RSSCTs) results confirmed equilibrium results that H700 is a superior sorbent compared to GAC in synthetic stormwater (SSW). However, H700 copper removal capacity was significantly reduced in background river water (RW) and by competing Pb^{2+} and Zn^{2+}. Alternatively, GAC RSSCTs performance were similar in RW compared to SSW and matched performance of H700 in the RW and metals competition solutions. Decreased copper sorption in RW when natural organic matter (NOM) is present is a significant concern due to the ubiquitous nature of NOM in stormwater. Treatment design parameters should include evaluation of decreased sorption performance in complex stormwater solutions. Field scale 50 percent breakthrough for H700 was estimated as 7.3 days in SSW (continuous stormflow with 100 ppb influent $[Cu^{2+}]$), compared to 2.2 and 2.0 days in RW and metals competition solutions, respectively. This large reduction in breakthrough time is important to consider when designing field scale treatment systems and planning for media replacement.

The DLM accurately described sorption as a function of pH and predicted equilibrium breakthrough of the RSSCTs. The calibrated DLM model can be used to

predict field scale performance under varying influent environmental pH conditions. Model predictions created a pathway for biochar application to field scenarios without extensive experimental requirements. Field scale equilibrium breakthrough for H700 was estimated as 19, 29, and 47 days in SSW (continuous stormflow with 31 ppb influent $[Cu^{2+}]$), at influent pH of 6.2, 6.5, and 6.8, respectively. The calibrated and validated DLM allows users to predict performance under varying field solution conditions without extensive experimental time and resources required to conduct batch and RSSCT performance evaluations.

7   Bibliography

Ahmad, Mahtab et al. 2013. "Trichloroethylene Adsorption by Pine Needle Biochars Produced at Various Pyrolysis Temperatures." *Bioresource technology* 143: 615–22.

———. 2014. "Biochar as a Sorbent for Contaminant Management in Soil and Water: A Review." *Chemosphere* 99: 19–33.

Atkinson, CJ, JD Fitzgerald, and NA Hipps. 2010. "Potential Mechanisms for Achieving Agricultural Benefits from Biochar Application to Temperate Soils: A Review." *Plant and soil*. http://link.springer.com/article/10.1007/s11104-010-0464-5 (October 13, 2014).

Awad, Yasser Mahmoud, Evgenia Blagodatskaya, Yong Sik Ok, and Yakov Kuzyakov. 2012. "Effects of Polyacrylamide, Biopolymer, and Biochar on Decomposition of Soil Organic Matter and Plant Residues as Determined by 14C and Enzyme Activities." *European Journal of Soil Biology* 48: 1–10.

Ayodele, Ajayi et al. 2009. "Numerical Analysis of the Impact of Charcoal Production on Soil Hydrological Behavior, Runoff Response and Erosion Susceptibility." *Revista Brasileira de Ciência do Solo* 33(1): 137–46.

Babić, B M, S K Milonjić, M J Polovina, and B V Kaludierović. 1999. "Point of Zero Charge and Intrinsic Equilibrium Constants of Activated Carbon Cloth." *Carbon* 37(3): 477–81.

Belyaeva, O N, and R J Haynes. 2012. "Comparison of the Effects of Conventional Organic Amendments and Biochar on the Chemical, Physical and Microbial Properties of Coal Fly Ash as a Plant Growth Medium." *Environmental Earth Sciences* 66(7): 1987–97.

Benjamin, Mark M. 2014. *Water Chemistry*. Waveland Press.

Bettini, Simone, Franco Ciani, and Valeria Franceschini. 2006. "Recovery of the Olfactory Receptor Neurons in the African Tilapia Mariae Following Exposure to Low Copper Level." *Aquatic Toxicology* 76(3–4): 321–28.

Beyers, Daniel W., and Michael S. Farmer. 2001. "Effects of Copper on Olfaction of Colorado Pikeminnow." *Environmental Toxicology and Chemistry* 20(4): 907–12.

Bhavsar, Satyendra P et al. 2004. "Development of a Coupled Metal Speciation-Fate Model for Surface Aquatic Systems." *Environmental toxicology and chemistry* 23(6): 1376–85.

Biederman, Lori A, and W Stanley Harpole. 2013. "Biochar and Its Effects on Plant Productivity and Nutrient Cycling: A Meta-Analysis." *GCB bioenergy* 5(2): 202–14.

Biniak, S, M Pakuła, and G S Szyman. 1999. "Effect of Activated Carbon Surface Oxygen- and / or Nitrogen-Containing Groups on Adsorption of Copper (II) Ions from Aqueous Solution †." 1(Ii): 6117–22.

Boehm, H P. 1994. "Some Aspects of the Surface Chemistry of Carbon Blacks and Other Carbons." *Carbon* 32(5): 759–69.

Bolan, Nanthi S et al. 2013. "Landfills as a Biorefinery to Produce Biomass and Capture Biogas." *Bioresource technology* 135: 578–87.

Borrok, D. M., and J. B. Fein. 2005. "The Impact of Ionic Strength on the Adsorption of Protons, Pb, Cd, and Sr onto the Surfaces of Gram Negative Bacteria: Testing Non-Electrostatic, Diffuse, and Triple-Layer Models." *Journal of Colloid and Interface Science* 286(1): 110–26.

Borrok, David, Benjamin F. Turner, and Jeremy B. Fein. 2005. "A Universal Surface Complexation Framework for Modeling Proton Binding onto Bacterial Surfaces in Geologic Settings." *American Journal of Science* 305(6–8 SPEC. ISS.): 826–53.

Buck, Kristen N, and Kenneth W Bruland. 2005. "Copper Speciation in San Francisco Bay: A Novel Approach Using Multiple Analytical Windows." *Marine Chemistry* 96(1–2): 185–98.

Buerge-Weirich, Diane et al. 2002. "Adsorption of Cu, Cd, and Ni on Goethite in the Presence of Natural Groundwater Ligands." *Environmental science & technology* 36(3): 328–36.

Cao, Xinde et al. 2011. "Simultaneous Immobilization of Lead and Atrazine in Contaminated Soils Using Dairy-Manure Biochar." *Environmental Science & Technology* 45(11): 4884–89. http://pubs.acs.org/doi/abs/10.1021/es103752u.

Cao, Xinde, and Willie Harris. 2010. "Properties of Dairy-Manure-Derived Biochar

Pertinent to Its Potential Use in Remediation." *Bioresource Technology* 101(14): 5222–28. http://dx.doi.org/10.1016/j.biortech.2010.02.052.

Carreau, Natalie D, and Greg G Pyle. 2005. "Effect of Copper Exposure during Embryonic Development on Chemosensory Function of Juvenile Fathead Minnows (Pimephales Promelas)." *Ecotoxicology and environmental safety* 61(1): 1–6.

Champagne, Pascale, and Chenxi Li. 2009. "Use of Sphagnum Peat Moss and Crushed Mollusk Shells in Fixed-Bed Columns for the Treatment of Synthetic Landfill Leachate." *Journal of Material Cycles and Waste Management* 11(4): 339–47.

Chan, K Y et al. 2007. "Assessing the Agronomic Values of Contrasting Char Materials on Australian Hardsetting Soil." In *Proceedings of the Conference of the International Agrichar Initiative*, , 19.

Chan, KY, L Van Zwieten, and I Meszaros. 2008. "Agronomic Values of Greenwaste Biochar as a Soil Amendment." *Soil Research*. http://www.publish.csiro.au/?paper=SR07109 (October 13, 2014).

Chen, Carl W., Daniel Leva, and Adam Olivieri. 1996. "Modeling the Fate of Copper Discharged to San Francisco Bay." *Journal of Environmental Engineering* 122(10): 924–34.

Chen, H X, Z L Du, Wei Guo, and Q Z Zhang. 2011. "Effects of Biochar Amendment on Cropland Soil Bulk Density, Cation Exchange Capacity, and Particulate Organic Matter Content in the North China Plain." *Ying yong sheng tai xue bao= The journal of applied ecology* 22(11): 2930–34.

Chen, Xincai et al. 2011. "Adsorption of Copper and Zinc by Biochars Produced from Pyrolysis of Hardwood and Corn Straw in Aqueous Solution." *Bioresource Technology* 102(19): 8877–84.

Cheng, Chih-Hsin, Johannes Lehmann, Janice E Thies, and Sarah D Burton. 2008. "Stability of Black Carbon in Soils across a Climatic Gradient." *Journal of Geophysical Research: Biogeosciences* 113(G2).

Christl, Iso, and Ruben Kretzschmar. 2001. "Interaction of Copper and Fulvic Acid at the Hematite-Water Interface." *Geochimica et Cosmochimica Acta* 65(20):

3435–42.

Chun, Yuan, Guangyao Sheng, Cary T Chiou, and Baoshan Xing. 2004. "Compositions and Sorptive Properties of Crop Residue-Derived Chars." *Environmental science & technology* 38(17): 4649–55.

Clary, Jane et al. 2017. Water Environment & Reuse Foundation *Final Report International Stormwater BMP Database - 2016 Summary Statistics*. http://www.bmpdatabase.org/Docs/03-SW-1COh BMP Database 2016 Summary Stats.pdf.

Coates, John, and R A Meyers Ed. 2000. "Interpretation of Infrared Spectra , A Practical Approach Interpretation of Infrared Spectra , A Practical Approach." *Encyclopedia of Analytical Chemsitry*: 10815–37.

Cole, R H, Frederick R E, Healy, R P, Rolan, R G. 1984. "Preliminary Findings of the Priority Pollutant Monitoring Project of the National Urban Runoff Program . ." *Water Pollut Control Fed* 56(7): 898–908.

Comans, Rob N.J., and Jack J. Middelburg. 1987. "Sorption of Trace Metals on Calcite: Applicability of the Surface Precipitation Model." *Geochimica et Cosmochimica Acta* 51(9): 2587–91.

Corapcioglu, M O, and C P Huang. 1987. "The Surface Acidity and Characterization of Some Commercial Activated Carbons." *Carbon* 25(4): 569–78.

Crittenden, John C et al. 1991. "Predicting GAC Performance with Rapid Small-Scale Column Tests." *Journal-American Water Works Association* 83(1): 77–87.

Crittenden, John C, John K Berrigan, and David W Hand. 1986. "Design of Rapid Small-Scale Adsorption Tests for a Constant Diffusivity." *Journal (Water Pollution Control Federation)*: 312–19.

Crittenden, John C, John K Berrigan, David W Hand, and Ben Lykins. 1987. "Design of Rapid Fixed-Bed Adsorption Tests for Nonconstant Diffusivities." *Journal of Environmental Engineering* 113(2): 243–59.

Davis, Allen P et al. 2003. "Water Quality Improvement through Bioretention: Lead, Copper, and Zinc Removal." *Water Environment Research* 75(1): 73–82.

Davis, Allen P, Mohammad Shokouhian, and Shubei Ni. 2001. "Loading Estimates of Lead, Copper, Cadmium, and Zinc in Urban Runoff from Specific Sources."

Chemosphere 44(5): 997–1009.

Delaney, Matt. 2015. "Northwest Biochar Commercialization Strategy Paper. Prepared for the Oregon Department of Forestry."

Dugan, Emmanuel et al. 2010. "Bio-Char from Sawdust, Maize Stover and Charcoal: Impact on Water Holding Capacities (WHC) of Three Soils from Ghana." In *19th World Congress of Soil Science, Symposium*, , 9–12.

Dzombak, David A, and Francois M M Morel. 1987. "Adsorption of Inorganic Pollutants in Aquatic Systems." *Journal of Hydraulic Engineering* 113(4): 430–75.

———. 1990. *Surface Complexation Modeling: Hydrous Ferric Oxide*. John Wiley & Sons.

Farley, Kevin J, David A Dzombak, and François M M Morel. 1985. "A Surface Precipitation Model for the Sorption of Cations on Metal Oxides." *Journal of Colloid and Interface Science* 106(1): 226–42.

Fu, Fenglian, and Qi Wang. 2011. "Removal of Heavy Metal Ions from Wastewaters: A Review." *Journal of environmental management* 92(3): 407–18.

Fuchs, Mark R, Manuel Garcia-Perez, Phillip Small, and Gloria Flora. 2014. "Campfire Lessons: Breaking Down the Combustion Process to Understand Biochar Production and Characterization."

Gabaldón, Carmen, Paula Marzal, Jose Ferrer, and Aurora Seco. 1996. "Single and Competitive Adsorption of Cd and Zn onto a Granular Activated Carbon." *Water Research* 30(12): 3050–60.

Gao, Yuan, and Gregory Korshin. 2013. "Effects of NOM Properties on Copper Release from Model Solid Phases." *Water research* 47(14): 4843–52.

Gaskin, Julia W et al. 2007. "Potential for Pyrolysis Char to Affect Soil Moisture and Nutrient Status of a Loamy Sand Soil."

Genç-Fuhrman, Hülya, Peter S Mikkelsen, and Anna Ledin. 2007. "Simultaneous Removal of As, Cd, Cr, Cu, Ni and Zn from Stormwater: Experimental Comparison of 11 Different Sorbents." *Water research* 41(3): 591–602.

Gerould, Joy-Marie Danielle. 2016. "Characterization of Biochar for Use in Treating Copper (II) Polluted Stormwater."

Glaser, Bruno, Johannes Lehmann, and Wolfgang Zech. 2002. "Ameliorating Physical and Chemical Properties of Highly Weathered Soils in the Tropics with Charcoal--a Review." *Biology and fertility of soils* 35(4): 219–30.

Glaser, Bruno, and William I Woods. 2004. *Amazonian Dark Earths: Explorations in Space and Time*. Springer.

Groot, Harry et al. 2017. "BIOCHAR AS AN INNOVATIVE WOOD PRODUCT: A LOOK AT BARRIERS TO REALIZATION OF ITS FULL POTENTIAL."

Hansen, James A. et al. 1999. "Chinook Salmon *(Oncorhynchus Tshawytscha)* and Rainbow Trout *(Oncorhynchus Mykiss)* Exposed to Copper: Neurophysiological and Histological Effects on the Olfactory System." *Environmental Toxicology and Chemistry* 18(9): 1979–91. http://doi.wiley.com/10.1002/etc.5620180917.

Hardie, Marcus et al. 2014. "Does Biochar Influence Soil Physical Properties and Soil Water Availability?" *Plant and Soil* 376(1–2): 347–61.

Houston, Laurie. 2017. "Forest to Farm Biochar: What Will It Take?" https://www.agclimate.net/2018/05/17/forest-to-farm-biochar-what-will-it-take/.

Hsieh, Chi-hsu, Allen P Davis, and Brian A Needelman. 2007. "Bioretention Column Studies of Phosphorus Removal from Urban Stormwater Runoff." *Water Environment Research* 79(2): 177–84. http://openurl.ingenta.com/content/xref?genre=article&issn=1061-4303&volume=79&issue=2&spage=177.

Huang, Hsiao-Wen. 2012. "The Assessment of Copper and Zinc Removal from Highway Stormwater Runoff Using Apatite II^{TM}."

Imani, Saber et al. 2011. "Hg, Cd and Pb Heavy Metal Bioremediation by Dunaliella Alga." *Journal of Medicinal Plants Research* 5(13): 2775–80.

Jiang, Jun, and Ren-kou Xu. 2013. "Application of Crop Straw Derived Biochars to Cu (II) Contaminated Ultisol: Evaluating Role of Alkali and Organic Functional Groups in Cu (II) Immobilization." *Bioresource technology* 133: 537–45.

Jiang, Ming-qin, Xiao-ying Jin, Xiao-Qiao Lu, and Zu-liang Chen. 2010. "Adsorption of Pb (II), Cd (II), Ni (II) and Cu (II) onto Natural Kaolinite Clay." *Desalination* 252(1–3): 33–39.

Johir, M. A.H. et al. 2009. "Treatment of Stormwater Using Fibre Filter Media."

Water, Air, and Soil Pollution: Focus 9(5–6): 439–47.

Jones, Benjamin E H, R J Haynes, and I R Phillips. 2010. "Effect of Amendment of Bauxite Processing Sand with Organic Materials on Its Chemical, Physical and Microbial Properties." *Journal of Environmental Management* 91(11): 2281–88.

Joshi, P. K. et al. 2011. "Bioremediation of Heavy Metals in Liquid Media Through Fungi Isolated from Contaminated Sources." *Indian Journal of Microbiology* 51(4): 482–87.

Joshi, U M, and R Balasubramanian. 2010. "Characteristics and Environmental Mobility of Trace Elements in Urban Runoff." *Chemosphere* 80(3): 310–18.

Julliard, A. K., D. Saucier, and L. Astic. 1996. "Time-Course of Apoptosis in the Olfactory Epithelium of Rainbow Trout Exposed to a Low Copper Level." *Tissue and Cell* 28(3): 367–77.

Jung, Chanil et al. 2015. "Competitive Adsorption of Selected Non-Steroidal Anti-Inflammatory Drugs on Activated Biochars: Experimental and Molecular Modeling Study." *Chemical Engineering Journal* 264: 1–9.

Kameyama, K, T Miyamoto, T Shiono, and Y Shinogi. 2012. "Influence of Sugarcane Bagasse-Derived Biochar Application on Nitrate Leaching in Calcaric Dark Red Soil." *Journal of Environmental Quality* 41(4): 1131–37.

Katz, Lynn E, and Kim F Hayes. 1995. "Surface Complexation Modeling: I. Strategy for Modeling Monomer Complex Formation at Moderate Surface Coverage." *Journal of colloid and interface science* 170(2): 477–90.

Kayhanian, M, C Suverkropp, A Ruby, and K Tsay. 2007. "Characterization and Prediction of Highway Runoff Constituent Event Mean Concentration." *Journal of environmental management* 85(2): 279–95.

Kennedy/Jenks Consultants. 2013. "City of Corvallis Trysting Tree Golf Course Trysting Tree Golf Course Recycled Water Feasibility Study City of Corvallis." (0791027).

Kim, Kwang Ho, Jae Young Kim, Tae Su Cho, and Joon Weon Choi. 2012. "Influence of Pyrolysis Temperature on Physicochemical Properties of Biochar Obtained from the Fast Pyrolysis of Pitch Pine (Pinus Rigida)." *Bioresource Technology* 118: 158–62. http://dx.doi.org/10.1016/j.biortech.2012.04.094.

Kuzyakov, Yakov et al. 2009. "Black Carbon Decomposition and Incorporation into Soil Microbial Biomass Estimated by 14C Labeling." *Soil Biology and Biochemistry* 41(2): 210–19.

Kwon, Seokjoon, and Joseph J Pignatello. 2005. "Effect of Natural Organic Substances on the Surface and Adsorptive Properties of Environmental Black Carbon (Char): Pseudo Pore Blockage by Model Lipid Components and Its Implications for N2-Probed Surface Properties of Natural Sorbents." *Environmental science & technology* 39(20): 7932–39.

Laird, David A et al. 2010. "Impact of Biochar Amendments on the Quality of a Typical Midwestern Agricultural Soil." *Geoderma* 158(3–4): 443–49.

Lee, S M, and Allen P Davis. 2001. "Removal of Cu (II) and Cd (II) from Aqueous Solution by Seafood Processing Waste Sludge." *Water Research* 35(2): 534–40.

Lee, Young J, Evert J Elzinga, and Richard J Reeder. 2005. "Cu (II) Adsorption at the Calcite--Water Interface in the Presence of Natural Organic Matter: Kinetic Studies and Molecular-Scale Characterization." *Geochimica et Cosmochimica Acta* 69(1): 49–61.

Legret, M, and C Pagotto. 1999. "Evaluation of Pollutant Loadings in the Runoff Waters from a Major Rural Highway." *Science of the Total Environment* 235(1–3): 143–50.

Lehmann, Johannes et al. 2002. "Slash-and-Char-a Feasible Alternative for Soil Fertility Management in the Central Amazon." In *Proceedings of the 17th World Congress of Soil Science*, , 1–12.

———. 2007. "Bio-Energy in the Black." *Frontiers in Ecology and the Environment* 5(7): 381–87.

———. 2008. "Australian Climate--Carbon Cycle Feedback Reduced by Soil Black Carbon." *Nature Geoscience* 1(12): 832.

———. 2011. "Biochar Effects on Soil Biota--a Review." *Soil biology and biochemistry* 43(9): 1812–36.

Li, Dong, William C Hockaday, Caroline A Masiello, and Pedro J J Alvarez. 2011. "Earthworm Avoidance of Biochar Can Be Mitigated by Wetting." *Soil Biology and Biochemistry* 43(8): 1732–37.

Liu, Pei et al. 2012. "Modification of Bio-Char Derived from Fast Pyrolysis of Biomass and Its Application in Removal of Tetracycline from Aqueous Solution." *Bioresource technology* 121: 235–40.

Lopez, David Anthony. 2015. "Examination of Immobilized TiO$_2$ Nanoparticle Photocatalytic Treatment of Stormwater by LilyPads."

Lu, Huanliang et al. 2013. "Characterization of Sewage Sludge-Derived Biochars from Different Feedstocks and Pyrolysis Temperatures." *Journal of Analytical and Applied Pyrolysis* 102: 137–43.

Lu, Yuefeng, and Herbert E Allen. 2001. "Partitioning of Copper onto Suspended Particulate Matter in River Waters." *Science of the Total Environment* 277(1–3): 119–32.

Luoma, Samuel N. 1983. "Bioavailability of Trace Metals to Aquatic Organisms—a Review." *Science of the total environment* 28(1–3): 1–22.

Major, Julie, Christoph Steiner, Adriana Downie, and Johannes Lehmann. 2012. "Biochar Effects on Nutrient Leaching." In *Biochar for Environmental Management*, Routledge, 303–20.

Manyà, Joan J. 2012. "Pyrolysis for Biochar Purposes: A Review to Establish Current Knowledge Gaps and Research Needs." *Environmental Science and Technology* 46(15): 7939–54.

Martinez-Villegas, Nadia, and Carmen Enid Martinez. 2008. "Solid-and Solution-Phase Organics Dictate Copper Distribution and Speciation in Multicomponent Systems Containing Ferrihydrite, Organic Matter, and Montmorillonite." *Environmental science & technology* 42(8): 2833–38.

Mcintyre, Jenifer K., David H. Baldwin, James P. Meador, and Nathaniel L. Scholz. 2008. "Chemosensory Deprivation in Juvenile Coho Salmon Exposed to Dissolved Copper under Varying Water Chemistry Conditions." *Environmental Science and Technology* 42(4): 1352–58.

Menendez, J A, M J Illán-Gómez, C A Leon y Leon, and L R Radovic. 1995. "On the Difference between the Isoelectric Point and the Point of Zero Charge of Carbons." *Carbon* 33(11): 1655–57.

Miedema, John. 2011. "The Sustainable Biochar System Collaborative Biochar

Research Initiative."
https://www.climatesolutions.org/sites/default/files/uploads/10.miedemapdf.pdf.

Mimiaga, Jim. 2016. "Biochar Seen as Potential Market for Forest." https://the-journal.com/articles/1952.

Mohan, Dinesh, Charles U Pittman, and Philip H Steele. 2006. "Pyrolysis of Wood/Biomass for Bio-Oil: A Critical Review." *Energy & fuels* 20(3): 848–89.

Mohan, Dinesh, Ankur Sarswat, Yong Sik Ok, and Charles U. Pittman. 2014. "Organic and Inorganic Contaminants Removal from Water with Biochar, a Renewable, Low Cost and Sustainable Adsorbent - A Critical Review." *Bioresource Technology* 160(October): 191–202. http://dx.doi.org/10.1016/j.biortech.2014.01.120.

Moran, David Taylor, J Carter Rowley III, George R Aiken, and Bruce W Jafek. 1992. "Ultrastructural Neurobiology of the Olfactory Mucosa of the Brown Trout, Salmo Trutta." *Microscopy Research and Technique* 23(1): 28–48.

Moreno-Piraján, J C, and L Giraldo. 2011. "Activated Carbon Obtained by Pyrolysis of Potato Peel for the Removal of Heavy Metal Copper (II) from Aqueous Solutions." *Journal of Analytical and Applied Pyrolysis* 90(1): 42–47.

Morley, Matthew C, Jennifer L Henke, and Gerald E Speitel Jr. 2005. "Adsorption of RDX and HMX in Rapid Small-Scale Column Tests: Implications for Full-Scale Adsorbers." *Journal of environmental engineering* 131(1): 29–37.

Mukherjee, A., A. R. Zimmerman, and W. Harris. 2011. "Surface Chemistry Variations among a Series of Laboratory-Produced Biochars." *Geoderma* 163(3–4): 247–55. http://dx.doi.org/10.1016/j.geoderma.2011.04.021.

Mukherjee, A, A R Zimmerman, and W Harris. 2011. "Surface Chemistry Variations among a Series of Laboratory-Produced Biochars." *Geoderma* 163(3–4): 247–55.

Mukherjee, Atanu, and Rattan Lal. 2013. "Biochar Impacts on Soil Physical Properties and Greenhouse Gas Emissions." *Agronomy* 3(2): 313–39.

Nadaroglu, Hayrunnisa, Ekrem Kalkan, and Nazan Demir. 2010. "Removal of Copper from Aqueous Solution Using Red Mud." *Desalination* 251(1–3): 90–95.

Namazian, Mansoor, and Sakineh Halvani. 2006. "Calculations of PKa Values of Carboxylic Acids in Aqueous Solution Using Density Functional Theory." *The Journal of Chemical Thermodynamics* 38(12): 1495–1502.

Nason, Jeffrey A et al. 2011. *Copper Speciation in Highway Stormwater Runoff as Related to Bioavailability and Toxicity to ESA-Listed Salmon*.

Nason, Jeffrey a, Matthew S Sprick, and Don J Bloomquist. 2012. "Determination of Copper Speciation in Highway Stormwater Runoff Using Competitive Ligand Exchange - Adsorptive Cathodic Stripping Voltammetry." *Water research* 46(17): 5788–98. http://www.ncbi.nlm.nih.gov/pubmed/22921394 (October 28, 2014).

Novak, J M et al. 2016. "Soil Health, Crop Productivity, Microbial Transport, and Mine Spoil Response to Biochars." *BioEnergy Research* 9(2): 454–64.

Novak, Jeff et al. 2016. "Biochars Impact on Water Infiltration and Water Quality through a Compacted Subsoil Layer." *Chemosphere* 142: 160–67. http://dx.doi.org/10.1016/j.chemosphere.2015.06.038.

Novak, Jeffrey M et al. 2012. "Biochars Impact on Soil-Moisture Storage in an Ultisol and Two Aridisols." *Soil Science* 177(5): 310–20.

———. 2018. "Remediation of an Acidic Mine Spoil: Miscanthus Biochar and Lime Amendment Affects Metal Availability, Plant Growth, and Soil Enzyme Activity." *Chemosphere* 205: 709–18.

Novak, JM, WJ Busscher, and DL Laird. 2009. "Impact of Biochar Amendment on Fertility of a Southeastern Coastal Plain Soil." *Soil …*. http://journals.lww.com/soilsci/Abstract/2009/02000/Impact_of_Biochar_Amendment_on_Fertility_of_a.6.aspx (October 13, 2014).

Nunes, B et al. 2015. "Ecotoxicological Effect of Zinc Pyrithione in the Freshwater Fish Gambusia Holbrooki." *Ecotoxicology* 24(9): 1896–1905.

Parker, J C, L W Zelazny, S Sampath, and W G Harris. 1979. "A Critical Evaluation of the Extension of Zero Point of Charge (ZPC) Theory to Soil Systems 1." *Soil Science Society of America Journal* 43(4): 668–74.

Phillips, Claire L et al. 2016. "Gasified Grass and Wood Biochars Facilitate Plant Establishment in Acid Mine Soils." *Journal of environmental quality* 45(3):

1013–20.

Pitcher, S K, R C T Slade, and N I Ward. 2004. "Heavy Metal Removal from Motorway Stormwater Using Zeolites." *Science of the Total Environment* 334: 161–66.

Provolt, Justin J. 2013. "Evaluation of Apatite II[TM] for Removal of Copper and Zinc from Highway Stormwater Runoff: Laboratory and Field Experiments."

Ragnar, Martin, Christofer T Lindgren, and Nils-Olof Nilvebrant. 2000. "PKa-Values of Guaiacyl and Syringyl Phenols Related to Lignin." *Journal of wood chemistry and technology* 20(3): 277–305.

Rajapaksha, Anushka Upamali et al. 2018. "Removal of Hexavalent Chromium in Aqueous Solutions Using Biochar: Chemical and Spectroscopic Investigations." *Science of the Total Environment* 625: 1567–73.

Ravat, Corinne, Jacques Dumonceau, and Fanny Monteil-Rivera. 2000. "Acid/Base and Cu (II) Binding Properties of Natural Organic Matter Extracted from Wheat Bran: Modeling by the Surface Complexation Model." *Water Research* 34(4): 1327–39.

Regmi, Pusker et al. 2012. "Removal of Copper and Cadmium from Aqueous Solution Using Switchgrass Biochar Produced via Hydrothermal Carbonization Process." *Journal of Environmental Management* 109: 61–69.

Robertson, A. P., and J. O. Leckie. 1997. "Cation Binding Predictions of Surface Complexation Models: Effects of PH, Ionic Strength, Cation Loading, Surface Complex, and Model Fit." *Journal of Colloid and Interface Science* 188(2): 444–72.

Ronsse, Frederik, Sven Van Hecke, Dane Dickinson, and Wolter Prins. 2013. "Production and Characterization of Slow Pyrolysis Biochar: Influence of Feedstock Type and Pyrolysis Conditions." *Gcb Bioenergy* 5(2): 104–15.

Rose, H E. 1951. "Fluid Flow Through Beds of Granular Material. Aspects of Fluid Flow, 135."

Rosselot, Kirsten Sinclair. 2006. "Copper Released from Brake Lining Wear in the San Francisco Bay Area." (January): 70.

Ryan, Adam C, Joseph R Tomasso, and Stephen J Klaine. 2009. "Influence of PH,

Hardness, Dissolved Organic Carbon Concentration, and Dissolved Organic Matter Source on the Acute Toxicity of Copper to Daphnia Magna in Soft Waters: Implications for the Biotic Ligand Model." *Environmental toxicology and chemistry* 28(8): 1663–70.

Sandahl, Jason F, David H Baldwin, Jeffrey J Jenkins, and Nathaniel L Scholz. 2007. "Article A Sensory System at the Interface between Urban Stormwater Runoff and Salmon Survival A Sensory System at the Interface between Urban Stormwater Runoff and Salmon Survival." *Environmental Science & Technology* 41(8): 2998–3004.

Sansalone, John J., and Steven G. Buchberger. 1997. "Partitioning and First Flush of Metals in Urban Roadway Storm Water." *Journal of Environmental Engineering* 123(2): 134–43. http://ascelibrary.org/doi/10.1061/%28ASCE%290733-9372%281997%29123%3A2%28134%29.

Schecher, W D, and D C McAvoy. 1992. "MINEQL+: A Software Environment for Chemical Equilibrium Modeling." *Computers, Environment and Urban Systems* 16(1): 65–76. http://www.scopus.com/inward/record.url?eid=2-s2.0-0026613115&partnerID=40&md5=84ed164c601c8d07b7da167af11420ce.

Shackley, Simon et al. 2010. "An Assessment of the Benefits and Issues Associated with the Application of Biochar to Soil." *Department for Environment, Food and Rural Affairs, UK Government, London.*

Shaheen, Donald G. 1975. 1 *Contributions of Urban Roadway Usage to Water Pollution*. Office of Research and Development, US Environmental Protection Agency.

Silvertooth, Jason R. 2014. "Evaluation of Copper Removal from Stormwater Runoff Using Compost and Apatite II^{TM}."

Singh, Bhupinder Pal, Annette L Cowie, and Ronald J Smernik. 2012. "Biochar Carbon Stability in a Clayey Soil as a Function of Feedstock and Pyrolysis Temperature." *Environmental science & technology* 46(21): 11770–78.

Singh, Gurdeep, and Narendra S Rawat. 1985. "Removal of Trace Elements from Acid Mine Drainage." *International journal of mine water* 4(1): 17–23.

Sohi, S P, Evelyn Krull, E Lopez-Capel, and R Bol. 2010. "A Review of Biochar and

Its Use and Function in Soil." In *Advances in Agronomy*, Elsevier, 47–82.

Sohi, Saran, Elisa Lopez-Capel, Evelyn Krull, and Roland Bol. 2009. "Biochar, Climate Change and Soil: A Review to Guide Future Research." *CSIRO Land and Water Science Report* 5(09): 17–31.

Sohi, SP, E Krull, E Lopez-Capel, and R Bol. 2010. "A Review of Biochar and Its Use and Function in Soil." *Advances in agronomy*. http://www.sciencedirect.com/science/article/pii/S0065211310050029 (October 13, 2014).

Speth, Thomas F. 1991. "Evaluating Capacities of GAC Preloaded with Natural Water." *Journal of environmental engineering* 117(1): 66–79.

Sposito, Garrison. 1981. "The Operational Definition of the Zero Point of Charge in Soils." *Soil Science Society of America Journal* 45(2): 292–97.

Stang, John. 2017. "State Working on Winery Wastewater Permit System." http://greatnorthwestwine.com/2017/03/31/state-working-winery-wastewater-permit-system/.

Steigerwald, Jessica Marie. 2018. "Comparison of Aqueous Cu2+, Pb2+ , and Zn2+ Adsorption with Pyrolyzed Hazelnut Shells and a Commercially Produced High-Carbon Fly Ash."

Streubel, J D et al. 2011. "Influence of Contrasting Biochar Types on Five Soils at Increasing Rates of Application." *Soil Science Society of America Journal* 75(4): 1402–13.

Sun, Hao, William C Hockaday, Caroline A Masiello, and Kyriacos Zygourakis. 2012. "Multiple Controls on the Chemical and Physical Structure of Biochars." *Industrial & Engineering Chemistry Research* 51(9): 3587–97.

Sun, Xueli, and Allen P Davis. 2007. "Heavy Metal Fates in Laboratory Bioretention Systems." *Chemosphere* 66(9): 1601–9.

Swami, Deepika, and D Buddhi. 2006. "Removal of Contaminants from Industrial Wastewater through Various Non-Conventional Technologies: A Review." *International Journal of Environment and Pollution* 27(4): 324–46.

Tan, Guangcai et al. 2016. "Sorption of Mercury (II) and Atrazine by Biochar, Modified Biochars and Biochar Based Activated Carbon in Aqueous Solution."

Bioresource technology 211: 727–35.

Tipping, Edward, John R Griffith, and John Hilton. 1983. "The Effect of Adsorbed Humic Substances on the Uptake of Copper (II) by Goethite." *Croatica Chemica Acta* 56(4): 613–21.

Tong, Xuejiao et al. 2012. "Adsorption of Cu (II) on Rice Straw Char From Acidic Aqueous Solutions." *Environmental Chemistry* 31(1): 64–68.

Uchimiya, Minori, SeChin Chang, and K. Thomas Klasson. 2011. "Screening Biochars for Heavy Metal Retention in Soil: Role of Oxygen Functional Groups." *Journal of Hazardous Materials* 190(1–3): 432–41. http://dx.doi.org/10.1016/j.jhazmat.2011.03.063.

US Climate Data. 2018. "US Climate Data." https://www.usclimatedata.com/climate/salem/oregon/united-states/usor0304.

US EPA. 2016. "National Recommended Water Quality Criteria-Aquatic Life Criteria Table."

———. 2018. "Superfund Site: Formosa Mine Riddle Oregon." https://cumulis.epa.gov/supercpad/cursites/csitinfo.cfm?id=1002616.

Uzoma, K C et al. 2011. "Influence of Biochar Application on Sandy Soil Hydraulic Properties and Nutrient Retention." *J. Food Agric. Environ* 9(3–4): 1137–43.

Verheijen, F, S Jeffery, a C Bastos, M Van Der Velde, et al. 2010. JRC Scientific and technical Report *Biochar Application to Soils: A Critical Review of Effects on Soil Properties, Processes and Functions*.

Verheijen, F, S Jeffery, A C Bastos, M der Velde, et al. 2010. "Biochar Application to Soils." *A critical scientific review of effects on soil properties, processes, and functions. EUR* 24099: 162.

Vijayaraghavan, K, Umid Man Joshi, and R Balasubramanian. 2010. "Removal of Metal Ions from Storm-Water Runoff by Low-Cost Sorbents : Batch and Column Studies." 136(October): 1113–19.

Vithanage, Meththika et al. 2015. "Mechanisms of Antimony Adsorption onto Soybean Stover-Derived Biochar in Aqueous Solutions." *Journal of environmental management* 151: 443–49.

Volesky, Bohumil. 2007. "Biosorption and Me." *Water research* 41(18): 4017–29.

Walaszek, M et al. 2018. "Sorption Behavior of Copper, Lead and Zinc by a Constructed Wetland Treating Urban Stormwater." *Applied Geochemistry*.

Weber, Walter J. 2004. "Preloading of GAC by Natural Organic Matter in Potable Water Treatment Systems: Mechanisms, Effects and Design Considerations." *Journal of Water Supply: Research and Technology-Aqua* 53(7): 469–82.

Westall, John C, John D Jones, Gary D Turner, and John M Zachara. 1995. "Models for Association of Metal Ions with Heterogeneous Environmental Sorbents. 1. Complexation of Co (II) by Leonardite Humic Acid as a Function of PH and NaClO4 Concentration." *Environmental science & technology* 29(4): 951–59.

Westall, John, and Herbert Hohl. 1980. "A Comparison of Electrostatic Models for the Oxide/Solution Interface." *Advances in Colloid and Interface Science* 12(4): 265–94.

Weyers, Sharon L, and Kurt A Spokas. 2011. "Impact of Biochar on Earthworm Populations: A Review." *Applied and Environmental Soil Science* 2011.

Witek-Krowiak, Anna, and D Harikishore Kumar Reddy. 2013. "Removal of Microelemental Cr (III) and Cu (II) by Using Soybean Meal Waste--Unusual Isotherms and Insights of Binding Mechanism." *Bioresource technology* 127: 350–57.

Woolf, D, JE Amonette, FA Street-Perrott, and J Lehmann. 2010. "Sustainable Biochar to Mitigate Global Climate Change." *Nature* .… http://www.nature.com/ncomms/journal/v1/n5/abs/ncomms1053.html (October 13, 2014).

Woolf, Dominic. 2008. "Biochar as a Soil Amendment: A Review of the Environmental Implications."

Wright Water Engineers and Geosyntec Consultants. 2011. "Pollutant Category Summary: Metals." *International Stormwater BMP Database*: 64.

Wu, Peng, and Yu-shan Zhou. 2009. "Simultaneous Removal of Coexistent Heavy Metals from Simulated Urban Stormwater Using Four Sorbents: A Porous Iron Sorbent and Its Mixtures with Zeolite and Crystal Gravel." *Journal of hazardous materials* 168(2–3): 674–80.

Wu, Xiang, Wang Huapin, Deng Nansheng, and Wu Feng. 2003. "Feasibility Study

on Heavy Metal Removal from Mine Water by Using Geological Material." *Fresenius Environmental Bulletin* 12(11): 1400–1406.

Xie, Xiongfei, Daniel E Giammar, and Zimeng Wang. 2016. "MINFIT: A Spreadsheet-Based Tool for Parameter Estimation in an Equilibrium Speciation Software Program." *Environmental science & technology* 50(20): 11112–20.

Yu, Liuqian et al. 2013. "Effects of Biochar Application on Soil Methane Emission at Different Soil Moisture Levels." *Biology and Fertility of Soils* 49(2): 119–28.

Zhang, P, R Ding, R Wallace, and T Bandosz. 2015. "Evaluation of Pharmaceuticals Removal by Sewage Sludge-Derived Adsorbents with Rapid Small-Scale Column Tests." In *AGU Fall Meeting Abstracts*,.

Zhang, Youchi, and Wensui Luo. 2014. "Adsorptive Removal of Heavy Metal from Acidic Wastewater with Biochar Produced from Anaerobically Digested Residues: Kinetics and Surface Complexation Modeling." *BioResources* 9(2): 2484–99. http://ojs.cnr.ncsu.edu/index.php/BioRes/article/view/4886.

Zhu, Chen. 2002. "Estimation of Surface Precipitation Constants for Sorption of Divalent Metals onto Hydrous Ferric Oxide and Calcite." *Chemical Geology* 188(1–2): 23–32.

Zimmerman, Andrew R, Bin Gao, and Mi-Youn Ahn. 2011. "Positive and Negative Carbon Mineralization Priming Effects among a Variety of Biochar-Amended Soils." *Soil biology and biochemistry* 43(6): 1169–79.

Zwieten, L V, B P Singh, and J Cox. 2012. "Chapter Four: Biochar Effects on Soil Properties." *Biochar in horticulture: prospects for the use of biochar in Australian horticulture. Horticulture Australia, NSW Department of Primary Industries*.

van Zwieten, L et al. 2010. "Effects of Biochar from Slow Pyrolysis of Papermill Waste on Agronomic Performance and Soil Fertility." *Plant and soil* 327(1–2): 235–46.

Van Zwieten, Lukas et al. 2009. "Biochar and Emissions of Non-CO2 Greenhouse Gases from Soil." *Biochar for environmental management: science and technology* 1: 227–50.

8   Appendix A

Appendix A contains supplemental information from the first manuscript (Chapter 4), "Defining mechanisms for copper removal by biochar using characterization, equilibrium testing and electrostatic modelling."

SRNOM Stock Preparation The SRNOM stock solution was prepared by adding 0.0250g of dry SRNOM powder and an initial 200 mL of distilled de-ionized (DDI) water to a 250 mL volumetric flask, adjusting the pH to 4.0 ± 0.1, and then filling the volumetric flask up to the 250 mL line with DDI water. This solution was then mixed in the dark for 24 hours prior to filtering (0.45 μm Millipore™ HAWP04700). The dissolved organic carbon (DOC) concentration of the stock solution was measured in triplicate (1: 20 dilution) using a Shimadzu TOC-V$_{CSH}$ total organic carbon analyzer (ASTM D757).
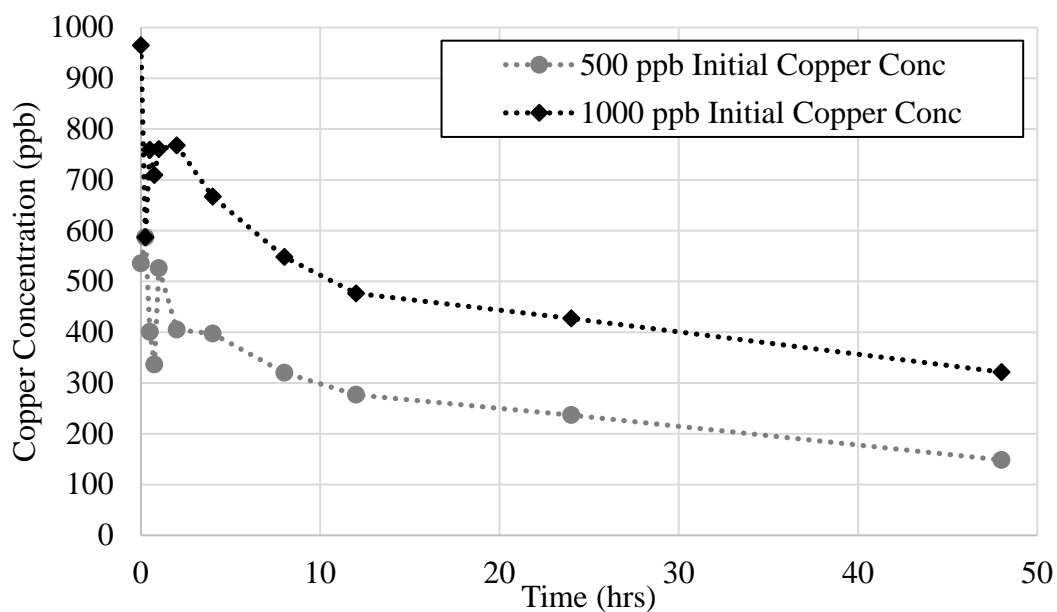
Figure 24 Batch Kinetics tests for H700 Biochar

9   Appendix B

Appendix B contains supplemental information from the second manuscript (Chapter 5), "Evaluating dynamic copper removal by hazelnut shell biochar in fixed-bed column experiments: synthetic stormwater, river water, and metals competition."

Table 7 Number of Filter Beds Treated for effluent column breakthrough of 2, 20, and 50 ppb Cu^{2+}

Effluent Copper Treatment level (ppb)	Number of Filter Beds Treated		
	2	20	50
H700 SSW	1813	2931	4195
GAC SSW	138	394	660
H700 RW	30	385	1244
GAC RW	178	622	1451
H700 Comp.	266	622	1125
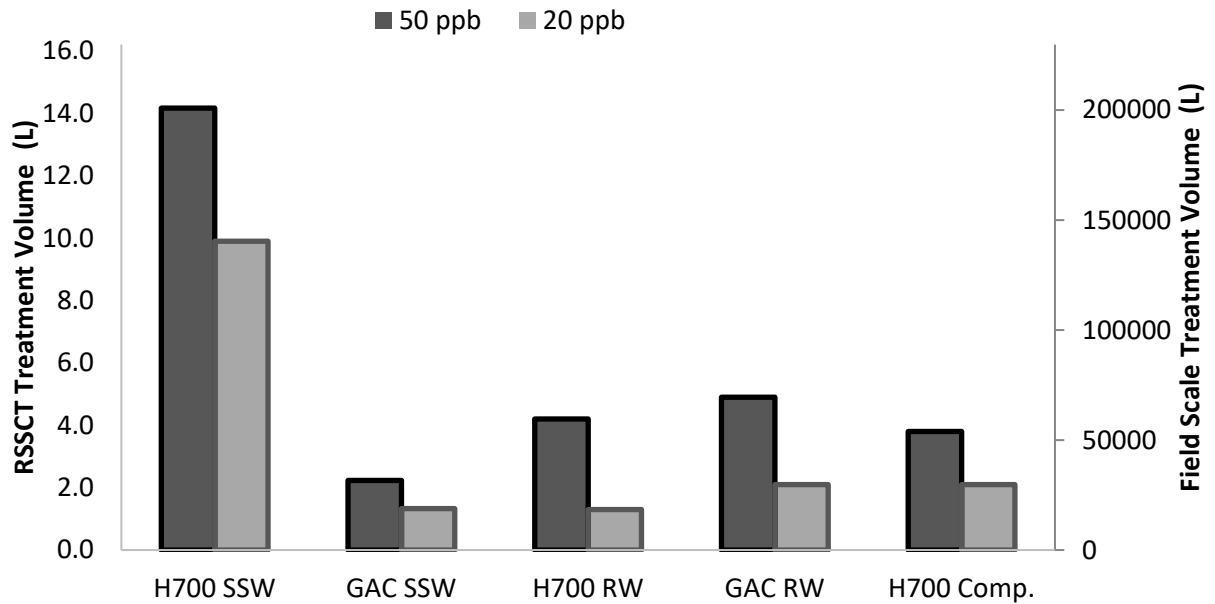
Figure 24 RSSCT and Field Scale Breakthrough Volumes to reach effluent treatment levels of 20 ppb (t_{B20}) and 50 ppb Cu^{2+} (t_{B50}).
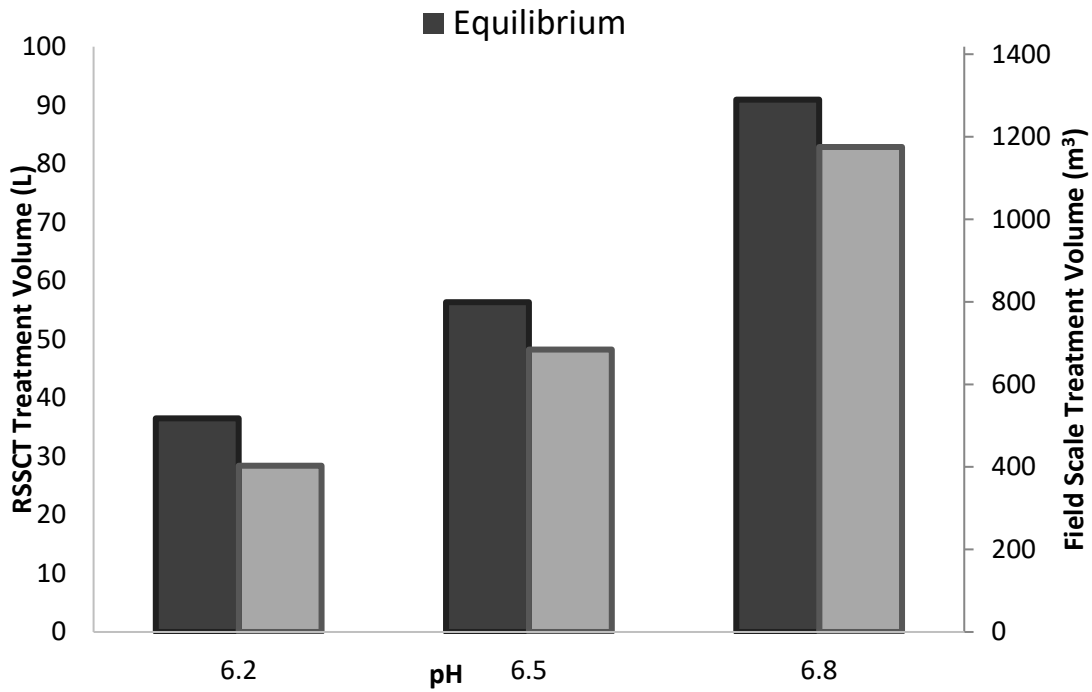
Figure 25 RSSCT and field scale DLM initial and equilibrium breakthrough volume predictions at influent copper concentration of 31 ppb
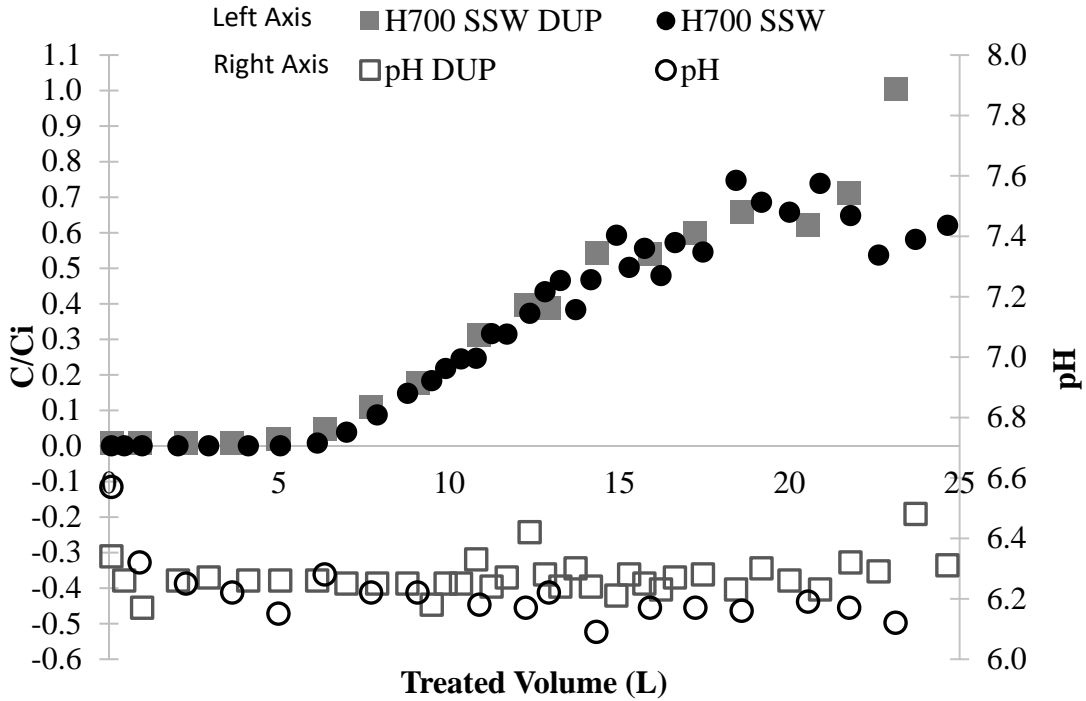

Figure 26 Duplicate H700 Synthetic Stormwater (SSW) RSSCT results and corresponding pH
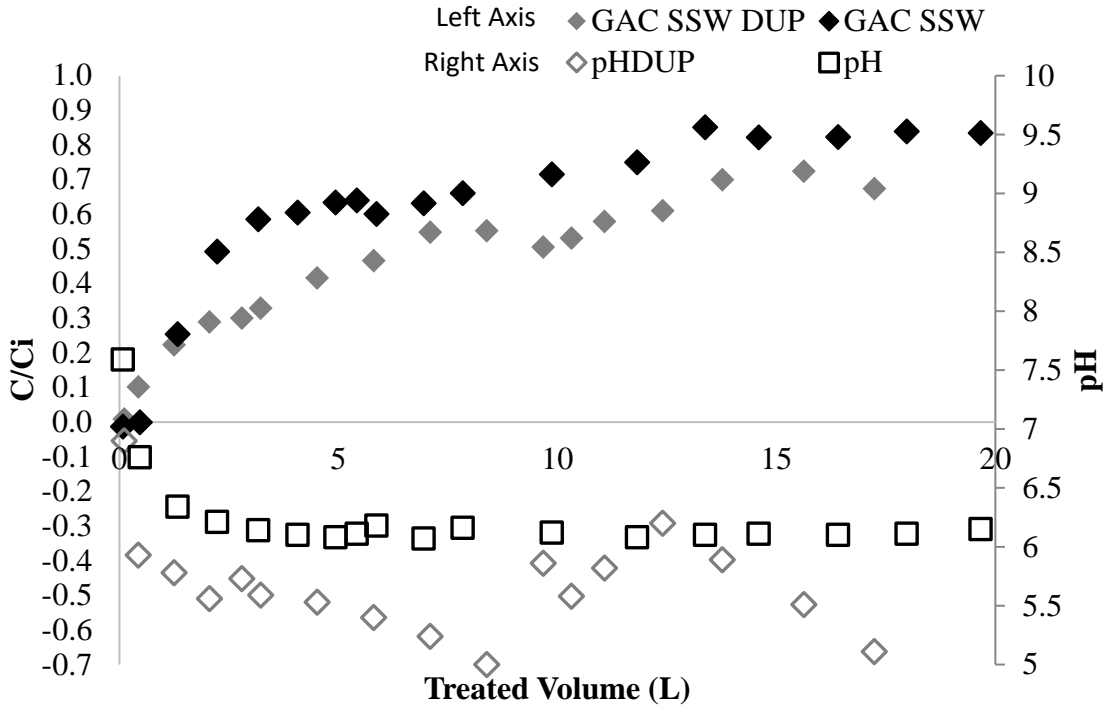
Figure 27 Duplicate GAC Synthetic Stormwater (SSW) RSSCT results and corresponding pH
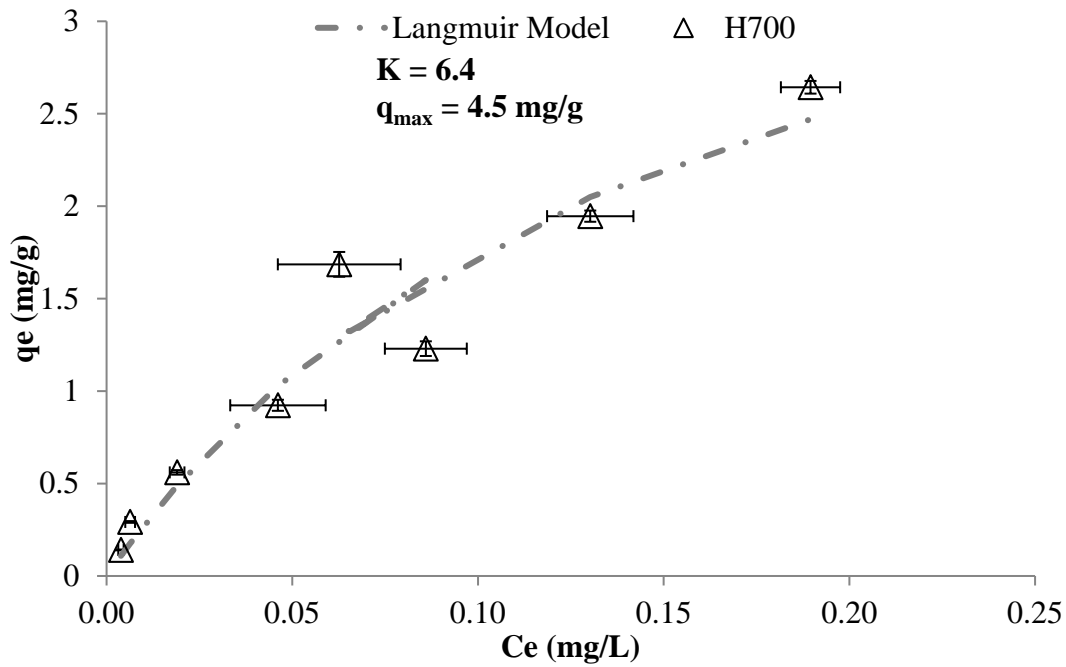

Figure 28 H700 Batch equilibrium isotherm data and Langmuir model parameters at final equilibrium pH of 7.4